PHYSICAL REVIEW LETTERS

VOLUME 3
JULY 1 - DECEMBER 15, 1959

Published by the
AMERICAN PHYSICAL SOCIETY

PHYSICAL REVIEW LETTERS

Containing short communications dealing with important new discoveries or topics of high current interest in rapidly changing fields of research, and abstracts of Articles to be published in future issues of THE PHYSICAL REVIEW.

Published by the
AMERICAN PHYSICAL SOCIETY

President

G. E. UHLENBECK
University of Michigan
Ann Arbor, Michigan

Vice-President

V. F. WEISSKOPF
Massachusetts Institute of Technology
Cambridge, Massachusetts

Secretary

K. K. DARROW
Bell Telephone Laboratories
(retired)

Office:
Columbia University
New York 27, New York

Treasurer

S. L. QUIMBY
Columbia University
New York 27, New York

Local Secretary for the Pacific Coast

WILLIAM A. NIERENBERG
University of California
Berkeley, California

Managing Editor

S. A. GOUDSMIT
Brookhaven National Laboratory
Upton, Long Island, New York

Editors

S. A. GOUDSMIT and S. PASTERNACK

Assistant Editor

P. J. LEURGANS

Publication Manager

M. J. FLEMING

Communications intended for this Journal should be short (about 800 words) and self-contained; they should not contain more than two figures. The results of an extended research program should not be presented as a series of Letters in place of a comprehensive Article.

Manuscripts, which must be in duplicate, should be submitted to S. A. Goudsmit, Editor, The Physical Review, Brookhaven National Laboratory, Upton, New York. The authors' institutions are requested to pay a publication charge of $35 per page which, if honored, entitles them to 100 free reprints. For abstracts, a publication charge of $8 will be requested.

Subscription Price

	U. S. and Canada	Elsewhere
Physical Review Letters		
Members of the American Physical Society	$ 5.00	$ 6.00
Nonmembers	10.00	11.00

Back Numbers

Single Copies	1.00
Complete Volumes	
I (July 1 - December 15, 1958)	9.00
II (January 1 - June 15, 1959)	9.00

Subscriptions, renewals, and orders for back numbers should be addressed to the American Institute of Physics, 335 East 45th Street, New York 17, New York.

Changes of address in the case of members of the American Physical Society should be addressed to the Treasurer; in case of other subscribers, to the American Institute of Physics.

Physical Review Letters is published semimonthly by the American Physical Society at Freeport, New York

Second-class mailing privileges held at Freeport, New York

EDITORIAL

With this issue we begin our second year of operation of PHYSICAL REVIEW LETTERS. The journal has received general approval and seems to be meeting a real need. The subscriptions, although slower than expected at the start, have increased rapidly and the financial situation is now reasonably healthy.

Unfortunately, the number of contributions has also increased. As we have pointed out before, the journal would lose its usefulness if it became so voluminous that its contents could not be scanned easily. Moreover, our facilities are limited and we cannot handle more than 15 to 20 Letters per issue. (The size of the current issue, which is 50% larger, cannot be maintained on a continuous basis.) We therefore must apply quite stringent criteria of importance and urgency, and require the full cooperation of contributors and referees in restricting the Letters to those whose rapid publication can be of greatest value.

There are two innovations on the cover of this issue of PHYSICAL REVIEW LETTERS, both designed to facilitate storage and use. The three heavy bars at the top designate the volume number, and the thin line near the bottom designates the issue number within the volume. Also, the back cover near the fold carries the volume number, page numbers, and year. Subscribers who do not bind their completed volumes may find it useful to mark the covers of volumes 1 and 2 correspondingly. (The spacing of the issue number lines is illustrated for an issue No. 7.)

S. A. Goudsmit and S. Pasternack

123622

PHYSICAL REVIEW
LETTERS

VOLUME 3 JULY 1, 1959 NUMBER 1

FIELD MIXING AND ASSOCIATED NEUTRON PRODUCTION IN A PLASMA*

A. C. Kolb and C. B. Dobbie
United States Naval Research Laboratory, Washington, D. C.

and

H. R. Griem
University of Maryland, College Park, Maryland, and
United States Naval Research Laboratory, Washington, D. C.
(Received June 4, 1959)

A series of experiments has been performed to determine the magnitude of the internal electric fields in a preheated deuterium plasma with a trapped internal axial magnetic field H_i, which is compressed by a large externally generated axial field H_e. It has been shown that E_θ fields of several hundred volts/cm can be readily produced by the rapidly changing internal magnetic fields and result in the production of neutrons from D-D reactions.

The electric field strength in the plasma can be controlled by varying separately (dH_e/dt), H_i, and the relative polarity of the internal and external fields. The highest E_θ fields are observed when the two magnetic fields, which are generated by separate condenser banks (the "preheater" and "main" banks) have opposite polarity. During the early stages of the compression, on the second half-cycle of the preheater and the first half-cycle of the main bank, the trapped magnetic field first increases in magnitude as the plasma radius diminishes and then decreases rapidly, reversing its direction as the two fields interpenetrate [Figs. 2(C), (E)]. Shortly after the internal magnetic field passes through zero, with $dH_i/dt \sim 10^{11}$ gauss/sec, a burst of neutrons is observed. For a trapped field of ~+10 000 gauss, which is reversed to -10 000 gauss in ~0.2 μsec, e.g., see Fig. 2(E), a kev deuteron can double its energy in about one Larmor period. Particles with energies sufficient to cause a D-D reaction can easily be produced in times of ~1 μsec by the induced electric field which transfers energy from the reversed trapped field to the plasma. The particles are confined by the external field when the internal field passes through zero since the external field from the second half-cycle of the preheater and the first half-cycle of the main bank are in the same direction and do not cancel one another.

The cancellation of a trapped reversed axial magnetic field from the first half-cycle by the penetration of an external field generated during the second half-cycle of a fast condenser discharge was first suggested by Furth[1,2] as the mechanism responsible for neutron production in other experiments.[3,4] (In these cases there was no trapped reversed field during the first half-cycle since there was no preheater field as in the present experiment.) This suggestion was based on earlier observations of Colgate[5] with rapidly oscillating axial fields (the "collapse" experiment), on field measurements of Anderson et al.[3] with inverse pinches, and also on experiments performed with the triaxial pinch.[6] The latter is a tubular pinch compressed between magnetic fields of opposite sign and neutrons are emitted near a current maximum with an isotropic en-

ergy distribution at a time of enhanced resistivity when there are rapidly cancelling reverse fields. Our experiment with axial confining fields in which the internal trapped field can be controlled lends support to the hypothesis of Furth for the trapped field origin of "second half-cycle neutrons" and does not appear to be consistent with the suggestion[7] that the energetic deuterons are produced by simple Joule and shock preheating with subsequent adiabatic compression by an external field. The cancellation of the trapped field apparently plays an essential role.

Also in this experiment the trapped field from the first half-cycle of the main condenser bank is observed to be trapped at the beginning of the second half-cycle [e.g., Fig. 2(H)] and then compressed by the rising external reversed field. This trapped field appears to be responsible for the excitation of large amplitude radial plasma oscillations observed previously[8] as well as providing a plausible mechanism for the neutron generation reported elsewhere.[3,4]

The experimental parameters employed for most of this investigation were: voltage 15 kv, capacitance 130-400 μf for the main bank and 20 kv, 1 μf for the preheater discharge; maximum current, 1.1×10^6 amp; maximum field, 100 000 gauss; total inductance 0.05 μh; coil inductance 0.04 μh; coil length 10 cm; coil diameter 5.7 cm i.d.; Pyrex tube 5.0 cm i.d. The electrical system is described more completely elsewhere.[8] No magnetic mirrors were used so that deuterons moving axially with energies above one kev could escape from the confining field in a few tenths of a microsecond. Therefore, the neutron generation is probably caused principally by a highly nonisotropic distribution of deuterons moving in a plane normal to the magnetic axis. The observation of neutrons with no mirror fields suggests that the presence of magnetic mirrors is not the dominant factor in the initial heating since deuterons are apparently raised to high energies in a short period of time by an induced E_θ field in the plasma.

Typical observations are shown in Figs. 1 and 2. The magnetic field from the second half-cycle of the preheater is trapped on its third half-cycle if there is no rf (1 kw, 27 Mc/sec)

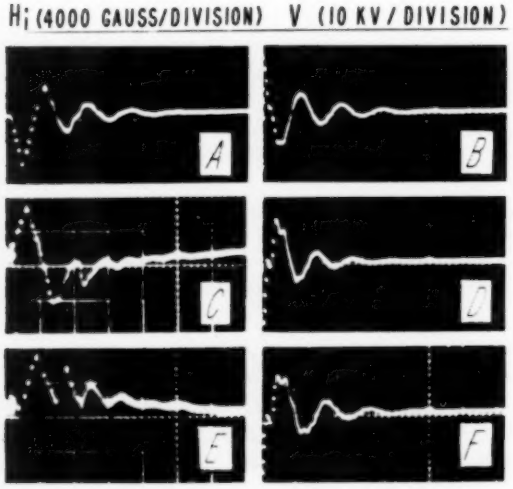

FIG. 1. Internal magnetic field H_i and voltage V across the coil for the preheater discharge: A, B one atmos air (no gas current); C, D 100 microns D_2 (no rf pre-excitation), C shows the trapped field on the third half-cycle; E, F 100 microns D_2 (rf pre-excitation), E shows the trapped field on the second half-cycle. The probe is positioned at the central plane of the coil. The time scale is 1 μsec/division. The dots serve to improve the clarity in the oscillograms.

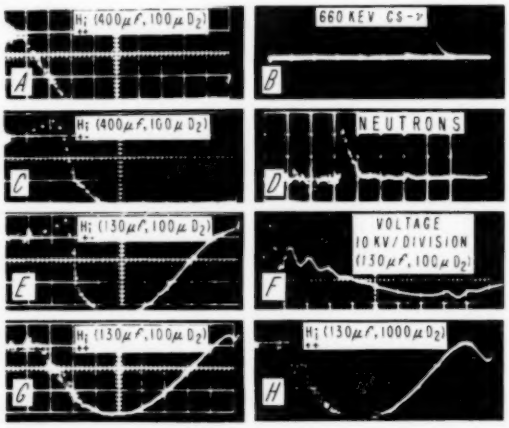

FIG. 2. Internal magnetic field H_i with internal and external fields in opposite directions (+-) C, E and in the same direction (++) A, G, H showing the compression and rapid reversal of the trapped preheater field (C, E) and the trapped field from the first half-cycle of the main bank (G, H). The voltage trace F corresponds to the field E; the modulation is due to the coupled preheater and main banks. The time of neutron emission is shown in D (corresponding to C) and the scintillations due to cesium γ-rays are shown in B for comparison. The scale for H_i is 15 000 gauss/division and the time scale is 1 μsec/division. The probe was positioned on the magnetic axis at the end of the coil for A and C and at the central plane for E, G, and H.

pre-excitation [Fig. 1(C)]. With rf pre-excitation the field from the first half-cycle is trapped and on the second half-cycle the internal field [Fig. 1(E)] has a direction opposite to the field external to the plasma. The magnetic probe signal with the tube filled with air at atmospheric pressure (no ionization) is shown in Fig. 1(A) for comparison. The difference in the voltages across the coil with air (1 atmos) [Fig. 1(B)] and deuterium (100 microns) [Figs. 1(D), (F)] shows a marked effect when a plasma is created and the load inductance is reduced accordingly.

The neutrons were identified with a BF_3 proportional counter surrounded by paraffin and the time of emission was determined with a lead-shielded (1 cm) plastic scintillator. Additional shielding is provided by the 7.5-cm wall of the steel coil. Figure 2(B) shows the pulse shape for individual scintillations obtained using 0.66-Mev γ-rays from a cesium source, which have about the same average pulse height as 2.5-Mev neutrons. The decay time for a single scintillation is determined by the amplifier. Neutrons are observed [Fig. 2(D)] if the main bank of condensers is discharged during the second half-cycle of the preheater when the trapped field has the correct reverse polarity.[9] The neutron emission lasts for ~0.2-2 μsec which, for densities of $\sim 10^{16}$ - 10^{17} cm^{-3}, corresponds to the expected scattering time for particles out the ends. If the internal magnetic field is in the same direction as the main external field [Figs. 2(A), (G)] it rises slowly in the plasma as compared to the case when the trapped field is in the opposite direction [Figs. 2(C), (E)]. After about 2 μsec the plasma radius from streak camera observations is comparable to the probe radius, and the field measured at later times is essentially the vacuum field.

The experiments have been repeated using a somewhat slower preheater discharge with the following parameters: 25-30 kv, 2 μf, 330 kc/sec. The highest neutron yield was observed if the main bank was fired near the voltage maximum at the beginning of the second half-cycle of the preheater. Hard x-rays (several hundred kev) were also recorded with the scintillation counter when hydrogen was substituted for deuterium. The x-ray emission occurred during four half-cycles of the main bank when there were large voltages across the coil. The neutrons appeared at lower coil voltages. The polarity of the trapped preheater field did not seem to be a critical factor in the x-ray production.

Discussions with Dr. Harold Grad and Dr. Harold Furth have been of considerable value in the interpretation of these experiments which were carried out with the technical assistance of Mr. L. J. Melhart and Mr. T. H. DeRieux.

---

*Jointly supported by the U. S. Atomic Energy Commission and the Office of Naval Research.

[1] H. P. Furth (private communication, Geneva Conference, 1958).

[2] Anderson, Furth, Stone, and Wright, Phys. Fluids 1, 489 (1959).

[3] Elmore, Little, and Quinn, Phys. Rev. Letters 1, 32 (1958); Proceedings of the Second United Nations International Conference on the Peaceful Uses of Atomic Energy, Geneva, 1958 (United Nations, Geneva, 1958), Vol. 32, p. 337, P/356.

[4] K. W. Allen and B. Niblett, Conference on Controlled Thermonuclear Reactions, Berkeley, 1959 (unpublished); W. Millar (unpublished) communicated by P. C. Thonemann; H. Hurwitz (private communication). The hard radiation reported by S. M. Osovets et al., Proceedings of the Second United Nations International Conference on the Peaceful Uses of Atomic Energy, Geneva, 1958 (United Nations, Geneva, 1958), Vol. 32, p. 311, P/2225 (see Fig. 24), may originate from the same mechanism. A trapped field from an auxiliary coil was rapidly compressed and cancelled during the collapse of a plasma loop.

[5] S. A. Colgate and R. E. Wright, Proceedings of the Second United Nations International Conference on the Peaceful Uses of Atomic Energy, Geneva, 1958 (United Nations, Geneva, 1958), Vol. 32, p. 145, P/368.

[6] Anderson, Baker, Ise, Kunkel, Pyle, and Stone, Bull. Am. Phys. Soc. 4, 119 (1955).

[7] Boyer, Little, Quinn, Sawyer, and Stratton, Phys. Rev. Letters 2, 279 (1959).

[8] A. C. Kolb, Proceedings of the Second United Nations International Conference on the Peaceful Uses of Atomic Energy, Geneva, 1958 (United Nations, Geneva, 1958), Vol. 31, p. 328, P/345.

[9] In earlier experiments [Griem, Kolb, and Faust, Phys. Rev. Letters 2, 281 (1959)] the existence of electron temperatures of $\sim 8 \times 10^6$°K were inferred from an analysis of the bremsstrahlung radiation in the soft x-ray region emitted from a dense deuterium plasma confined by an externally generated magnetic field. No neutrons were observed with the scintillation counter which has a sensitivity of 1.5×10^{-4} count/neutron. This negative result is consistent with the measured density, temperature, and volume of the plasma. No trapped reverse field was present in this case and the induced E_θ fields were too small (a few volts/cm) to generate neutrons by the mechanism discussed here.

NEW APPROACH IN THE THEORY OF SATELLITE ORBITS*

John P. Vinti
National Bureau of Standards, Washington, D. C.
(Received April 27, 1959)

If O is a center for the earth and if Oz points along the polar axis and Ox towards the vernal equinox, the oblate spheroidal coordinates ξ, η, ϕ, defined by

$$x = c[(\xi^2+1)(1-\eta^2)]^{1/2}\cos\phi, \quad (0<\xi<\infty)$$
$$y = c[(\xi^2+1)(1-\eta^2)]^{1/2}\sin\phi, \quad (-1\leq\eta\leq 1)$$
$$z = c\xi\eta,$$

turn out to be a useful system of coordinates for investigating the motion of an earth satellite.

In this coordinate system any axially symmetric potential $V(\xi,\eta)$ that results in separability of the Hamilton-Jacobi equation must have the general form

$$V(\xi,\eta) = (\xi^2+\eta^2)^{-1}[f(\xi)+g(\eta)].$$

The most general solution of Laplace's equation compatible with such a form is

$$V = C + b_0\,\mathrm{Re}(\xi+i\eta)^{-1} + b_1\,\mathrm{Im}(\xi+i\eta)^{-1} + b_2(\xi^2+\eta^2)^{-1}\left[2\xi\tan^{-1}\xi+\eta\ln\left(\frac{1+\eta}{1-\eta}\right)\right],$$

where the logarithmic term has a singularity everywhere on the z axis. We therefore place $b_2=0$ and we also place $C=0$ to make V vanish at infinity.

Expansion of $(\xi+i\eta)^{-1}$ in spherical harmonics leads naturally to the following choices for the adjustable constants b_0 and c:

$$b_0 c = -GM, \quad c^2 = (I_p - I_t)/M,$$

where G is the gravitational constant, M is the mass of the earth, and I_p and I_t are, respectively, the polar and transverse moments of inertia of the earth.

The above V then everywhere gives the r^{-1} term and the second harmonic exactly. For the fourth harmonic it yields an amplitude which has about half of Jeffreys' value[1] or about 86% of the value obtained by King-Hele and Merson,[2] from analysis of data on satellite orbits. Since these authors indicate a standard deviation of 16%, the resulting value for the fourth harmonic agrees with their value within the limits of observational error. Even the sixth harmonic, of amplitude 1.3×10^{-9}, falls within the (admittedly wide) amplitude limits, $(0.1\pm1.5)\times10^{-6}$, given by King-Hele and Merson.

[The term $b_1\,\mathrm{Im}(\xi+i\eta)^{-1}$ leads to odd harmonics, with amplitudes all proportional to the first harmonic amplitude δ/R, where R is the equatorial radius and δ is the distance OC from the coordinate center O to the center of mass C. Thus if O is taken as coincident with C, all the odd harmonics drop out, so that the potential $V(\xi,\eta)$ here derived always has symmetry with respect to a plane through C, perpendicular to the polar axis. It remains an open question whether use of a displaced center O, noncoincident with C, which would give rise to first, third, ..., harmonics with amplitudes δ/R, $0.00109\delta/R$, ..., could usefully represent equatorial asymmetry, as found by O'Keefe, Eckels, and Squires.[3]]

The net result of the present work is a reduction of the problem of satellite motion to quadratures, for a potential whose even harmonics are exact through the second, and whose fourth harmonic is comparable with empirical values. The kinetic equations of motion have been set up formally, in terms of certain integrals, which are now being evaluated. The effects of drag, of axial asymmetry, and of higher odd harmonics remain to be handled by perturbation theory.

This paper had its inspiration in the earlier work of Sterne[4] and of Garfinkel,[5] who also reduced the problem to quadratures, for potentials with approximate second harmonics.

---

*This work was supported by the U. S. Air Force, through the Office of Scientific Research of the Air Research and Development Command.

[1] Harold Jeffreys, The Earth (Cambridge University Press, Cambridge, 1952), second edition, Chap. IV.

[2] D. G. King-Hele and R. H. Merson, Nature 183, 881 (1959).

[3] O'Keefe, Eckels, and Squires, Science 129, 565 (1959).

[4] T. E. Sterne, Astron. J. 62, 96 (1957).

[5] B. Garfinkel, Astron. J. 63, 88 (1958).

PROTONS IN THE EARTH'S MAGNETIC FIELD*

Stanley C. Freden and R. Stephen White
Lawrence Radiation Laboratory, University of California, Livermore, California
(Received May 28, 1959)

The identity, flux, and energy distribution of particles trapped in the earth's magnetic field have been determined for those particles which penetrate more than 6 g/cm² of material.

A small stack of nuclear emulsions has been exposed to the particles in the lower Van Allen radiation belt.[1] The stack consisted of 10 sheets of Ilford *K*.5 emulsion, $1\frac{3}{8}$ in. $\times 1\frac{3}{8}$ in. $\times 600\ \mu$, enclosed in a water-tight stainless steel box which was mounted on the instrument board $1\frac{3}{4}$ in. from the side wall of the nose cone of a Thor-Able ballistic missile. The normal to this wall was parallel to the plane of the emulsions.

The missile was launched from Cape Canaveral on April 7. It reached a maximum altitude of 1230 km and spent about 15 minutes above 1000 km between the latitudes of 20°N and 3°N. The nose cone was recovered in the South Atlantic and returned for analysis. The emulsions were in excellent condition.

The particles that penetrated 5 g/cm² of nose cone wall, 0.032 in. of stainless steel emulsion box, and a minimum of 1 mm of nuclear emulsion have been identified and their numbers and energies measured; these correspond to protons and electrons with energies greater than 75 Mev and 12 Mev, respectively. The separation of protons from electrons was done unambiguously for proton energies up to 700 Mev by measuring the ionization of their tracks, only. The background of π mesons and other particles that arose from trapped proton or cosmic-ray interactions in the walls of the nose cone was negligible. No attempt was made to determine the angular distribution of the charged particles in the belt because the nose cone of the missile was not oriented in space. Therefore, in all the results which follow, an isotropic distribution has been assumed.

All proton energies were measured using the g^* method of ionization.[2] Normalization was obtained for g^*'s from 5 to 7 using the tracks of protons which had residual ranges of 8 to 14 mm in the emulsions. The energies of these stopping protons were determined from their ranges. The scanning for tracks was done 5 mm in from the edge of the emulsion that was nearest the nose cone wall where accurate g^* measurements could be taken. In addition, scanning was done 1 mm from the edge to pick up low-energy protons which did not penetrate to 5 mm. All particles whose vertical angles were within ±15° of the emulsion plane and whose horizontal angles, in the plane of the emulsion, were within ±15° of the normal to the wall of the nose cone were accepted for measurement. The estimated absorber thickness in the backward direction was used to correct the proton spectrum for the number of protons which crossed the scan lines in the wrong direction. The calculated correction varied continuously from 10% at 75 Mev to 25% at 700 Mev. This was checked experimentally at 100 Mev.

Emulsions which underwent the same history as those exposed to the Van Allen belt except for being aboard the missile were scanned for background tracks. The proton background was small. After the background of tracks of plateau ionization was subtracted out, no electron signal remained. An upper limit of 1% is placed on the ratio of the number of electrons to protons that can penetrate 6 g/cm² of material.

The resulting value, N, the absolute number of protons Mev^{-1} sterad^{-1} sec^{-1} cm^{-2}, outside the nose cone at an altitude of about 1200 km is plotted versus the proton energy T in Fig. 1 on a log-log plot. The data approximate a straight line from the minimum detectable energy of 75 Mev to the maximum observed energy of 700 Mev. The data are represented by

$$N = N_1 T^{-n}, \tag{1}$$

where a least-squares fit to the data gives $n = 1.84 \pm 0.08$ and $N_1 = (2.1^{+1.0}_{-0.7}) \times 10^3$ protons Mev^{-1} sterad^{-1} sec^{-1} cm^{-2}. The data also fit an exponential

$$N = N_0 e^{-T/T_0}, \tag{2}$$

with $T_0 = 120 \pm 5$ Mev, and $N_0 = 0.84 \pm 0.07$ proton Mev^{-1} sterad^{-1} sec^{-1} cm^{-2}.

At least two theories have received considerable attention for the origin of the trapped particles in the earth's magnetic field: (1) Solar injection.[1] Since a solar origin would give protons of a few Mev, at most, it seems unable to account for the high-energy protons found in this experiment. (2) Earth neutron albedo. In this theory neutrons from cosmic-ray interactions in

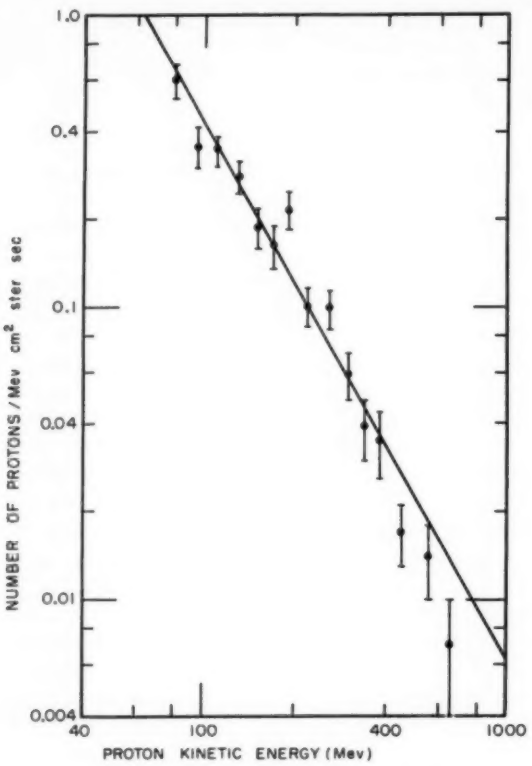

FIG. 1. The absolute energy spectrum of protons above 75 Mev in the lower Van Allen radiation belt at an altitude of 1200 km. The line is a least-squares fit of the equation $N=N_1T^{-n}$ to the data and gives $N_1=(2.1^{+1}_{0.7})\times10^3$ protons Mev^{-1} sterad^{-1} sec^{-1} cm^{-2} and $n=1.84\pm0.08$.

the upper atmosphere travel to the region of trapping and there decay into protons and electrons.[3-5] The earth neutron albedo can explain the data since high-energy neutrons are formed in cosmic-ray stars in the atmosphere in sufficient abundance to give the number of protons observed here.

Singer[3] predicted a velocity distribution that was proportional to $v^{-0.6}$. This distribution is transformed to give an energy distribution proportional to $T^{-0.8}$. Hess[6] made use of the neutron energy distribution that he measured high in the atmosphere to predict the neutron flux in the trapping region. From that he obtained a proton energy distribution proportional to $T^{-1.3}$ for $T_p \geq 100$ Mev (see the accompanying Letter). Neither of these distributions is as steep as the experimental data. If only the data for proton energies <300 Mev are used, $n=1.56\pm0.12$ and $N_1=(5.2^{+4.0}_{-2.3})\times10^2$ protons Mev^{-1} sterad^{-1} sec^{-1} cm^{-2}. This difference in n can be explained by the larger orbits and the subsequently greater loss of the high-energy protons.

The omnidirectional proton flux, J_{75}, i.e., the number of protons above 75 Mev which pass through a sphere of 1 cm^2 cross section per sec, is found by multiplying Eq. (1) by 4π and integrating over all proton energies greater than 75 Mev. The resulting value of J_{75} is 800 ± 200 protons cm^{-2} sec^{-1} If the power law with $n=1.56$ is used to integrate down to a proton energy of 10 Mev, the resulting omnidirectional flux is 3×10^3 protons cm^{-2} sec^{-1} which is not in agreement with the value of 100 to 1000 that was obtained from previous data.[1] It appears that a still smaller value of n should be used at low energies. Better agreement with this previous result is obtained by using the exponential fit which gives an omnidirectional flux of 1100 protons cm^{-2} sec^{-1}

The radiation level at the position of the emulsion stack inside the nose cone due to electrons and electromagnetic radiation is less than 50 mr/hr. Using the exponential extrapolation of the proton data, the radiation level in space at 1200 km due to protons is estimated to be 1 r/hr.

It is a pleasure to acknowledge the assistance and cooperation of personnel in the Space Technology Laboratories both at Los Angeles and at Cape Canaveral, General Electric–Missile and Space Vehicle Department, and Avco–Research and Advanced Development Division. We thank John Lindner for coordinating the experiment with the missile requirements. We are grateful to Al Oliver for assembly of the stacks. We especially thank Miss Patricia Banks, Mrs. Irene Brown, Miss Claudia Crane, Mrs. Theodora Hilliard, Mrs. Beverly Lagiss, Mrs. Bobby Sawyer, Mrs. Nancy Stratton, Mrs. Sophie Ward, and Mrs. Elizabeth Wilson for locating the proton tracks and for taking measurements on them.

---

* Work was performed under the auspices of the U. S. Atomic Energy Commission.

[1] Van Allen, Ludwig, Ray, and McIlwain, "Observations of High-Intensity Radiation by Satellites 1958 Alpha and Gamma," IGY Satellite Series Number 3, 73, Natl. Acad. Sci., Washington, D. C. (1958); Van Allen, McIlwain, and Ludwig, J. Geophys. Research 64, 271 (1959); J. A. Van Allen and L. A. Frank, Nature 183, 430 (1959).

[2]P. H. Fowler and D. H. Perkins, Phil. Mag. 46, 587 (1955).
[3]S. F. Singer, Phys. Rev. Letters 1, 171 (1958).
[4]S. F. Singer, Phys. Rev. Letters 1, 181 (1958).
[5]P. J. Kellogg, Nuovo cimento 11, 48 (1959).
[6]Wilmot N. Hess, following Letter [Phys. Rev. Letters 3, 11 (1959)].

VAN ALLEN BELT PROTONS FROM COSMIC-RAY NEUTRON LEAKAGE

Wilmot N. Hess
Lawrence Radiation Laboratory, University of California, Berkeley, California
(Received June 1, 1959)

One of the sources of particles for the Van Allen radiation belt is the decay of cosmic-ray neutrons leaking out of the atmosphere of the earth. Recently the cosmic-ray neutron energy spectrum has been measured,[1] and from this, by use of a multigroup neutron-diffusion calculation,[2] the neutron leakage has been calculated (Fig. 1). Some of the neutrons leaking out of the atmosphere decay in the earth's magnetic field and are trapped. From this leakage we can calculate the equilibrium proton energy spectrum in the inner Van Allen belt.

The calculated neutron leakage is given by $\phi(E) = 0.8E^{-2}$ neutron/cm^2 Mev sec in the region from 10 Mev to 1 Bev. The decay density of neutrons, dn/dV, is given approximately by

$$\frac{dn}{dV}(E,R) = \left[\frac{1}{v\gamma L}\exp\left(-\frac{R}{v\gamma L}\right)\right] \times \phi(E)\left(\frac{R_e}{R}\right)^2 \text{ neutron decays/cm}^3 \text{ Mev sec},$$

where L = neutron mean life, R_e = radius of earth, v = neutron velocity, R = distance from earth's center, and γ is the time-dilation factor. Protons resulting from neutron decays have very nearly the energy of the parent neutron. This gives us, for the proton source,

$$S(E) \cong k_1[\phi(E)/\beta\gamma].$$

Whereas the loss mechanism for electrons in the Van Allen belt is multiple small-angle Coulomb scattering, the loss mechanism for protons is slowing down by collisions with bound electrons.[3]

In order to calculate the equilibrium proton energy spectrum we must consider the continuity equation for the slowing-down process. Following Singer[3] we can write

$$\frac{dN(E)}{dt} = S(E) - \frac{d}{dE}\left[N(E)\frac{dE}{dt}\right] = 0$$

for the steady state, where $N(E)$ is the equilibrium proton energy spectrum. This continuity equation follows the flow of protons along an energy axis. Now we can write $dE/dt = (dE/dx) \times (dx/dt) = (dE/dx)\beta c$; then, by substituting into the continuity equation, we get

$$\frac{k_1\phi(E)}{\beta\gamma} = \frac{d}{dE}\left[\left(k_2E^{-n}\right)\left(\beta c\frac{dE}{dx}\right)\right],$$

where we have taken $N(E) = k_2E^{-n}$. Approximating β, $\beta\gamma$, and dE/dx as functions of E, we can write[4]

$$\beta = 0.0885\ E^{0.344},$$

$$\beta\gamma = 0.0393\ E^{0.545},$$

$$dE/dx = 1.16\ E^{-0.586} \text{ Mev/cm of NTP air}.$$

These are all accurate to 5% or less in the energy region 80 Mev to 700 Mev. The continuity equation now becomes

$$k_3E^{-2.545} = \frac{d}{dE}\left[k_4E^{-n-0.242}\right] = k_5E^{-n-1.242}$$

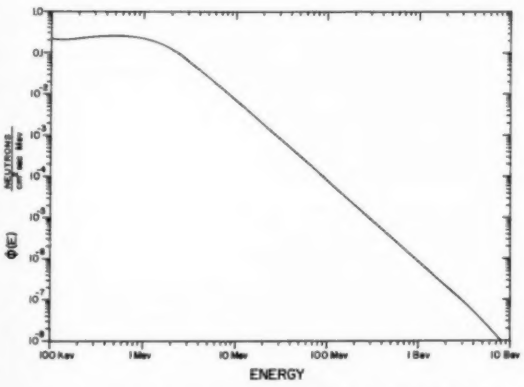

FIG. 1. The energy spectrum of the cosmic-ray neutrons that leak out of the atmosphere of the earth.

This gives, for the desired equilibrium proton energy spectrum,

$$N(E) = k_2 E^{-\eta} = k_2 E^{-1.30}$$

This is shown plotted in Fig. 2, extended down to 1 Mev by refitting $\beta, \beta\gamma$, and dE/dx and repeating the process above. The peak in the spectrum is at about 1 Mev. There are two reasons for this; first, this is about the position of the peak in the neutron leakage spectrum (see Fig. 1), and secondly, below this energy, charge-exchange reactions on neutral hydrogen remove the particles quite rapidly.[5] One can see that the equilibrium spectrum is flatter than the source spectrum. This says that the proton effective lifetime increases with the proton energy, as might be expected from the nature of the loss mechanism. We can find the lifetime here by using the "leaking bucket" equation as Van Allen[6] has done:

$$\text{Input} = \text{output} = \text{contents}/\tau.$$

The mean life τ in this problem is given by

$$\tau = \text{contents/input} = k_6[T^{-1.31}/T^{-2.55}] = k_6 T^{1.24}.$$

Freden and White, in the accompanying Letter, report measurement of the proton spectrum of the inner Van Allen belt.[7] The shape of our spectrum agrees well with theirs from 90 Mev to about 200 Mev. They find considerably fewer protons above 200 Mev than are predicted by the present analysis. There are at least three possible causes of this difference. (a) The neutron-leakage angular distribution is a function of energy.[2] This has been neglected, and although it is not obvious how it would, this might change the spectrum. (b) A 500-Mev proton at a distance of one earth radius from the surface has a radius of gyration of 600 km. This is so large that this particle will reach appreciably further into the atmosphere of the earth at its mirror point than lower energy particles, and thus its lifetime will be shorter. (c) This large radius of gyration means that this particle will be quite susceptible to nonadiabatic processes, which will lower its energy. For example, time fluctuations in the earth's magnetic field[8] would act on this particle (to remove it) more readily than on lower energy particles.

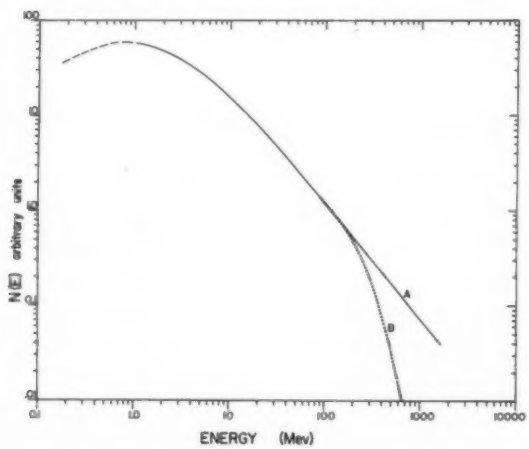

FIG. 2. The equilibrium energy spectrum of protons in the Van Allen radiation belt. A, the spectrum calculated in this report. B, the measured spectrum of Freden and White, fitted by an exponential law $N(E) = k \exp(-E/125)$ and normalized at 100 Mev.

If we evaluate the constant in the expression for the proton lifetime, we get

$$\tau = 2.1 \times 10^{-10} M l^{1.24} \text{ sec},$$

where M is the thickness of air (in cm) that must be traveled by the particle in its trajectory to equal 1 cm of air at NTP:

$$M = \frac{\text{atoms/cm}^3 \text{ at NTP}}{\text{atoms/cm}^3 \text{ along real path}} = \frac{6 \times 10^{19}}{Y}.$$

Following Christofilos' analysis,[9] we get

$$Y = (N_0/\psi)(h/r_0)^{1/2},$$

where N_0 = mirror-point density, $\psi \times r_0$ = length of magnetic line from mirror point to equator, r_0 = mirror-point radius, and h = scale height of atmosphere. If we take $N_0 = 10^5$ atoms/cm^3 (for about 1100 km, according to Johnson[10]) and $\psi = 2$ and $h = 100$ km, we get $Y = 5.7 \times 10^3$ atoms/cm^3. This gives $\tau = 6 \times 10^8$ sec for a 100-Mev proton. Now if we use the neutron decay density $dn/dV \cong (1/v\gamma L)\,\phi(E)$, we can evaluate the absolute value of the proton flux, F, to be expected in the inner Van Allen belt by using the leaking-bucket formula, $I = C/\tau$. We get

$$F = Cv = I\tau v = (dn/dV)\tau v,$$

$$F = (1/\gamma L)\Phi\tau.$$

Integrating $\phi(E)$ from 40 Mev up, we get the total neutron flux $\Phi = 0.019$ neutron/cm^2 sec. This gives, for the proton flux, $F = 1 \times 10^4$ protons/cm^2 sec. This agrees well with what Van Allen finds for the penetrating component of the inner belt,[11] which, according to the neutron-leakage source model, will be all fast protons.

This calculation is not an exact one, but it does show that the lifetime and flux predicted by the neutron-leakage source have reasonable values.

Detailed calculations on the neutron-leakage source are now under way and will be published later.

[1]Hess, Patterson, Wallace, and Chupp, Phys. Rev. (to be published).

[2]Hess, Canfield, and Lingenfelter, University of California Radiation Laboratory (unpublished data, 1959).

[3]J. A. Welch, Air Force Special Weapons Center, Albuquerque, New Mexico (private communication); M. P. Nakada, Lawrence Radiation Laboratory, Livermore, California (private communication); F. S. Singer, Phys. Rev. Letters 1, 181 (1958).

[4]Aron, Hoffman, and Williams, Atomic Energy Commission Report AECU-663, 1951 (unpublished).

[5]G. Stuart, Phys. Rev. Letters 2, 417 (1959).

[6]Van Allen, McIlwain, and Ludwig, J. Geophys. Research 64, 271 (1959).

[7]S. C. Freden and R. S. White, preceding Letter [Phys. Rev. Letters 3, 9 (1959)].

[8]J. A. Welch, Air Force Special Weapons Center, Albuquerque, New Mexico (private communication).

[9]N. C. Christofilos, University of California Radiation Laboratory Report UCRL-5407, 1958 (unpublished).

[10]Francis S. Johnson, Lockheed Missile and Space Division Report LMSD-49719, 1959 (unpublished).

[11]J. A. Van Allen and L. A. Frank, Nature 183, 430 (1959).

POLARIZATION OF THE Al^{27} NUCLEI IN RUBY*

J. A. Cowen, W. R. Schafer, and R. D. Spence
Department of Physics, Michigan State University, East Lansing, Michigan
(Received May 14, 1959; revised manuscript received June 1, 1959)

In the course of a series of studies of the relaxation process of the aluminum nucleus in ruby we have found that it is possible to observe either enhanced nuclear absorption or emission signals by driving a microwave transition of the chromium impurity. The crystal, containing 0.1% chromium, was cooled to 4.2°K and was irradiated with microwave power at 9300 Mc/sec. The dc magnetic field and the frequency of the nuclear resonance spectrometer were adjusted so that one of the transitions of the chromium ion ($S=\frac{3}{2}$) and at least one of the transitions of the Al^{27} nucleus ($I=\frac{5}{2}$) were simultaneously observed on the oscilloscope. The aluminum nuclear resonance signal in ruby consists of five components arising from the interaction of the quadrupole moment of the nucleus with the crystalline electric field.

With the magnetic field adjusted so that the chromium spin resonance occurred at the low-field end of the magnetic field sweep, all the components of the aluminum nuclear resonance showed an enhancement [Fig. 1(a)] if sufficient microwave power was applied. With the magnetic field adjusted so that the chromium spin resonance occurred at the high-field end of the sweep, all of the components of the nuclear resonance gave strong emission signals [Fig. 1(b)] if sufficient microwave power was applied. The exact position in the magnetic field sweep at which the largest enhanced or emission signals occur depends on the orientation of the crystal and on the microwave transition being excited. The dependence of the emission signal on the microwave power level is shown in Fig. 2. The maximum enhancement observed thus far is about 30. The effects are strongly temperature dependent as indicated by the fact that they disappear rapidly as the system warms up from helium temperature. No effects have been observed at liquid air temperature. When the

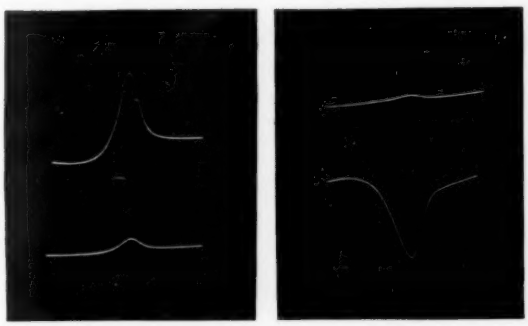

(a) (b)

FIG. 1. One component of the nuclear magnetic resonance signal in Al^{27}. (a) Top: enhanced signal; bottom: signal with no microwave power. (b) Top: signal with no microwave power; bottom: emission signal.

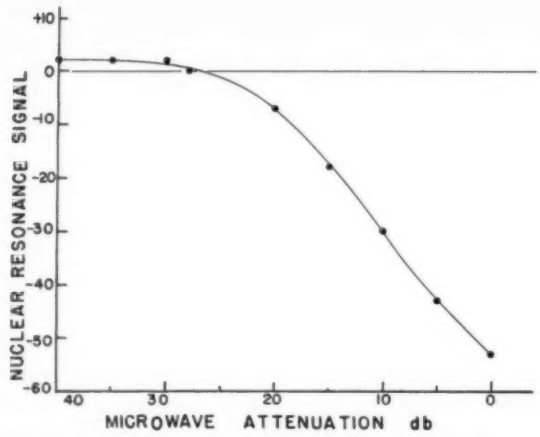

FIG. 2. The amplitude of the inverted nuclear resonance signal in arbitrary units as a function of microwave power.

microwave power is applied to the system, the enhanced or emission signals build up exponentially with a characteristic time which varies from less than a second to a few seconds depending on the orientation of the crystal.

These results can be explained in terms of the dynamic polarization process discussed by Abragam and Proctor[1] and others.[2] They consider a system in which the nuclear spin-lattice relaxation time is much greater than the electronic spin-lattice relaxation time. A mutual spin flip may take place inducing either $\Delta m_I = +1$ or $\Delta m_I = -1$ transitions if the frequency at which the electronic system is irradiated is the sum or difference of the electronic and nuclear resonance frequencies. If H_m is the amplitude of the modulation field and H_0 the dc magnetic field, then $\Delta m_I = +1$ transitions are induced when the frequency of the microwave source satisfies

$$\nu = (\gamma_S - \gamma_I)(H_0 - H_m), \tag{1}$$

and $\Delta m_I = -1$ transitions are induced when

$$\nu = (\gamma_S + \gamma_I)(H_0 + H_m). \tag{2}$$

The resulting change in population of the nuclear levels produces an enhanced absorption signal for case (1) and a stimulated emission signal for case (2). It does not appear that in the absence of the microwave power the spin-lattice relaxation times of the system satisfy the condition imposed by Abragam and Proctor, but there is definite evidence that the nuclear relaxation time increases appreciably in the presence of the microwave power. The energy levels of the chromium ion in ruby are complicated by large zero-field splitting and as a result they are strongly angle dependent and quite impure except at fields higher than those used in our experiment (~3000 gauss). Nevertheless, all orientations and all transitions examined thus far have given at least a small amount of polarization.

We wish to thank Dr. Chihiro Kikuchi and Dr. John Lambe of the University of Michigan Willow Run Laboratories for their interest, assistance, and encouragement. We also wish to thank Dr. N. Bloembergen of Harvard University for several helpful comments.

---

* Supported by the National Science Foundation and the Air Force Office of Scientific Research.

[1] A. Abragam and W. Proctor, Compt. rend. 246, 2253 (1958).

[2] Uebersfeld, Motchane, and Erb, J. phys. radium 19, 843 (1958).

EVIDENCE FOR ANISOTROPY OF THE SUPERCONDUCTING ENERGY GAP FROM ULTRASONIC ATTENUATION*

R. W. Morse, T. Olsen,† and J. D. Gavenda
Physics Department, Brown University, Providence, Rhode Island
(Received May 15, 1959)

The Bardeen, Cooper, and Schrieffer theory of superconductivity has shown remarkably good agreement with most experiments considering that a single isotropic energy gap has been used.[1] However, there are disagreements, particularly with respect to specific heats, as was emphasized by Boorse in a recent Letter.[2] A likely explanation of such discrepancies is that the energy gap in most superconductors is appreciably anisotropic.[3] Thus the specific heat variation with T would be determined near the transition temperature (T_c) by some average value of the gap, while at low temperatures the smaller values would dominate.

In order to demonstrate whether or not the energy gap depends upon the electron's position on the Fermi surface, an experiment must select electrons from a fairly limited region of the surface. Such is the case with the ultrasonic attenuation. If the electronic mean free path (l) is large compared to the wavelength (λ), then a sound wave having vector $\vec{q}$ scatters electrons from state $\vec{k}$ to $\vec{k}'$, where $\vec{k}' = \vec{k} \pm \vec{q}$. In addition, a phonon is absorbed or emitted; i.e., $E(\vec{k}') = E(\vec{k}) \pm \hbar\omega$, where ω is the angular frequency of the sound wave. These conditions of momentum and energy conservation are satisfied only by a particular group (or groups) of electrons on the energy surface. Since $\hbar\omega$ is small, then $\Delta E = (\Delta\vec{k})\cdot(\nabla_k E)$, or $\hbar\omega = \vec{q}\cdot(\nabla_k E)$, where ∇_k is the gradient operator in k space. Since the electronic group velocity is $\vec{v}_0 = \hbar^{-1}\nabla_k E$, the required electrons are those for which $v_0\cos\theta = v_s$, where v_s is the velocity of sound and θ is the angle between $\vec{q}$ and $\vec{v}_0$. Thus the scattered electrons are ones which drift in the direction of the wave with the speed of sound and so remain in a constant phase of the wave. For a spherical energy surface these electrons lie on a ring perpendicular to the direction of the sound propagation, and since $v_0 \gg v_s$, this ring of electrons is nearly an equatorial one.[4]

As has been shown previously,[5] the temperature dependence of the longitudinal wave attenuation in superconductors is determined in the Bardeen-Cooper-Schrieffer theory by the energy-gap temperature variation. By this theory the ratio of the superconducting attenuation coefficient (α_s) to that in the normal state (α_n, a constant) is given by

$$\alpha_s/\alpha_n = 2(e^{\epsilon/kT}+1)^{-1}, \qquad (1)$$

where 2ϵ is the temperature-dependent energy gap. Thus measurements of α_s/α_n as a function of T for waves in various directions in a single crystal, by selecting different groups of electrons, should show up any significant anisotropy of ϵ.

We have made measurements of longitudinal wave attenuation at frequencies up to 80 Mc/sec in oriented single crystals of tin at temperatures down to 1.00°K. From these observations it appears that $2\epsilon_0$, the energy gap as $T \to 0$, varies at least between $3.2kT_c$ and $4.3kT_c$. The samples were oriented such that propagation was along [001], [100], and [110]. Figure 1 shows the measurements along two of these directions and displays the extreme behaviors. Observations

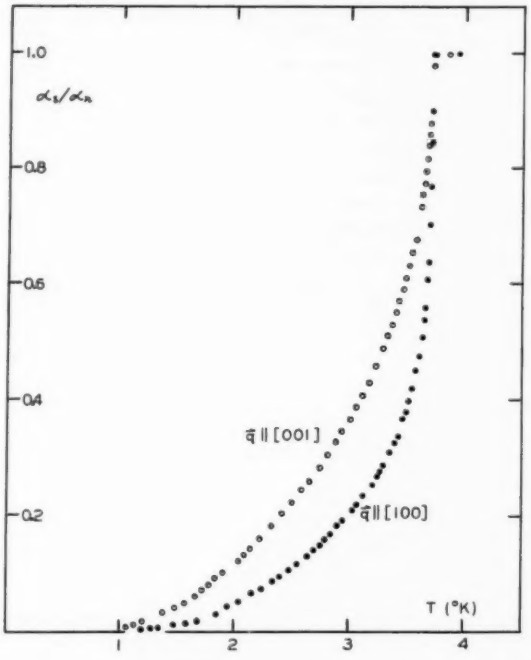

FIG. 1. Normalized longitudinal wave attenuation in tin. Propagation along [001] is at 72 Mc/sec; that along [100] is at 42 Mc/sec.

reported earlier by Bohm and one of us,[5] which were made on a different [001] crystal with different equipment, agree closely with the [001] measurements shown here. It should be noted that in all the measurements made, the condition $\lambda \gg l$ was amply satisfied (ql is estimated to be 20 or more).

The energy gap anisotropy is most effectively demonstrated if $\log(\alpha_s/\alpha_n)$ is plotted versus T_c/T since this curve should approach a straight line for large T_c/T, the slope being determined by ϵ_0. In order to do this, however, an extrapolation of α_s to $T=0$ must be made in order to find α_n and to eliminate attenuations of nonelectronic origin. This was done by choosing that extrapolation which gave the best straight-line limit when $\log(\alpha_s)$ is plotted vs T_c/T. The measurements for the three orientations when plotted in this way are shown in Fig. 2. The estimates of $2\epsilon_0$, determined by the straight-line portions of the curves, are as follows: [001], $(3.2\pm0.1)kT_c$; [100], $(4.3\pm0.2)kT_c$; and [110], $(3.8\pm0.1)kT_c$.

Naturally, the attenuation in any one direction would not necessarily reflect a single value for $2\epsilon_0$ since the scattering involves an average around a ring of the Fermi surface (or perhaps more than one in tin). Thus the values for $2\epsilon_0$ given above probably represent only approximate values for dominant parts of the surface. However, the large qualitative differences observed seem most reasonably explained by energy gap variations of at least the magnitude indicated above. Such differences cannot be explained by variations among the samples since the same sample was used for measurements along [001] and [110]. Furthermore, measurements in one crystalline direction at different frequencies and on different samples gave very similar results.

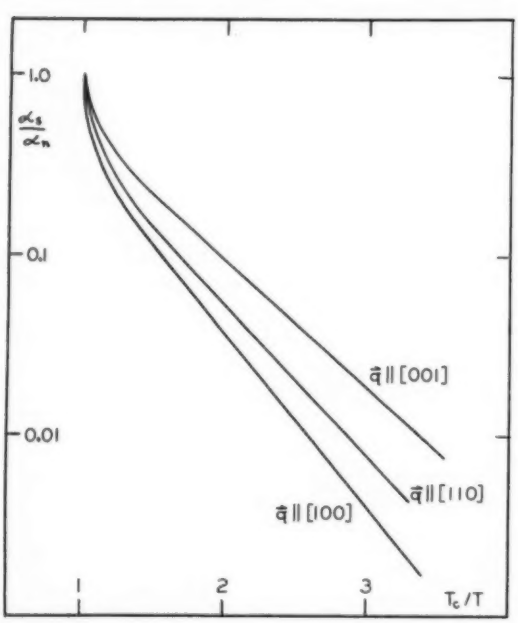

FIG. 2. Plots of $\log(\alpha_S/\alpha_n)$ vs T_C/T for longitudinal waves along different crystalline axes in tin. Propagation along [110] is at 76 Mc/sec. Measurements for the other directions are those shown in Fig. 1.

It should be noted that Eq. (1) does not give a very good fit to the experimental points shown in Fig. 1 when the single energy gaps quoted above are used. In particular, the experimental decrease just below T_c is steeper than indicated by these energy gaps. This suggests that in each direction of propagation there are some electrons involved which have an energy gap higher than the value estimated by the slope of Fig. 2. Thus one obtains a good fit to the experimental curve for [001], for example, by assuming that 80% of the electrons have $3.2kT_c$ and 20% have $4.3kT_c$ for $2\epsilon_0$.

Similar measurements are being made with shear waves. Because of the introduction of a plane of polarization, these should be more selective in choosing electrons on the Fermi surface than are longitudinal waves.

---

*Work supported by the U.S. Air Force Office of Scientific Research.

†On leave from the University of Oslo, Oslo, Norway.

[1]Bardeen, Cooper, and Schrieffer, Phys. Rev. 108, 1175 (1957).

[2]H. A. Boorse, Phys. Rev. Letters 2, 391 (1959).

[3]This possiblity, which has been suggested by a number of persons, was discussed at the International Conference on the Electronic Properties of Metals at Low Temperatures, Geneva, New York, August 25-29, 1958 (unpublished).

[4]It is probable that the group velocity of a given group of electrons becomes modified in the superconducting state [see Bardeen, Rickayzen, and Tewordt, Phys. Rev. 113, 982 (1959)]. This effect, however, does not alter the argument that propagation in different directions involves different electrons.

[5]R. W. Morse and H. V. Bohm, Phys. Rev. 108, 1094 (1957).

SPECIFIC HEAT MEASUREMENTS AND THE ENERGY GAP IN SUPERCONDUCTORS*

Leon N. Cooper
Brown University, Providence, Rhode Island
(Received May 13, 1959)

It has recently been pointed out by Boorse[1] that the low-temperature ($T_c/T \gtrsim 4$) specific heats of various superconductors seem to deviate from the theoretical curve calculated by Bardeen, Schrieffer, and the author.[2] We should like to suggest that the theory of superconductivity proposed in reference 2 contains a possible explanation of these deviations.

If instead of the constant electron-electron interaction used in reference 2 for the detailed calculation of electrodynamic and thermal properties, one uses the electron-electron interaction $V(\vec{k}, \vec{k}')$ which is nonconstant and anisotropic as might be expected in actual metals, one finds the results of reference 2 altered only in that the square of the energy gap $\epsilon_0^2(T)$ is everywhere replaced by $\mathcal{F}\mathcal{F}^*(\vec{k}, T)$, while the criterion for the existence of the superconducting state is that the integral equation

$$\mathcal{F}(\vec{k}) = -\tfrac{1}{2}\sum_{\vec{k}'} \mathcal{F}(\vec{k}')V_{\vec{k}\vec{k}'}\frac{\tanh[(\beta/2)E(\vec{k}';T)]}{E(\vec{k}', T)} \qquad (1)$$

have a nonzero solution for $\mathcal{F}$. Here $\beta = 1/kT$, $E(\vec{k}';T) = (\epsilon^2 + \mathcal{F}\mathcal{F}^*)^{1/2}$, and $V_{\vec{k}\vec{k}'} = V_{\vec{k}'\vec{k}}$ due to arguments of time-reversal invariance.

It is seen that $\mathcal{F}\mathcal{F}^*$, which now plays the role of the square of the energy gap, is a function of $\vec{k}$ as well as of T; thus the energy of a single-particle excitation depends upon the direction as well as the magnitude of its momentum vector.[3] This might result in the appearance of single-particle excitations which seem [e.g., in absorption experiments] to lie below the "energy gap." If, for example, in a particular material there was a small region of the Fermi surface over which the energy gap was smaller than that over the rest of the surface, the single-particle excitations in this region might appear to lie below the "energy gap" determined by the gross behavior of the entire surface.

Further one would expect anisotropies in measurements which pick out a direction in a crystal and which are sensitive to excitations from selected portions of the Fermi surface. One such would be the absorption of ultrasound in a superconductor. Recently Morse, Olsen, and Gavenda[4] have in fact observed a variation of the rate of ultrasonic attenuation with direction in a single crystal of tin.

With regard to the low-temperature specific heat measurements, the "upward curvature" of the specific heat of aluminum pointed out by Boorse in the region $T_c/T \gtrsim 4$ would be another consequence of a variation in the energy gap over the Fermi surface. To provide a very simple illustration: if the energy gap had a value ϵ_{01} over one region of the Fermi surface and a value of ϵ_{02} over the rest of the surface, the logarithm of the electronic specific heat of the superconductor would be expected to assume roughly the following form at low temperatures:

$$\ln\left(\frac{C_{es}}{\gamma T_c}\right) \simeq \text{constant} + \tfrac{3}{2}\ln\left(\frac{T_c}{T}\right) + \ln\left[a_1 \exp\left(-\frac{\epsilon_{01}}{kT_c}\frac{T_c}{T}\right) + a_2 \exp\left(-\frac{\epsilon_{02}}{kT_c}\frac{T_c}{T}\right)\right]. \qquad (2)$$

If $a_1 \gg a_2$ and $\epsilon_{01}/kT_c > \epsilon_{02}/kT_c$, the first term in the square brackets would dominate the second for T_c/T small, while the second would dominate for T_c/T large. The logarithm of the specific heat would then change its slope in going from the region of dominance of the first term to that of the second, producing an upward curvature.

One test of these ideas could be made by a direct comparison of the variation of the energy gap in a given material as determined by the ultrasonic attenuation and by the low-temperature electronic specific heat.

---

*This work was supported in part by the U.S. Atomic Energy Commission.

[1]H. A. Boorse, Phys. Rev. Letters 2, 391 (1959). See also for references to the measurements.

[2]Bardeen, Cooper, and Schrieffer, Phys. Rev. 108, 1175 (1957).

[3]This fact, which has been recognized by several other authors, among them P. W. Anderson, A. B. Pippard, and V. Heine, was discussed at the International Conference on the Electronic Properties of Metals at Low Temperatures, Geneva, New York, August 25-29, 1958 (unpublished). Anderson has also pointed out the relevance of a possible anisotropy of the energy gap to specific heat measurements.

[4]Morse, Olsen, and Gavenda, preceding Letter [Phys. Rev. Letters 3, 15 (1959)].

NUCLEAR QUADRUPOLE RESONANCE IN METALLIC INDIUM*

R. R. Hewitt† and W. D. Knight
Department of Physics, University of California, Berkeley, California
(Received May 28, 1959)

Subsequent to the observation of the nuclear quadrupole resonance in gallium,[1] a resonance was also found in indium. Since the nuclear spin of In^{115} is 9/2, one expects to find four resonances with frequencies in the ratio of 1:2:3:4 in a tetragonal crystal.

Following a suggestion of R. H. Hammond that the lattice of the indium sample was probably strained badly, another sample was prepared in which dry, annealed indium spheres (2-4 microns diameter) were mixed loosely in quartz powder. The other lines for In^{115}, and also the weaker ones for the less abundant isotope, In^{113}, were then successfully detected. The quadrupole coupling constants for In^{115} and In^{113} are 45.24 ± 0.02 Mc/sec and 44.60 ± 0.1 Mc/sec, respectively, at 4.2°K. The ratio of these frequencies agrees with the corresponding ratio measured by a different method.[2]

The average temperature coefficient of the quadrupole coupling constant between 4.2°K and 77°K is 5×10^{-4}/°K. This is to be compared with the value 9×10^{-5}/°K for gallium, and 6×10^{-5}/°K for niobium in ferroelectric $KNbO_3$ in the same temperature range.

The result is of interest for several reasons. First, the nuclear quadrupole resonance may be studied in the superconductor. Second, the contribution of the quadrupole energy to the low-temperature specific heat[3] may be calculated. Finally, the temperature dependence of the quadrupole coupling may be compared with that obtained[4] for In^{111} in the experiment on γ-ray asymmetry.

We wish to thank M. Pomerantz and R. Hammond for helpful discussions.

---

*This research was partly assisted by the Alfred P. Sloan Foundation and the Office of Naval Research.

†Alfred P. Sloan Postdoctoral Fellow on leave from the University of California at Riverside, California.

[1]Knight, Hewitt, and Pomerantz, Phys. Rev. 104, 271 (1956).

[2]P. Kusch and T. G. Eck, Phys. Rev. 94, 1799 (1954).

[3]G. Seidel and P. H. Keesom, Phys. Rev. Letters 2, 261 (1959).

[4]R. M. Steffen, Bull. Am. Phys. Soc. 2, 231 (1957).

THEORY OF NEGATIVE-MASS CYCLOTRON RESONANCE

D. C. Mattis and M. J. Stevenson
Research Laboratory, International Business Machines Corporation, Poughkeepsie, New York
(Received May 19, 1959)

In recent communications[1,2] Dousmanis et al. suggest that the re-entrant energy contours of the heavy-hole bands in Ge and Si[3] could contribute a negative resistivity component to the overall resistivity of these materials, possibly related to a nonequilibrium density of carriers in these re-entrant states. Such a phenomenon could be observed under cyclotron resonance conditions (H_{dc} along [100] axis, electric field transverse to H_{dc}) as an emission spectrum centered about the cyclotron frequency of these states, or as a reduction in the strength of the background absorption at that frequency.

We have examined this idea in some detail, and find that except under very restrictive conditions, these states will in general add a normal, positive resistivity contribution to the material independently of their population. Therefore, indisputable experimental evidence of any emissive properties at the cyclotron frequency of the carriers in these "dimple" states will be shown to reveal more about the nature of conduction in the valence band of Ge and Si than merely the existence of these re-entrant energy contours, or deviations from thermal equilibrium, or a combination of these.

As an introduction to the analysis consider the expression for the integrated absorption coefficient A, calculated for a hypothetical system of carriers of constant, isotropic effective mass m^*. Under crossed dc magnetic and rf electric fields, the carriers will be stimulated by the

latter to make transitions between Landau levels (denoted by quantum number n). We obtain

$$A = (\pi e^2/2m^*)\sum (n+1)[f(n,\vec{k}) - f(n+1,\vec{k})]$$
$$= (\pi e^2/2m^*)\sum f(n,\vec{k}) = \pi e^2 N/2m^*. \quad (1)$$

The sum in Eq. (1) is over all quantum numbers, only n changing in a transition. The result we obtain is a sum rule independent of the magnetic field, namely, that the integrated absorption depends only upon the total density of carriers, N.

Were it possible to isolate carriers in a region of opposite band curvature where the energy is given by $E = E_0 - p^2/2m^*$, such that over the whole range where carriers exist the effective mass $-m^*$ is constant, isotropic, and negative, the integrated absorption coefficient would be

$$A = (\pi e^2/2|m^*|)\sum (n+1)[f(n+1,\vec{k}) - f(n,\vec{k})]$$
$$= -\pi e^2 N/2|m^*|. \quad (2)$$

This system of negative masses is emissive, just as the system of positive masses was absorptive. Now, it might be argued that the sign of the mass determines whether a system of particles is emissive or absorptive. We believe this point of view to be unsound. Our arguments, to be developed below, will indicate that in the case of distributions which can be characterized by a function of energy alone, emission will occur only if there is a maximum energy cutoff on the states of interest (such as E_0 in the case of negative masses discussed above) combined with an unbalanced "inverted" distribution. These arguments do not hold when the distribution is anisotropic, as is the case for the NEMAG (negative-effective mass amplifiers and generators) suggested by Krömer.[4] However, in experiments where holes are optically excited, thermal scattering of the holes along a surface of constant energy is presumably rapid enough that the population of states along such a contour may be taken to be constant. We idealize the experiments of Dousmanis et al. by means of the following assumptions:

1. Holes are excited up to the optical phonon energy E_{opt}. (Those created at higher energies will rapidly emit optical phonons and fall to this energy or below.)

2. A negative transverse mass $-m_T$ and positive longitudinal mass m_L will be assumed constant for carriers within narrow cones of half-angle α whose axes lie along the [100] axes of Ge and Si. Beyond this cone, the heavy holes under consideration have a positive effective mass m_P, whose magnitude is sufficiently different from m_T that the conductivity at frequencies near $\omega_T = eH/m_T c$ will be determined largely by the properties of the carriers within the cones. We shall consider the possibility that m_T, m_L, or α vary with energy.

3. Steady state is described by a distribution function $f(E)$ dependent only on energy. The microwave fields are a small perturbation, whose effects we shall describe by the Boltzmann equation. Thus, under cyclotron resonance conditions, with the magnetic field along the axis of one of the cones, we find a frequency-dependent conductivity given by[5]

$$\sigma(\omega) = \frac{-Ne^2\int_0^\alpha d\theta\, \sin^3\theta \int dp\, p^2 v^2 [df(E)/dE](\tau + i\omega\tau^2)/[(\omega_T\tau)^2 + (1+i\omega\tau)^2]}{2\int_0^\alpha d\theta \sin\theta \int dp\, p^2 f(E)}$$
$$= \frac{-Ne^2\alpha^2 \int dE\, E^{3/2}(df/dE)(\tau + i\omega\tau^2)/[(\omega_T\tau)^2 + (1+i\omega\tau)^2]}{2m_L \int dE\, E^{1/2} f(E)} \quad (3)$$

The second expression follows if $\alpha^2 \ll 1$. The total density of carriers within the cone is taken to be N, and the momentum relaxation time τ obeys $\omega_T\tau \gg 1$ for a well-defined resonance. A dispersion relation valid near the axis of the cone is

$$E = \tfrac{1}{2}p^2(\cos^2\theta/m_L - \sin^2\theta/m_T) \cong \tfrac{1}{2}p^2/m_L$$
$$= \tfrac{1}{2}v^2(m_L\cos^2\theta - m_T\sin^2\theta) \cong \tfrac{1}{2}v^2 m_L, \quad (\alpha^2 \ll 1) \quad (4)$$

and was used to express the variables of Eq. (3) in terms of the energy.

If ω_T and τ vary slowly with energy compared with $f(E)$, the numerator of Eq. (3) can be integrated by parts, and we obtain

$$\sigma(\omega) = \frac{3Ne^2\alpha^2}{4m_L}\left[\frac{\tau + i\omega\tau^2}{(\omega_T\tau)^2 + (1+i\omega\tau)^2}\right]. \quad (5)$$

It is easily verified that $\mathrm{Re}[\sigma(\omega)] > 0$, so that we have a direct check that under reasonable assump-

tions the conductivity, and hence the absorption for the system under consideration is positive.

If all the hypotheses we stated are not valid, there will exist possibilities for these negative masses to amplify resonant radiation. We envisage two distinct situations: the first involves a cutoff energy $E_C < E_{opt}$, such that for $E > E_C$ the shape of the energy contours has changed sufficiently that no particles[6] above this cutoff energy can contribute to the resonance at ω_T. If such is true for the energy band structure of the heavy holes in Ge or Si, emission would be observed at ω_T provided

$$\int_0^{E_C} dE\, E^{3/2}\, df/dE > 0.$$

This last condition is tantamount to an inversion of the population of these low-lying energy levels, which could be achieved by a mechanism such as selective recombination of slow carriers.

If the band structure does not permit such a drastic change in m_T, a second situation is conceivable whereby the distribution function while still of cubic symmetry shows some anisotropy.

If, for example,

$$f = f_1(E) + f_2(|\vec{p}|), \qquad (6)$$

those particles distributed according to f_1 will absorb radiation, whereas the contribution of the carriers with negative transverse mass $-m_T$ distributed according to f_2 can be shown to be emissive, and peaked about the frequency ω_T. Whether emission or absorption predominates at that frequency will depend on the relative magnitudes of f_1 and f_2.

In this connection we propose that light may not provide the best mechanism for obtaining a selective excitation of such carriers. A possible alternative excitation technique could utilize microwave impact ionization of impurity centers in p-type Ge by resonant absorption at the cyclotron frequency ω_P of the positive-mass heavy holes. With a double resonant cavity system, the changes in the rf conductivity may then be studied with a low-power probing signal at the resonance frequency of the negative-mass holes, ω_T. Such a technique would result in the presence of positive-charge carriers only, and with proper circular polarization the effects of the negative-mass holes can be separated from those of the positive-mass holes.

In concluding, we express our thanks to colleagues of this laboratory—to Mr. W. Kopka for computational work on the IBM 704 computer, and to Dr. S. Koenig, Dr. R. Landauer, and Dr. E. Adams for their interest and helpful suggestions.

[1]G. C. Dousmanis, Phys. Rev. Letters 1, 55 (1958).
[2]G. C. Dousmanis et al., Phys. Rev. Letters 1, 404 (1958).
[3]Dresselhaus, Kip, and Kittel, Phys. Rev. 98, 368 (1955).
[4]H. Krömer, Proc. Inst. Radio Engrs. 47, 397 (1959).
[5]For method of derivation, see, for example, D. Mattis and G. Dresselhaus, Phys. Rev. 111, 403 (1958).
[6]This is an idealization. In reality we would not necessarily expect a sharp cutoff and there would be overlap in the spectra of states above and below E_C.

ROLE OF NEGATIVE EFFECTIVE MASS IN NEGATIVE RESISTANCE

Peter Kaus
University of Southern California, Los Angeles, California
(Received May 21, 1959)

Experiments on cyclotron resonance of negative-mass carriers in germanium have been reported.[1] The distribution of carriers (heavy holes) is not an equilibrium distribution, since the carriers were produced by optical excitation partly from acceptors and partly across the gap. The authors find a new resonance for the opposite sense of circular polarization to the positive-mass resonance line and the resonance corresponds to a decreased absorption. It has also been proposed to construct amplifiers using negative-effective-mass carriers in a nonequilibrium distribution maintained by auxiliary power sources.[2]

The decreased cyclotron resonance absorption as well as the proposed amplifiers depend on the negative resistance aspect of negative-effective-mass carriers. It is therefore of interest to investigate the relationship between negative effective mass, carrier distribution, and negative

resistance.

The stationary states in a crystal are described by Bloch functions, $\Psi_n(\vec{k},\vec{r}) = e^{i\vec{k}\cdot\vec{r}}U_n(\vec{k},\vec{r})$, with energy eigenvalues $E_n(\vec{k})$. Dropping the band subscript n, the corresponding group velocity is

$$\vec{v}(\vec{k}) = (1/\hbar)\vec{\nabla}_k E(\vec{k}). \quad (1)$$

Within well-known limits of validity the motion of an electron under the influence of a force $\vec{F}$ is given by

$$d\vec{k}/dt = (1/\hbar)\vec{F}. \quad (2)$$

Differentiating (1) with respect to the time and combining with (2), the equation of motion becomes

$$dv_i/dt = \sum_j (1/m^*)_{ij} F_j, \quad (3)$$

where a component of the reciprocal effective-mass tensor

$$(1/m^*)_{ij} = (1/\hbar^2)\partial^2 E/\partial k_i \partial k_j, \quad (4)$$

may be positive or negative.

A one-dimensional example is given in Fig. 1. Since every band has a lower and upper bound in energy, there is a positive and negative effective-mass region in every band. Consider a carrier in the negative effective-mass region [Fig. 1(a)]. If a force in the positive x direction is applied, the carrier moves in the positive k direction regardless of the energy band picture. It therefore moves to a region of smaller velocity or it accelerates in the negative x direction. If we think of a current associated with this motion, then the change in current is in the negative x direction or opposite to the applied force. A single carrier with negative effective mass, therefore, contributes to negative resistance.

For the same band consider now an equilibrium distribution at low temperature. Assume that the Fermi level is high up in the band [Fig. 1(b)]. The inflection point has been drawn at a low k value, so that many more negative-mass states are occupied than positive-mass states. At first glance it may appear that consequently this distribution would exhibit negative resistance to all applied forces at thermal equilibrium, or that it would emit rather than absorb.

This conclusion would be in obvious contradiction to the second law of thermodynamics. The sides of the crystal would charge up, producing

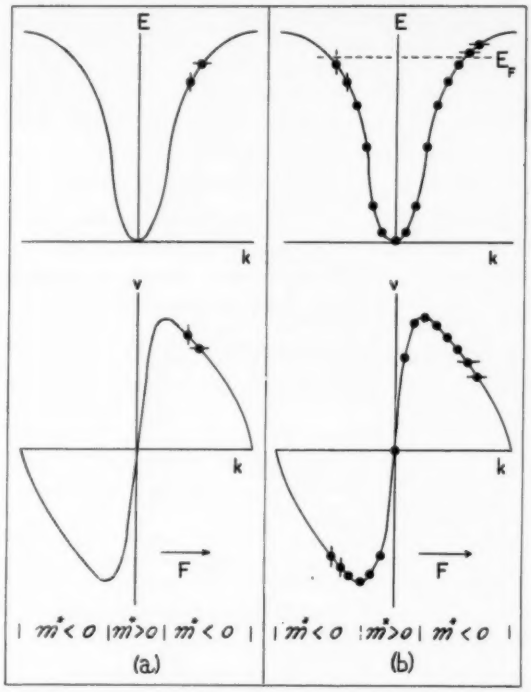

FIG. 1. Schematic representation of energy and velocity as a function of k for a simple one-dimensional band. The black dots represent occupied states. The black dots with a vertical line are states occupied at $t=0$, but unoccupied at $t=\Delta t$; the black dots with a horizontal line are states unoccupied at $t=0$, but occupied at $t=\Delta t$.

a field which would enhance the current. The original field is then seen to be unnecessary to produce a current which can be made to do work.

In the present example it is easy to see that the resistance of the distribution in Fig. 1(b) is in fact positive. Every carrier moves in the positive k direction at the same rate, according to (2). The total effect, therefore, is to add positive velocity to the total distribution of velocity. This conclusion is evidently seen to be independent of the shape of the energy band or the position of the Fermi level. However, this simple picture holds only at very low temperatures.

In the next section some necessary conditions for negative resistance are developed for a general distribution at a finite temperature.

The contribution of a quantum state to the current density is given by

$$\vec{j}(\vec{k}) = (1/L^3)(e/\hbar)\vec{\nabla}_k E(\vec{k}). \quad (5)$$

The time derivative of the current contribution

(5) is obtained using (1) and (2):

$$\frac{dj_i(\vec{k})}{dt} = \left(\frac{1}{L^3}\right)\left(\frac{e}{\hbar}\right)\sum_j \frac{\partial v_i(\vec{k})}{\partial k_j} F_j. \tag{6}$$

Let $g(\vec{k})$ be a general steady nonequilibrium distribution function. The function is maintained by the application of some auxiliary forces not contained in F_j. We now want to test the response of the distribution to a small incremental force F_j.

The change in the total current density is obtained by integrating (6) over the distribution $g(\vec{k})$:

$$\frac{dJ_i}{dt} = \left(\frac{1}{L^3}\right)\left(\frac{e}{\hbar}\right)\sum_j \int \frac{\partial v_i(\vec{k})}{\partial k_j} F_j g(\vec{k}) d\vec{k}. \tag{7}$$

If in particular we chose an electric field $\mathcal{E}$ for the incremental field, the derivative of the current density becomes

$$\frac{dJ_i}{dt} = \left(\frac{1}{L^3}\right)\left(\frac{e^2}{\hbar}\right)\sum_j \int \frac{\partial v_i(\vec{k})}{\partial k_j} \mathcal{E}_j g(\vec{k}) d\vec{k}. \tag{8}$$

In the following considerations nothing new emerges if the relaxation time τ is introduced. The derivative dJ_i/dt is then to be replaced for small incremental fields $\vec{\mathcal{E}}$ by the expression $\Delta J_i/\tau$, where ΔJ_i is the increment of current density over the steady-state current density.

The sign of the diagonal conductivity term, σ_{ii}, is therefore given by the sign of the integral

$$S_{ii} = \int \frac{\partial v_i(\vec{k})}{\partial k_i} g(\vec{k}) d\vec{k}. \tag{9}$$

We can write the integral (9) in the form

$$S_{ii} = \iint \bar{S}_{ii}(k_j, k_l) dk_j dk_l,$$

where

$$\bar{S}_{ii}(k_j, k_l) = \int \frac{\partial v_i(k_i, k_j, k_l)}{\partial k_i} g(k_i, k_j, k_l) dk_i. \tag{10}$$

The corresponding resistance is certainly positive if $\bar{S}_{ii}(k_j, k_l)$ is positive for all k_j and k_l.

Integrating (10) by parts and taking advantage of the equality of v_i at opposite edges of the zone, we obtain

$$\bar{S}_{ii}(k_j, k_l) = -\int v_i \frac{\partial g}{\partial k_i} dk_i, \tag{11}$$

or

$$\bar{S}_{ii}(k_j, k_l) = -\frac{1}{\hbar}\int \frac{\partial E}{\partial k_i}\frac{\partial g}{\partial k_i} dk_i. \tag{12}$$

From (12) it is clear that if the distribution function always decreases with increasing energy along a line (k_j, k_l) constant, then the corresponding contribution $\bar{S}_{ii}(k_j, k_l)$ to the conductivity is positive. If this is the case for all lines (k_j, k_l) constant, then S_{ii} is positive and the corresponding resistance is positive.

A necessary condition for negative resistance is therefore the following: "A distribution $g(\vec{k})$ cannot correspond to negative resistance in the i direction unless $\partial g/\partial E$ is positive along some line (k_j, k_l) constant."

The reversal of population demanded by this necessary condition depends in no way on the band structure. An obvious conclusion is that the equilibrium distribution [Fig. 1(b)] corresponds to positive resistance regardless of the number of negative-mass carriers or the position of the Fermi surface.

It would be misleading to conclude that negative mass has therefore no bearing on negative resistance. We can put Eq. (9) into the form

$$S_{ii} = \hbar \int [g(\vec{k})/m^*_{ii}(\vec{k})] d\vec{k}. \tag{13}$$

Singe $g(\vec{k})$ is positive definite, another necessary condition for negative resistance is seen to be: "A distribution $g(\vec{k})$ cannot correspond to negative resistance in the i direction unless some states corresponding to negative effective mass m^*_{ii} are occupied."

A distribution consisting entirely of negative-mass carriers [Fig. 1(a)] always corresponds to negative resistance. This is of course consistent with the first condition, since the lowest energy states along a line in k space always correspond to positive effective mass in the direction of the line. If only negative-mass states are occupied, the necessary reversal of population must have taken place.

It must be pointed out here that the reversal of population demanded in the first necessary condition is not a reversal of the total population at

one energy. It is not necessary that

$$\frac{dg}{dE}=\sum_j \int_s \frac{\partial g}{\partial k_j}\,\frac{\partial k_j}{\partial E}\,ds,$$

with the integral performed over a surface of constant energy, be positive for some such surface. The necessary condition for negative resistance in the i direction only demands that $\partial g/\partial E$ along some line in the i direction be positive. In Ge and Si with warped heavy-hole bands, the necessary reversal may only correspond to a redistribution from the thermal equilibrium distribution along constant-energy surfaces.

Most of these conclusions were simultaneously and independently reached by Dr. C. Kittel. I am very grateful to him for making his results available. I would also like to thank Dr. F. Herman for several discussions.

[1]Dousmanis, Duncan, Thomas, and Williams, Phys. Rev. Letters 1, 404 (1958).

[2]H. Krömer, Phys. Rev. 109, 1856 (1958); Proc. Inst. Radio Engrs. 47, 397 (1959).

BIMOLECULAR ELECTROLUMINESCENT TRANSITIONS IN GaP

E. E. Loebner and E. W. Poor, Jr.
RCA Laboratories, Princeton, New Jersey
(Received March 19, 1959; revised manuscript received June 1, 1959)

In this Letter we describe direct observations of bimolecular band-to-band transitions at rectifying junctions in single crystals of gallium phosphide and indium phosphide.

The presence of bimolecular recombination kinetics is deduced from the nearly square dependence of the emitted radiation on the injection current. Additional evidence for band-to-band electroluminescence is supplied by an analysis of the spectral distributions of the absorption coefficient, the electroluminous emittance, and the photovoltaic response of gallium phosphide crystal rectifiers. These band-to-band radiative transitions differ in a number of ways from those occurring via localized levels.[1]

The above-mentioned square dependence has been discussed by van Roosbroeck and Shockley[2] and looked for without success in germanium by Newman[3] who found a linear dependence. So far only Aigrain and Benoit[4] observed a square dependence in germanium, when a very sensitive detection technique was used. Braunstein,[5] who investigated band-to-band radiative transitions of injected carriers in Ge-Si alloys, GaAs, GaSb, and InP, found a linear dependence in all cases, in agreement with Newman's observations.[3]

Our GaP samples were grown by I. Hegyi of these Laboratories from gallium solution by the method of Wolff, Keck, and Broder[6] using a 5-day programmed heat-cool cycle with a peak temperature of about 1200°C. The crystals were flat hexagonal platelets with major faces parallel to (111) planes and an area of a few square millimeters. They were a few tenths of a mm thick. The crystal structure, determined by J. White, was that of sphalerite with a lattice constant of 5.449 A. The impurity with the highest concentration was copper with approximately 5-50 parts per million. Care was taken to avoid using crystals that had inclusions of free gallium or free phosphorus.

Undoped GaP crystals appear to contain grown junctions beneath the surface, which resemble somewhat those found in single crystals of silicon carbide grown by commercial processes.[7] A highly n-type conducting layer is separated from the bulk by a rectifying junction and most likely also by a nearly intrinsic layer. Ohmic contacts to the crystal bulk can be made by alloying indium through the junction or by electrical burnout of the junction layer.

The opto-electronic characteristics of the rectifiers were displayed directly on an oscilloscope. The radiation was detected by RCA 1P21 and 7102 multiplier phototubes after having been spectrally analyzed by a Perkin Elmer monochromator. Transmission data were obtained using a model 14M Cary recording spectrophotometer.

Figure 1 is a photograph of five oscilloscope traces displaying the mutual and time dependence of the GaP rectifier parameters light (L), current (I) and voltage (V) for a 60-cps sinusoidal 8-volt rms excitation. Trace A is a plot of L vs I, which shows essentially a square depen-

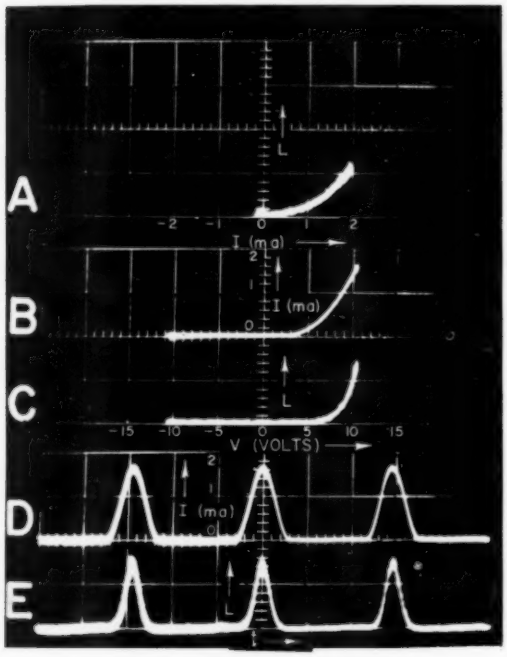

FIG. 1. Photographs of oscilloscope signals obtained from an electroluminescing GaP crystal rectifier. *A*—electroluminous emittance vs current; *B*—current vs voltage; *C*—electroluminous emittance vs voltage; *D*—current vs time; *E*—electroluminous emittance vs time.

dence of light on current. Traces *B* and *C* show the *I-V* and *L-V* characteristics, respectively. It is seen that current and light appear only on the forward bias portion of the cycle. Traces *D* and *E* show the time dependence of *I* and *L*, respectively. The light at all times is perfectly in phase with both the current and the voltage.

Microscopic observations show the light to be emitted uniformly over an area of about 10^{-3} cm^2 from a depth of several microns below the surface. In the cases on hand, only the light clearing the electrode whisker participates in the data contribution.

Various results pertaining to the spectral characteristics of our samples are seen in Fig. 2. Our optical absorption measurements lead us to a room temperature estimate of an energy gap value for GaP of 2.20 to 2.21 ev. This estimate results from a fit of the Macfarlane-Roberts expression[8] to an α vs h plot for values of the absorption coefficient, α, between 10 and 150 cm^{-1} at

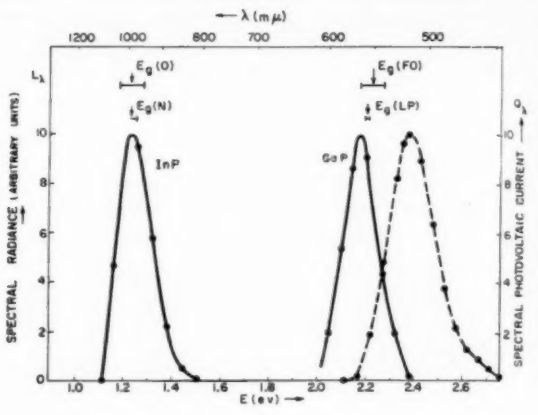

FIG. 2. Spectral opto-electronic responses of GaP and InP. Radiance indicated by ——. Short-circuit photovoltaic current indicated by ----. Letters in parenthesis indicate the following workers and references: O—Oswald (reference 13); N—Newman (reference 13); FO—Folberth and Oswald (reference 9); LP—Loebner and Poor (this Letter).

several temperatures. Assuming the presence of a single phonon assisting in the optical transition, its energy is estimated to be 0.026 ev, which gives an equivalent temperature of about 300°K. Excess absorption at lower energies and higher temperatures is probably due to optical transitions at dislocations or some other crystal imperfections. As seen from Fig. 2, the energy gap value obtained by us is in good experimental agreement with that quoted in the literature.[9]

The dashed curve on Fig. 2 represents the spectral response of the short-circuit photovoltaic current in the same junction for which the electroluminous spectrum has also been obtained. The photoelectric current flows in the direction opposite to that producing electroluminescence, while the photovoltage has the same polarity as that producing electroluminescence, in agreement with the cases of SiC and CdTe.[10] The analysis of the photocurrent spectral response is identical to that of Wysocki, Loferski, and Rappaport.[11] For $h\nu$ just greater than E_g, $\ln(Q_{\lambda max} - Q_\lambda)$ is plotted against α. This gives a straight line, whose slope, 10^{-2} cm, is a measure of the distance that the photons pass through GaP. The relatively rapid falloff of Q_λ at high energies indicates a carrier diffusion length very much shorter than 10^{-2} cm.[11]

The spectral radiance of the very same GaP rectifier during electroluminescence is also seen on Fig. 2. The radiation peaks at photon energies

of 2.20 ± 0.02 ev with a half-width of a few kT. This value is a few hundredths of an electron volt lower than the peak obtained from the van Roosbroeck-Shockley theory[2] using the calculated α's (derived from the Macfarlane-Roberts analysis), but agrees well with the peak obtained using the above-discussed additional low-energy absorption. It is interesting to note that a comparison of the high-energy side of the spectral curve of electroluminous emittance to the van Roosbroeck-Shockley theory indicates a photon travel through GaP of about 10^{-2} cm. This is in rather good agreement with the value obtained from the photocurrent vs $h\nu$ analysis. Some of the additional low-$h\nu$ emission is most likely due to defect sites mentioned above. These and self-absorption cause the peak to shift somewhat to lower energies.

We conclude that most of the electroluminescent phenomena on hand are quite distinct from those originating from recombinations via defect states as reported previously.[1,12] In all the latter cases the photon distribution peaks at energies lower than the energy gap value obtained from free carrier recombination electroluminescence reported in this Letter, or from the analysis of other optical data. Also in all defect center recombination cases a linear dependence of the light on current has been found. The agreement between the above-discussed characteristics of electroluminescence, optical absorption, and photoelectric response leads us to identify the electroluminescent phenomenon as one primarily due to band-to-band bimolecular transitions.

We have also seen bimolecular recombination kinetics for radiative transitions of carriers injected across a rectifying junction in indium phosphide. Braunstein[5] reported the presence of recombination radiation in InP at an energy close to the band gap. We have obtained the spectral distribution of this radiation. It is shown in Fig. 2. The position of the peak at 1.25 ev is in good agreement with the band gap values reported in the literature.[13]

The authors wish to express thanks to R. Braunstein, A. R. Moore, and J. I. Pankove for helpful discussions.

[1]E. E. Loebner and E. W. Poor, Jr., Bull. Am. Phys. Soc. 4, 45 (1959).
[2]W. van Roosbroeck and W. Shockley, Phys. Rev. 94, 1558 (1954).
[3]R. Newman, Phys. Rev. 91, 1313 (1953).
[4]P. Aigrain and C. Benoit à la Guillaume, J. phys. radium 17, 709 (1956); C. Benoit à la Guillaume, Compt. rend. 243, 704 (1956).
[5]J. R. Haynes and H. B. Briggs, Phys. Rev. 86, 647 (1952).
[6]Wolff, Keck, and Broder, Phys. Rev. 94, 753 (1954).
[7]O. W. Lossew, Physik. Z. 32, 692 (1931); L. Patrick, J. Appl. Phys. 28, 765 (1957); D. Ruecker, Z. angew. Phys. 10, 254 (1958).
[8]G. G. Macfarlane and V. Roberts, Phys. Rev. 97, 1714 (1955); 98, 1865 (1955).
[9]O. G. Folberth and F. Oswald, Z. Naturforsch. 9a, 1050 (1954).
[10]O. W. Lossew, Doklady Akad. Nauk S.S.S.R. 29, 363 (1940); O. Z. Van Doorn and D. de Nobel, Physica 22, 338 (1956).
[11]Wysocki, Loferski, and Rappaport, Signal Corps Engineering Laboratories Report, Fort Monmouth, New Jersey, 1958 (unpublished).
[12]Wolff, Hebert, and Broder, Semiconductors and Phosphors, edited by M. Schoen and H. Welker (Interscience Publishers, Inc., New York, 1958), p. 547.
[13]F. Oswald, Z. Naturforsch. 9a, 181 (1954); M. Glicksman, Bull. Am. Phys. Soc. 3, 120 (1958); R. Newman, Phys. Rev. 111, 1518 (1958).

ELECTRON SPIN RESONANCE EXPERIMENTS ON SHALLOW DONORS IN GERMANIUM

G. Feher, D. K. Wilson,* and E. A. Gere
Bell Telephone Laboratories, Murray Hill, New Jersey
(Received June 4, 1959)

Electron spin resonances on shallow donors in silicon have been studied by several authors.[1-3] In germanium there are various factors which make the observation of electron spin resonance signals more difficult and, so far, no resonances have been reported on shallow impurity states. The recent conflicting experimental results pertaining to the donor ground state in germanium[4,5] led us to reinvestigate the electron spin resonance behavior in this material. In the present Letter we wish to report on the observation of electron spin resonances from both bound and nonlocalized electrons in germanium. The results indicate that the ground state of the arsenic and phosphorus donors in germanium is a singlet.

The experiments were performed at temper-

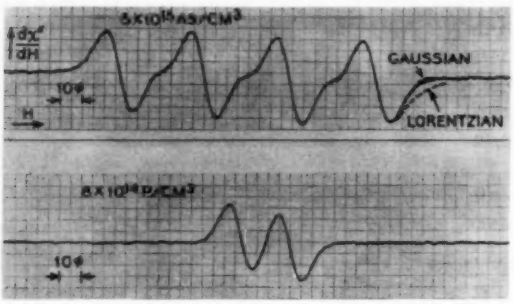

FIG. 1. Electron spin resonance signal from arsenic and phosphorus donors in germanium with the magnetic field H parallel to the [100] direction. $T \simeq 1.3°K$; $\nu_e \simeq 9000$ Mc/sec.

atures between 1.3°K and 4°K and microwave frequencies of ~9000 Mc/sec and ~24 000 Mc/sec. The details of the spectrometer have been described elsewhere.[6]

At low donor concentrations the electrons are localized on the impurity and a resolved hyperfine interaction with the donor nucleus is observed. This is illustrated for arsenic ($I = \frac{3}{2}$) and phosphorus ($I = \frac{1}{2}$) doped germanium in Fig. 1. The experimental results on the line width ΔH (full width between inflection points of $d\chi''/dH$), hyperfine splitting, and g values are summarized in Table I. The experiments on the arsenic-doped sample were repeated at 24 000 Mc/sec. The g value, ΔH (with H parallel to [100]), and hf splitting were found to be the same as at the lower frequency. For comparison purposes the data on silicon[1,3] are also listed in Table I.

The g shift in germanium is about two orders of magnitude larger than in silicon. It is proportional to $\lambda/\Delta E$, where λ is the spin-orbit coupling which in the valence band of germanium is an order of magnitude larger than in silicon and ΔE is the energy separation of the nearest bands that are admixed. The large observed g shift may have contributed to the fact that these lines have previously been missed.

The line widths quoted in Table I were obtained with H parallel to the [100] direction. When H deviates from this direction an appreciable line broadening occurs. This broadening together with the necessary small donor concentration in germanium makes the observation of the lines more difficult than in silicon. The broadening may arise, either from the anisotropic part of the hf interaction with the germanium nuclei or from a spread in g values due to a local perturbation of the donor wave function[7] (e.g., due to strains or overlaps). The observed Gaussian line shape is consistent with either picture. Experiments are under way to shed light on this question.

The magnitude of the hf splitting is about a factor of two smaller than in silicon. By a simple extrapolation of the theory of shallow donors in silicon due to Kohn and Luttinger,[8,9] one expects the hf splitting in germanium to be approximately an order of magnitude smaller than in silicon. This discrepancy with the experimental results is consistent with the large observed line width and indicates that the peaking of the conduction band wave functions at the nuclei is about

Table I. Summary of electron spin resonance data on phosphorus- and arsenic-doped germanium and silicon.[a,b] Because of different passage conditions[b] the line width in silicon has to be multiplied by 0.85 before comparing it to germanium.

Donor	Donor concentration (cm^{-3})	g value	Line width ΔH (oersteds)	Total hf splitting (oersteds)	$\lvert\psi(0)\rvert^2$ (cm^{-3})
		Germanium			
Phosphorus	8×10^{14}	1.5631 ± 0.0003	10	21	0.21×10^{24}
Arsenic	5×10^{15}	1.5701 ± 0.0003	11	107	0.87×10^{24}
		Silicon			
Phosphorus	1.5×10^{16}	1.99850	2.8	42	0.43×10^{24}
Arsenic	1.8×10^{16}	1.99837	3.2	212	1.73×10^{24}

[a]See reference 1.
[b]See reference 3.

a factor of six larger in germanium than in silicon. However, in deciding whether the singlet or the triplet is the lowest state only the presence of an appreciable isotropic hf interaction is important. Kohn and Luttinger[8,9] have shown that the ground-state wave function can be made up of a linear combination of four wave functions corresponding to the four minima of the conduction band. For three of these combinations (which form the degenerate triplet state) the value of the wave function at the origin is zero, and therefore cannot give rise to the observed isotropic hyperfine interaction. The singlet state is formed from a linear combination that has a finite value of $|\psi(0)|^2$ and should give rise to a hf splitting. The experimental observation of a splitting indicates therefore that the ground state is the singlet. The absolute amplitude of the signal and its variation with temperature excludes the possibility that one is observing an excited state.

At high donor concentrations[10] the electron is no longer localized on a particular impurity but moves throughout the crystal giving rise to a conduction process ("impurity band conduction") even at the lowest temperatures. Under these conditions the hyperfine interactions are averaged out and a single resonance line is observed.[11] The line width for such nonlocalized electrons in germanium is found to be anisotropic as illustrated in Fig. 2 which shows the results on a phosphorus-doped sample (10^{17} P/cm^3, $T = 1.3$°K, $\nu_e \simeq 9000$ Mc/sec). The width presumably arises from a spread in electronic g values which, in contrast to silicon,[11] are incompletely averaged out by motional narrowing.[12] An increase in temperature from 1.3°K to 4°K decreased the line width in the above phosphorus sample by ~10%. Similarly, an increase in the concentration from 3×10^{16} P/cm^3 to 10^{17} P/cm^3 decreased the line width in the [100] direction from 6 oersteds to 4 oersteds. These results and the observed Lorentzian line shape support the picture of a motionally narrowed line.[12]

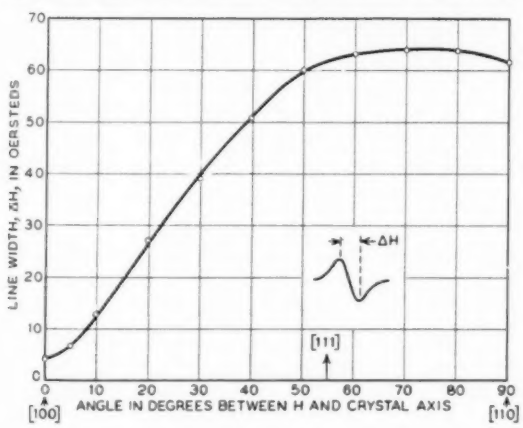

FIG. 2. Line width as a function of the orientation of the magnetic field with respect to the crystalline axes. $T \simeq 1.3$°K; $\nu_e \simeq 9000$ Mc/sec; 10^{17} P/cm^3. In this impurity concentration range one observes a single resonance line due to nonlocalized electrons.

The electronic g value of the nonlocalized electrons was found to be isotropic and approximately equal to the g value of the bound electrons (e.g., for 10^{17} P/cm^3, $g = 1.5636 \pm 0.0003$; and for 10^{17} As/cm^3, $g = 1.5698 \pm 0.0003$). This indicates that in this concentration of "impurity banding" the electron spends most of its time on the impurity.

Antimony-doped germanium was investigated in the concentration range between 10^{15} Sb/cm^3 and 3×10^{16} Sb/cm^3. The line shape was found to be extremely asymmetric and the g value varied between ~1.6 with H parallel to the [100] direction and 1.9 with H parallel to the [110] direction. This striking difference in behavior indicates that either the triplet-singlet levels overlap or that perhaps the triplet is lower in antimony. Strain experiments are in progress which should decide on this question.

We profited greatly from discussion with many members of the Bell Telephone Laboratories. In particular we wish to acknowledge the stimulating discussions with W. Kohn, P. W. Anderson, and G. Weinreich. We also wish to thank G. Bemski and J. Eisinger for their help in the 24000-Mc/sec experiment.

---

*This work was performed in partial fulfillment of the requirements for a Ph.D. degree from Rutgers University, New Brunswick, New Jersey.

[1]Fletcher, Yager, Pearson, Holden, and Merritt, Phys. Rev. 94, 1392 (1954); Fletcher, Yager, Pearson, and Merritt, Phys. Rev. 95, 844 (1954).

[2]A. Honig and A. F. Kip, Phys. Rev. 95, 1686 (1954).

[3]G. Feher, Phys. Rev. (to be published).

[4]Weinreich, Boyle, White, and Rogers, Phys. Rev. Letters 2, 96 (1959).

[5]H. Fritsche, Bull. Am. Phys. Soc. 4, 185 (1959).

[6]G. Feher, Bell System Tech. J. 26, 449 (1957).

[7]This would cause a mixing of the singlet and triplet states. However, in the [100] direction the four conduction band minima are equivalent and the mixing would not cause a broadening. This picture is consistent with the result that the narrowest line is ob-

served in the [100] direction.

[8]W. Kohn and J. Luttinger, Phys. Rev. 97, 883 (1955).

[9]W. Kohn, in Solid State Physics, edited by F. Seitz and D. Turnbull (Academic Press, New York, 1957), Vol. 5.

[10]In silicon this occurs at concentrations of the order of 10^{17}-10^{18} donors/cm^3. Because of the larger impurity Bohr radii in germanium, the corresponding concentrations are lower by between one and two orders of magnitude.

[11]In silicon this line was first observed by Portis, Kip, Kittel, and Brattain, Phys. Rev. 90, 988 (1953).

[12]P. W. Anderson and P. R. Weiss, Revs. Modern Phys. 25, 269 (1953).

ABSORPTION OF COMPRESSIONAL WAVES IN SOLIDS FROM 100 TO 1000 Mc/sec

J. Lamb, M. Redwood, and Z. Shteinshleifer
Electrical Engineering Department, Imperial College, London, England
(Received May 25, 1959)

We have determined the absorption of compressional waves in crystal quartz [X-direction], fused silica, germanium [100], and silicon [111]: the crystallographic directions specify the direction of propagation. Measurements were made by the "pulse technique" using guided waves in cylindrical specimens.[1-3] The dependence of the amplitude absorption coefficient on frequency is shown in Figs. 1-4.

In contrast to the findings of Granato and Truell and their co-workers[4-7] for germanium, we observed little difference between the absorption values for five crystals of silicon from different sources. These had dislocation densities—revealed by etch pits—from a few hundred to over 10^4 per cm^2. Two specimens were n-type with average resistivities of 0.1 and 14 ohm-cm, and three were p-type with resistivities of 3.20 and 30 ohm-cm. The axis of each cylinder was within 3° of the [111] direction. The absorption values in all five specimens agreed to within ±5%.

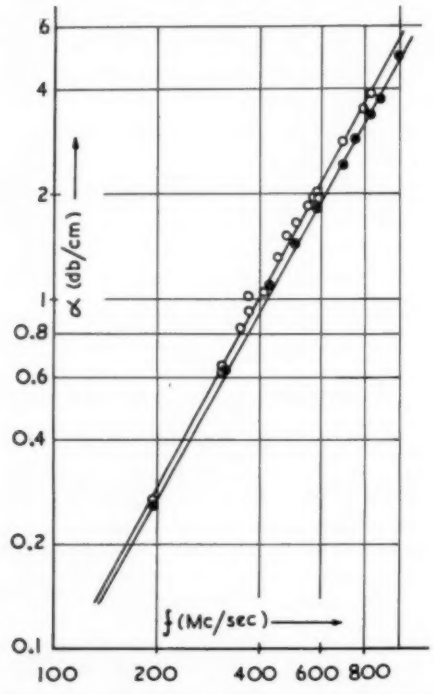

FIG. 1. Log(absorption coefficient) versus log(frequency) in crystal quartz. Propagation is along the X-axis. ○ = 20°C; ● = −77°C. At 20°C, α is proportional to $f^{1.82}$.

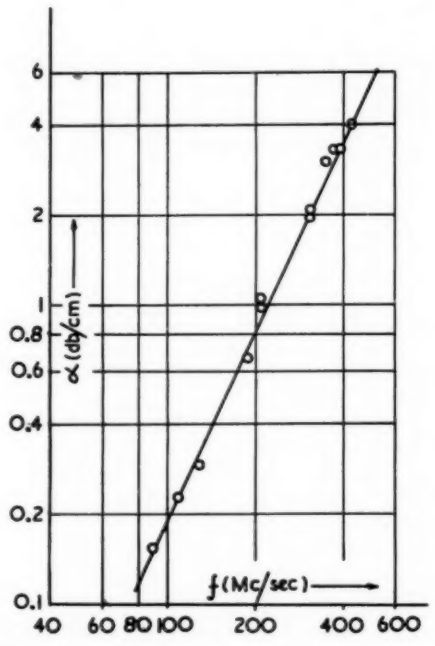

FIG. 2. Log(absorption coefficient) versus log(frequency) in fused silica (Thermal Syndicate, O.G. grade) at 18°C: α is proportional to $f^{2.12}$.

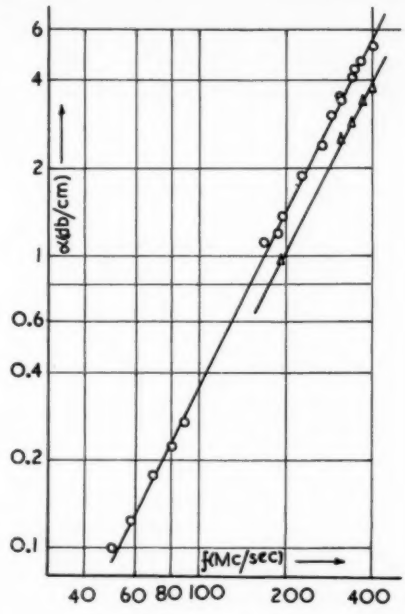

FIG. 3. Log(absorption coefficient) versus log(frequency) in germanium. Propagation is parallel to the [100] direction. o = 18°C; Δ = -158°C; the absorption is proportional to $f^{1.98}$ at 18°C.

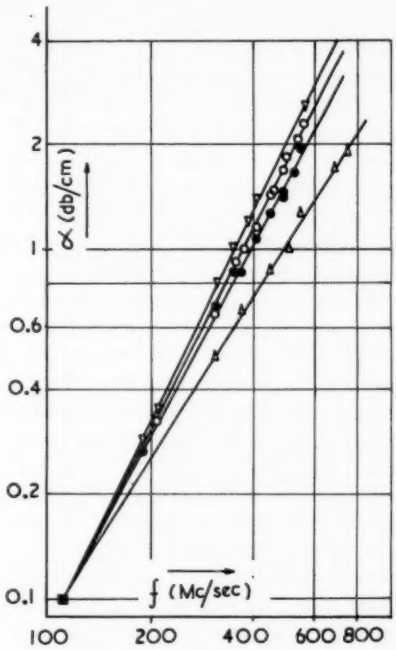

FIG. 4. Log(absorption coefficient) versus log(frequency) in silicon. Propagation is parallel to the [111] direction. ∇ = 197°C; o = 20°C; ● = -77°C; Δ = -158°C. At 197°C, α is proportional to $f^{2.0}$ and at -158°C to $f^{1.54}$.

Granato and Truell[6] found a wide range of absorption values in different specimens of germanium; their lowest values are close to, but slightly higher than, our values (Fig. 3).

At 20°C the absorption coefficient, α, for silicon and for germanium is approximately proportional to the square of the frequency. As a rough approximation, this is also true for crystal quartz and fused silica.

The values for crystal quartz at 1000 Mc/sec give quantitative support to estimates which have been made using other techniques.[8,9] We are continuing this work.

We wish to thank Mr. R. I. Walker of the Services Electronics Research Laboratory and Dr. K. Hoselitz of the Mullard Research Laboratory who supplied the crystals of silicon, and Mr. S. E. Bradshaw of the General Electric Company's Research Laboratory who provided crystals of germanium for this work.

[1]M. Redwood and J. Lamb, Proc. Inst. Elec. Engrs. B103, 773 (1956).
[2]M. Redwood, Proc. Phys. Soc. (London) B70, 721 (1957).
[3]M. Redwood, J. Acoust. Soc. Am. 31, 442 (1959).
[4]R. Truell and J. Bronzo, Phys. Rev. 90, 152 (1953).
[5]A. Granato and K. Lücke, J. Appl. Phys. 27, 583, 789 (1956).
[6]A. Granato and R. Truell, J. Appl. Phys. 27, 1219 (1956).
[7]Teutonico, Granato, and Truell, Phys. Rev. 103, 832 (1956).
[8]K. N. Baranskii, Doklady Akad. Nauk S.S.S.R., 114, 517 (1957) [translation: Soviet Phys. Doklady 2, 237 (1957)]; Akad. Nauk S.S.S.R. (Crystallography), 2, 299 (1957).
[9]H. E. Bömmel and K. Dransfeld, Phys. Rev. Letters 1, 234 (1958).

EFFECTS OF RARE EARTH IMPURITIES ON FERRIMAGNETIC RESONANCE IN YTTRIUM IRON GARNET

J. F. Dillon, Jr., and J. W. Nielsen
Bell Telephone Laboratories, Murray Hill, New Jersey
(Received June 11, 1959)

The first published ferrimagnetic resonance work on single-crystal yttrium iron garnet[1] (YIG) gave room-temperature line widths which were narrower than those observed for any other compound up to that time. However, the curve $\Delta H(T)$ showed a maximum at 40 or 50°K, and the variation of the field for resonance with crystal direction,[2] i.e., the surface $H_{res}(hkl)$, indicated that the anisotropy surface at liquid helium temperatures was convoluted beyond anything reported previously. Since then one of the authors (JFD)[3] and others[4] have observed much narrower lines and, associated with them, $\Delta H(T)$ curves[5] with much lower maxima which were, however, still near 50°K. These crystals did not show the wide excursions of $H_{res}(hkl)$ at low temperatures. In view of the clear possibility that these effects were caused by the presence of rare earth impurities, a series of YIG crystals doped with each of the rare earth ions were grown in order to identify experimentally the factors responsible for the line-width peak and the anomalous anisotropy. Recently Kittel[6] has considered theoretically the effect of rare earth ions on ferrimagnetic resonance in the rare earth garnets and in rare-earth-doped YIG. This paper gives an extract of the data obtained on YIG, containing small concentrations of rare earth ions. These show quite clearly that the line-width peak is at least predominantly a matter of rare earth impurities, that it is not always at 40 or 50°K, and that the anomalous anisotropy is associated also with the same impurities.

The crystals used were grown from flux. Highly polished spheres of 0.015- to 0.019-in. diameter made by the two-pipe technique[7] were mounted on sapphire rods with the [110] axes along the axis. The experiments were done near 9.3 and 24.0 kMc/sec using TE_{102} mode rectangular cavities in transmission. The high-frequency cavity was situated within a double Dewar. Data were obtained over a wide temperature range by boiling away the cryogenic liquid and allowing the cavity to warm at a rate determined by the heat leak. Temperature was measured with a thermocouple or a carbon resistance thermometer in contact with the wall of the cavity.

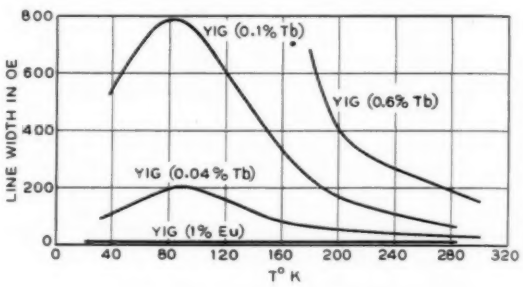

FIG. 1. Variation of ferrimagnetic resonance line width with temperature for several rare-earth-doped YIG crystals. Dopings are given in atomic percent on the figure. Line width is the field interval between points of half the maximum absorption. The data for YIG(0.6%Tb) were taken at 9.3 kMc/sec, the others at 24 kMc/sec.

The line widths were determined from recordings made of the absorption against magnetic field. All field measurements were made by nuclear magnetic resonance techniques.

Figure 1 shows the $\Delta H(T)$ curves for four different samples. We shall discuss in this Letter only two impurity ions, terbium and europium. We have introduced the terbium in three different concentrations.[8] Comparing the three YIG(Tb) samples, we see that the line width increases monotonically with terbium concentration. There is a pronounced peak in the line width at about 90°K for the YIG(0.04% Tb) and perhaps slightly lower for the YIG(0.1% Tb). The europium-doped sample serves as a demonstration of the very different effect encountered in introducing various rare earth ions. Whereas the ground state of Tb^{+++} is $^7F_6$, that of Eu^{+++} with its less than half-filled shell has the singlet ground state $^7F_0$. Since $J=0$, we might expect to a first approximation that the europium impurities will not contribute to the line width of the main iron resonance.

Figure 2 shows $H_{res}(hkl)$ in (110) for YIG(0.1% Tb) as well as for a nominally pure YIG made with a specially purified yttrium oxide. The former shows a surface even more convoluted than that reported before for a sample with unspeci-

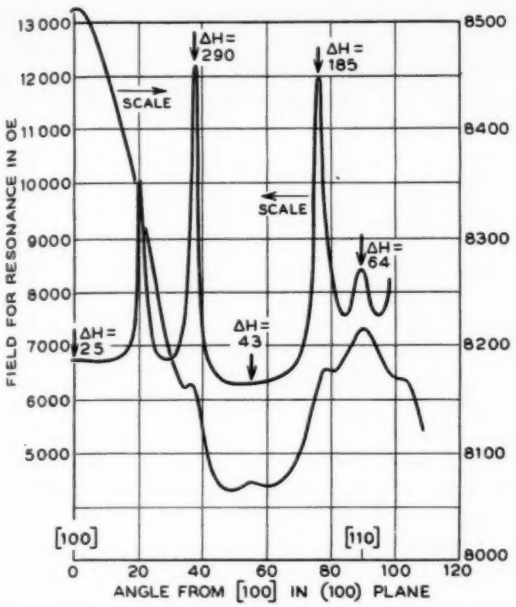

FIG. 2. Field for resonance at 1.5° K, against angle in the (110) plane for YIG free of intentional rare earth doping (scale at right, $f = 23\,192$ Mc/sec) as contrasted with the corresponding plot for YIG doped with 0.1% terbium (scale at left, $f = 22\,990$ Mc/sec). Line widths are given for several of the maxima and minima of the curve for the doped sample to show the line-width anisotropy.

fied impurities.[2] The curve for the YIG is grossly similar to that observed at room temperature, but there are a number extra peaks several degrees wide and perhaps forty oersteds high superimposed on the expected simple curve. It appears now that a number of the rare earth ions will have distinctive anisotropy and $H_{res}(hkl)$ surfaces associated with them. A comparison of the two curves of Fig. 2 suggests that one of the impurities in our YIG is terbium present in a concentration of a few parts in a million.

A. M. Clogston and L. R. Walker have joined one of the authors (JFD) in attacking the theoretical problem set by these plots and corresponding data on YIG doped with other rare earth ions.

A large anisotropy in line width is observed to be associated with the anomalous $H_{res}(hkl)$ surface. In the case of the YIG(0.1% Tb) at 1.5°K, several of these values are given on Fig. 2. Thus within a single crystal we have available a range of damping parameters.

These are being studied to gain an understanding of the physical processes involved in the damping associated with ferrimagnetic resonance.

We intend to describe in detail the effects of small concentrations of the other rare earth ions in YIG on $\Delta H(hkl)$, $H_{res}(hkl)$, and g, all as a function of temperature, in subsequent papers.

The authors acknowledge with thanks many discussions with A. M. Clogston, E. G. Spencer, and R. C. LeCraw. H. E. Earl provided valuable technical assistance.

---

[1]J. F. Dillon, Jr., Phys. Rev. 105, 759 (1957).
[2]J. F. Dillon, Jr., Phys. Rev. 111, 1476 (1958).
[3]J. F. Dillon, Jr., Bull. Am. Phys. Soc. 2, 128 (1957).
[4]Le Craw, Spencer, and Porter, Phys. Rev. 110, 1311 (1958).
[5]Spencer, Le Craw, and Clogston, following Letter [Phys. Rev. Letters 3, 32 (1959)].
[6]C. Kittel (to be published).
[7]W. L. Bond, Rev. Sci. Instr. 25, 401 (1954).
[8]The authors are grateful to K. Storks of these Laboratories for measuring the rare earth ion concentration in the samples by x-ray fluorescence analysis. These are used to label the curves on Fig. 1. The doping percentages used in this paper, e.g., YIG (X%), represent the atomic fraction $X/(X+Y)$ in YIG.

LOW-TEMPERATURE LINE-WIDTH MAXIMUM IN YTTRIUM IRON GARNET

E. G. Spencer, R. C. LeCraw, and A. M. Clogston
Bell Telephone Laboratories, Murray Hill, New Jersey
(Received June 11, 1959)

Measurements of the ferromagnetic resonance line-width maximum in single-crystal yttrium iron garnet (YIG) were previously reported by Dillon.[1] His data show that the line width increases with decreasing temperature, reaches a maximum below liquid nitrogen temperature, and decreases again to approximately the room-temperature value at liquid helium temperatures. We have been investigating the nature of this line-width maximum at low temperatures to determine if the effect is intrinsic to ferromagnetic resonance and to determine its origin. The line widths reported in this paper are determined from the absolute absorption of the sample and the saturation magnetization vs T curve measured on single-crystal YIG. The large effects on the line width ΔH at room temperature due to inhomogeneous broadening by scattering from pits on the surface of a YIG sphere were evaluated previously.[2] Consequently, we measured ΔH vs T for a series of three spheres prepared using polishing papers having mean grit sizes of 15, 5, and 0.3 microns, respectively. These measurements were made at 9300 Mc/sec. Figure 1 shows that the ratios of maximum line widths to room temperature line widths are 2.5, 4, and 13, respectively, the larger ratios occurring for the better polished spheres. It is also clearly shown that the contribution to the line width due to surface preparation is essentially additive over the temperature range. We conclude therefore that the low-temperature line-width maximum is an intrinsic property of the material and not of the surface. Further, if perfect polishing were attained the line-width maximum would still be approximately 6 oersteds in this sample.

Earlier investigations on the same samples[3] have shown a small but repeatable frequency dependence of line width at room temperature. The line width ΔH (full width between half maximum values) is 0.44 oersted at 3000 Mc/sec and 0.52 oersted at 9300 Mc/sec along the [111] axis. Taking these measurements over the temperature range, there are three essential features. See Fig. 2. The line width maximum at 3000 Mc/sec is reduced by 40% in magnitude and is shifted from 40°K to 30°K. Also it is seen that the room-temperature frequency dependence of

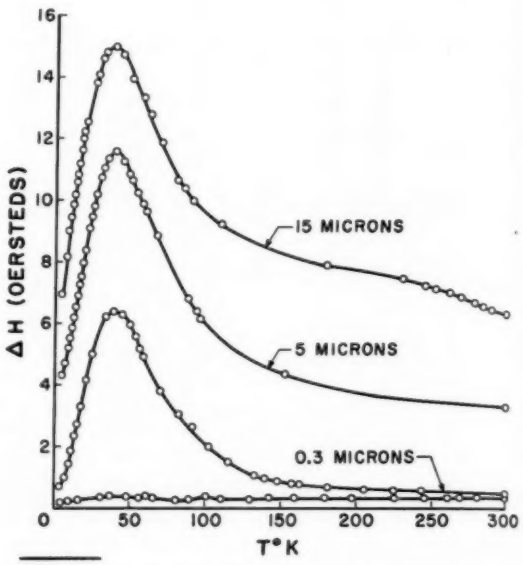

FIG. 1. ΔH vs T for single-crystal spheres of YIG 0.014 to 0.017 inch in diameter. H_{dc} oriented along the [111] axis. The labels on the curves indicate the mean grit size of the final polishing paper used to prepare the spheres. The lowest curve is Fig. 3 repeated here for comparison.

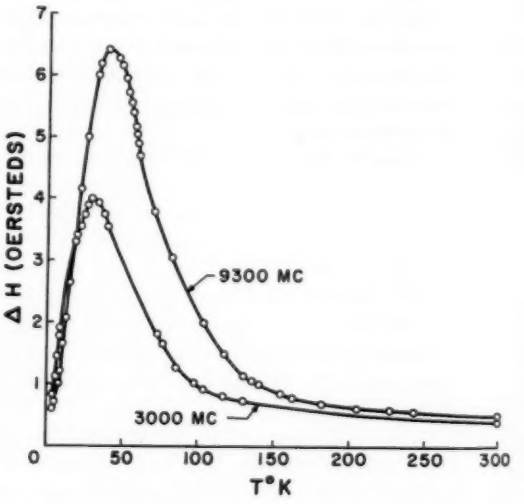

FIG. 2. ΔH vs T measured at 9300 and 3000 Mc/sec. H_{dc} oriented along the [111] axis.

line width is related to the mechanism of the low-temperature line-width maximum.

In considering the constituents that are used in growing[4] YIG, we recognized that the bulk yttrium oxide contains significant rare earth impurities. Further, the measured[5] spin-lattice relaxation times of the rare earth ions indicated that these ions could contribute strongly to the observed temperature variation of line widths in YIG. A detailed theory of this effect has been prepared by Kittel.[6]

The problem of purifying the yttrium oxide with respect to the rare earths was taken to Dr. Mark M. Woyski, of the Lindsay Chemical Division of the American Potash and Chemical Company. By using multiple exchange columns and by special processing against a small yield, he achieved at least a thousandfold reduction in the total rare earth content. The estimated total rare earth impurities are less than 0.1 part per million.

The results for YIG grown from the special purity yttrium oxide are given in Fig. 3 and for comparison superimposed on Fig. 1. It is seen that the rare earth contribution[7] to the ΔH maximum has been reduced from approximately 6 oersteds to slightly over 0.1 oersted, a ratio of about 50:1. It is tempting to identify the fine structure with individual rare earth ions, especially if we associate the peak at 100°K with Dillon and Nielsen's terbium line. Additional measurements will be needed to eliminate the possibility of other mechanisms, such as weakly interacting magnetostatic modes. An over-all feature of the data is the general decrease in line width from room temperature to liquid helium temperatures. This is the first time, to our knowledge, that this trend has been observed in ferromagnetic resonance. It is probable that the line width in this sample is limited by inhomogeneous broadening brought about by crystal imperfections, surface effects, and the rare earth ions near 4.2°K; and by thermal[3,8] processes at higher temperatures.

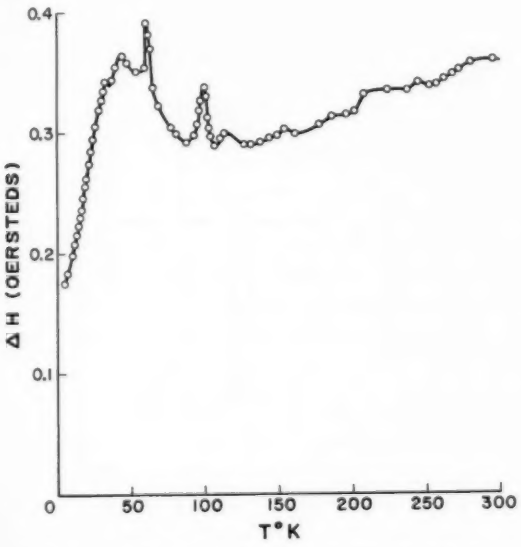

FIG. 3. ΔH vs T on a 0.020-inch diameter YIG sphere grown from yttrium oxide containing total rare earth impurities estimated to be less than 0.1 ppm. H_{dc} oriented along the [111] axis.

From the practical point of view it is interesting to note that $\mu''(\text{res}) = 14\,000$ at 4.2°K. From the theoretical point of view it can be expected that measurements on single-crystal YIG grown from such purity will yield more precise evaluation of the fundamental mechanism involved in spin-wave scattering and spin-lattice relaxation phenomena.

We should like to thank J. W. Nielsen for his advice through many discussions on the chemistry of garnets, and for his growing the garnets on which these data are based; J. F. Dillon for many helpful discussions; and H. E. D. Scovil for discussions on his measurements of rare earth relaxation.

[1]J. F. Dillon, Phys. Rev. 105, 759 (1957).

[2]LeCraw, Spencer, and Porter, Phys. Rev. 110, 1311 (1958).

[3]R. C. LeCraw and E. G. Spencer, J. Appl. Phys. 30, 185-S (1959).

[4]J. W. Nielsen, J. Appl. Phys. 29, 390 (1958); J. W. Nielsen and E. F. Dearborn, J. Phys. Chem. Solids 5, 202 (1958).

[5]B. Bleaney and H. E. D. Scovil, Proc. Phys. Soc. (London) A64, 204 (1951).

[6]C. Kittel, post-deadline paper 1959 Boston meeting of the American Physical Society; Phys. Rev. (to be published).

[7]J. F. Dillon and J. W. Nielsen in the preceding Letter [Phys. Rev. Letters 3, 30 (1959)] report on measurements in which deliberate amounts of specific rare earth ions have been added; this procedure allows them to measure effects due to particular ions.

[8]T. Kasuya, Progr. Theoret. Phys. (Kyoto) 12, 802 (1954).

OXIDES WHICH SHOW A METAL-TO-INSULATOR TRANSITION AT THE NEEL TEMPERATURE

F. J. Morin
Bell Telephone Laboratories, Murray Hill, New Jersey
(Received June 5, 1959)

In a previous paper[1] it was pointed out that the lower oxides of titanium and vanadium behave like metals. It was suggested that this was so because in the oxides at the beginning of the $3d$ series the nonbonding (t_{2g}) orbitals extend out far enough to overlap and form a narrow conduction band. It was also pointed out that polycrystalline samples of Ti_2O_3 and V_2O_3 appear to show a transition from metal to insulator at the Néel temperature. Now, this transition has been confirmed with single crystals of these oxides and also found to occur in the oxides VO and VO_2. This Letter reports electrical conductivity measurements made on polycrystalline TiO,[2] and on single crystals of Ti_2O_3,[3] VO, V_2O_3, and VO_2,[4] as additional evidence for the existence of a conduction band of t_{2g} orbitals, and suggests a model to explain the conductivity transitions which are found.

The single-crystal samples were 0.1 mm in size, too small for the usual four-point measurement, so two pressure contacts were used. Therefore, the absolute value of conductivity quoted is somewhat in doubt due to contact resistance and dimensional uncertainty. To obtain a Ti_2O_3 sample of suitable uniformity, a small fragment was broken from a large boule. It was unoriented. The vanadium oxide crystals were easily oriented from their growth habit. The TiO sample was a small rectangular bar and was measured by the four-point method.

Typical conductivity curves are shown in Fig. 1. In addition to these results, TiO was found to be a metal over the whole temperature range investigated: 300°K to 1.5°K. The transition temperatures from conductivity measurements are summarized in Table I and compared with those from heat capacity (C_p) and magnetic susceptibility (χ). In V_2O_3 and VO the transitions were very abrupt, with no measurable time or temperature dependence. In VO_2 and Ti_2O_3 the transitions were spread out over a range of temperature as shown in Table I, and some time dependence of conductivity was observed on cooling. Above the transition temperature, in the metallic state, all of the oxides showed a positive temperature coefficient of resistance typical of metals. If it is assumed that all the d electrons are available for transport in this state, the electron mobility lies approximately in the range 10^{-1} (TiO) to 10^{-2} (VO) cm²/volt sec indicative of a very narrow conduction band. Finding a hysteresis about the Néel transition seems a little unusual. It should be recalled, however, that C_p and χ measurements have been made most frequently only with increasing temperature. The C_p entries and the first two χ entries in Table I are of this kind and compare well with the transition temperature

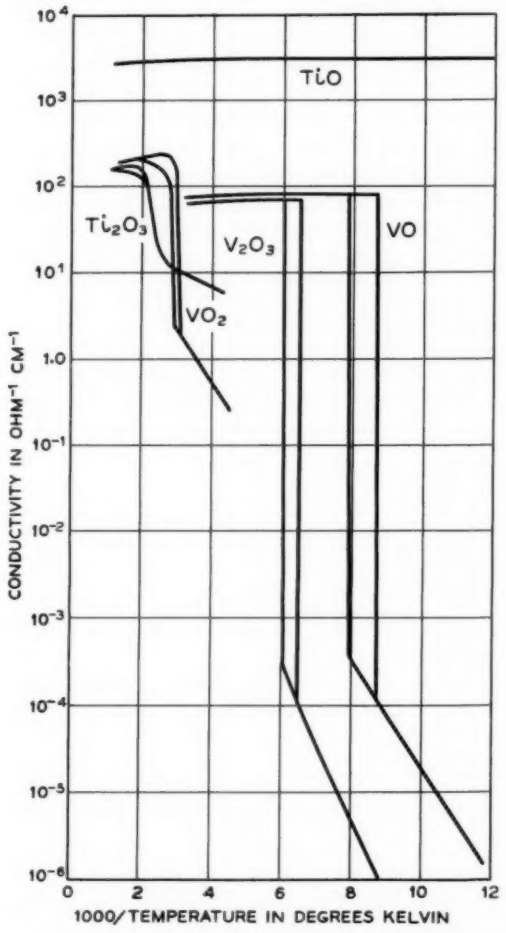

FIG. 1. Conductivity as a function of reciprocal temperature for the lower oxides of titanium and vanadium. Measurements were made along the [100] direction in VO, and along the c axis in V_2O_3 and VO_2.

Table I. Conductivity transition temperatures in degrees Kelvin are compared with Néel temperature from heat capacity, C_p, and magnetic susceptibility, χ.

Oxide	Structure	Conductivity cooling	Conductivity heating	C_p	χ
TiO	rock salt	...	...	...	...
VO	rock salt	114	126	...	...
V_2O_3	corundum	153	165	169[a]	168[b]
VO_2	monoclinic[c]	340-325	335-350	340[d]	340[e]
Ti_2O_3	corundum	500-400	400-500	473[f]	390-490[g]

[a]C. T. Anderson, J. Am. Chem. Soc. 58, 564 (1936).
[b]J. Wucher, J. recherches centre natl. recherche sci. Labs. Bellevue (Paris) 4, 254 (1952).
[c]Slightly distorted rutile structure; G. Andersson, Acta Chem. Scand. 10, 623 (1956).
[d]J. Jaffray and A. Dumas, J. recherches centre natl. recherche sci. Labs. Bellevue (Paris) 5, 360 (1953-54).
[e]E. Hoschek and W. Klemm, Z. anorg. u. allgem. Chem. 242, 63 (1939).
[f]B. F. Naylor, J. Am. Chem. Soc. 68, 1077 (1948).
[g]See reference 2.

measured by conductivity on heating. The last χ entry was measured both with heating and cooling and shows a hysteresis.[5]

In TiO and VO, which are rock salt structures, each cation is connected to its twelve nearest neighbor cations by overlapping t_{2g} orbitals. In the metallic state these orbitals constitute a partially filled band. This band contains six states per atom and is one third full in TiO and one half full in VO. Let the crystal become an antiferromagnet with the spin alignment reversing between (111) planes of cations as found in NiO for example. Then electrons on one half of the nearest neighbors have spin up and on the other half have spin down. Thus the band is split into two sets of bands, one set for spin up and one set for spin down. In VO each set of bands contains three lower states per atom which are full and three higher states per atom which are empty. Thus VO is an insulator below the transition temperature. In TiO the lower bands are only two thirds filled so TiO shows no transition to an insulator. This model is similar to one suggested by Slater[6] for MnO, in which each set of bands contains five lower states per atom which are filled and five higher states per atom which are empty. However, in MnO the t_{2g} orbitals do not overlap, the band width is zero, and the crystal is an insulator both above and below the transition.

The situation in the remaining oxides is much more complicated for reasons of structure and also because the transition in conductivity occurs even though the t_{2g} orbitals are partially empty. A more general point of view has been suggested by Anderson[7] and is based on the observation that antiferromagnets which involve indirect exchange are insulators. It is suggested that there are two processes in competition: (1) the correlation effect which tends to localize the d electrons and which is aided by setting the cation spins in an antiferromagnetic alignment; (2) the tendency of electrons to delocalize themselves by spreading into a band and thereby gaining kinetic energy. That these two processes are fairly energetic is indicated by the conductivity change of a factor 10^6 in VO and V_2O_3 at the transition. A splitting of the conduction band by ~ 0.4 ev is required to produce this amount of change in the carrier concentration. This may be compared with the energy of the Néel temperature which is only ~ 0.01 ev and which may represent the energy difference between the two competing processes. This more general point of view also offers an alternative explanation for the difference between TiO and VO. The electron mobility in TiO is ten times that in VO. This suggests that the conduction band is much wider in TiO so the electrons gain enough kinetic energy on spreading into it that the metallic state is always lower in energy than the antiferromagnetic state. The transition in all of the oxides can be described by a partially filled band which splits into an upper band which is empty and a set of lower occupied levels which are localized and have an antiferromagnetic spin alignment.

[1]F. J. Morin, Bell System Tech. J. 37, 1047 (1958).

[2]Sample obtained from A. D. Pearson and described in J. Phys. Chem. Solids 5, 316 (1958).

[3]Sample obtained from Linde Company.

[4]Crystals of the vanadium oxides were grown by H. Guggenheim by the hydrothermal process.

[5]Additional evidence was obtained that a hysteresis at the Néel transition is not unusual. With R. G. Shulman the nuclear magnetic resonance of Co^{59} in CoO was measured with slow warming and cooling about T_N. The transition was gradual, and on cooling appeared to occur several °K below the warming transition.

[6]J. C. Slater, Handbuch der Physik (Springer-Verlag, Berlin, 1956), Vol. 19.

[7]P. W. Anderson, Phys. Rev. (to be published) and private communication.

MULTILEVEL PULSED-FIELD MASER FOR GENERATION OF HIGH FREQUENCIES*

S. Foner, L. R. Momo, and A. Mayer†
Lincoln Laboratory, Massachusetts Institute of Technology, Lexington, Massachusetts
(Received June 1, 1959)

A proposed[1,2] multilevel pulsed-field ruby maser has been successfully operated at 4.2°K as an oscillator at both 12.61 kMc/sec and 19.15 kMc/sec with a pumping frequency of 12.61 kMc/sec. The results demonstrate the feasibility of generating or amplifying very high frequencies on a pulsed basis by conversion of magnetic field energy, supplied to an inverted spin distribution, into coherent radiation. The principles of operation and characteristics of the maser, and field dependence of spin-lattice relaxation time are discussed.

The pertinent transitions and the energy level diagram of Cr^{3+} in Al_2O_3 for applied fields perpendicular to the c axis[3] are shown in Fig. 1. For simplicity, the $\Delta M=2$ transition between levels 1 and 3 is saturated[4] at a pump frequency $\nu_3=\nu_1+\nu_2$, corresponding to a fixed dc bias field, H_0, above any field where cross relaxation effects[5] may occur, such as at ν_5. The cw three-level maser[6] would operate at $\nu_2 \ll \nu_3$, when $H=H_0$, with an inverted spin population between levels 2 and 1. If H is now increased to H_i in a time short compared to the spin-lattice relaxation time, oscillation or amplification should be obtainable at any frequency $\nu_i > \nu_2$ for which suitable maser cavity resonances occur. A gain of energy in the ratio of ν_i/ν_2 over the continuous three-level maser is obtained at the expense of energy extracted from the pulsed magnetic field. Wavelengths of about 1 mm would be generated at a field of 100 kilo-oersteds.

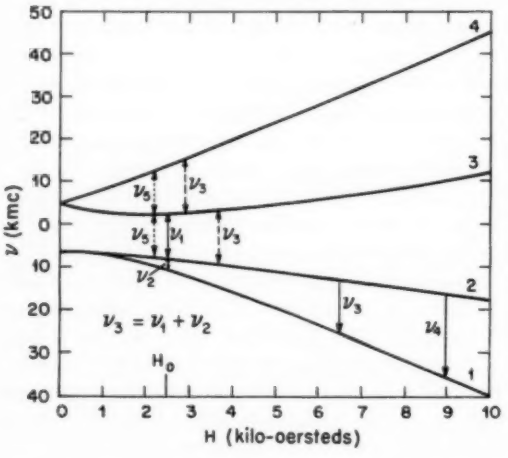

FIG. 1. Energy level diagram for Cr^{3+} in Al_2O_3 with applied field perpendicular to c axis. Operating points for pumping at $\nu_3=\nu_1+\nu_2$, and emission at ν_3 and ν_4 are indicated.

The maser reflection cavity, a solid rectangular parallelpiped of ruby,[7] was designed with the two lowest modes (TE_{101} and TE_{102}) occurring at ν_3 = 12.61 kMc/sec and ν_4 = 19.15 kMc/sec, respectively, with undercoupled loaded cavity Q's of about 2000 and 4800, respectively. The pump power and radiated energy were transmitted to and from the single cavity coupling iris by a tapered dielectric transition section attached to K_u-band waveguide. Both the dielectric transition and cavity were coated with a 0.001-in. silver plating in order to assure uniform penetration of the pulsed magnetic field throughout the cavity volume. The pulsed field, H_p, was generated in a solenoid (13 cm length, 7 cm i.d.) by discharge of a 2000-μf variable voltage capacitor bank.[8] A peak field of 9.4 kilo-oersteds was obtained at 1000 volts with a half-period of about 3 milliseconds [see Figs. 2(A), 2(B)]. The maser cavity assembly and surrounding glass Dewars were inserted in the solenoid, and the entire assembly was fixed between the pole faces of an electro-

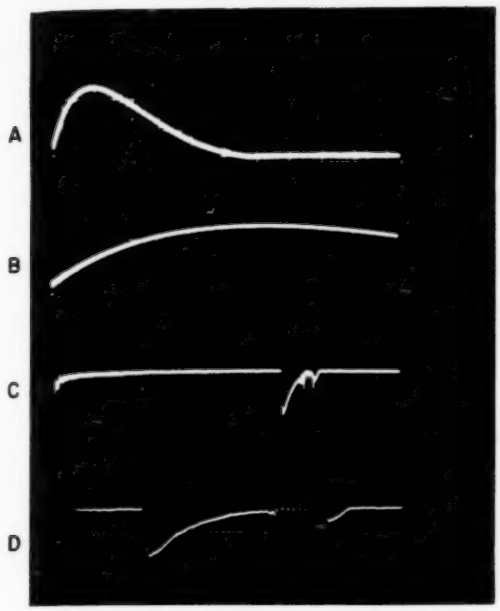

FIG. 2. Oscillograms of pulsed-field maser operation at 4.2°K. (A) Pulsed magnetic field versus time—horizontal time scale 500 μsec/cm. (B) Pulsed magnetic field versus time—horizontal time scale 100 μsec/cm. (C) Envelope detector output showing 19.15-kMc/sec emission of pulsed-field maser—horizontal scale 100 μsec/cm. Emission is obtained during both rise and decay of field pulse. (D) 19.15-kMc/sec emission—horizontal time scale expanded to 20 μsec/cm. An intense burst of radiation occurs at the onset of emission, accounting for the short blank portion of the oscillogram.

magnet. The field orientations were: H_{rf} perpendicular to the c axis, and H_0 perpendicular to both the c axis and to H_p. The mutually orthogonal orientation of H_0, H_p, and the c axis assured that the resultant H was always greater than H_0, and furthermore, that H always remained perpendicular to the c axis. The field dependence of the energy levels therefore remained as indicated in Fig. 1.

The pumping power was gated off within 50 μsec of the start of the pulsed field rise, and oscillations were observed at either ν_3 or ν_4 during the traversal of H_p through the appropriate resonance. Within the accuracy of the pulsed field measurement, emission occurred as predicted from Fig. 1. When the pump power was not turned off, population redistribution between levels 4-3 and 3-2 was observed (see Fig. 1). Typical oscillation characteristics at 4.2°K for the ν_4 mode are shown in Figs. 2(C) and 2(D). The expanded scale of Fig. 2(D) shows the pulsating character[9] of the oscillations, and the sensitive dependence of the emission pulses on the particular magnetic field sweep rate. The number of pulses and total energy output could be controlled by varying the pulsed-field sweep rate—the more rapid traversals resulted in lower peak output, and for a sufficiently fast rise time, no oscillations were observed. In this way it was possible to avoid emission at ν_3 completely, and yet obtain ν_4 emission at the peak of the pulsed field. When only a small portion of the inverted spin system radiated at ν_4, further emission at ν_3 was observed during the field decay. The peak power output at ν_4 was greater than 300 μw, and the integrated output energy for a typical case, e.g., Fig. 2(D), was greater than 0.04 erg. In both cases measurements were made of energy arriving at the crystal detector. Calculations show that a total energy of about 2 ergs would be available in the cavity if complete saturation between levels 1-3 were obtained, and if cavity losses and the spin-lattice relaxation were neglected. A considerable increase in efficiency is expected from an optimized microwave system.

Operation of this particular pulsed field maser would be limited to low magnetic fields if the spin-lattice time varied inversely as some large power of the magnetic field.[10] Measurements of spin-lattice relaxation time in ruby[11] at 4.2°K combined with the present results at ν_4 indicate that such a dependence is not yet dominant. Results of experiments as a function of temperature and field will be presented elsewhere.

An alternate scheme of multiple pumping[1,12] would circumvent most of the spin-lattice time field dependency, and would minimize requirements on the pulsed field system. Spin inversion with $\Delta M = 1$ transitions between levels 1-2, 2-3, and 3-4 in that order may be attained with a relatively small pulsed magnetic field at a reasonable pump frequency ν_j. With appropriate orientations of H_0 and H_p, and with a suitable maser material of large zero-field splitting, emission at a $\Delta M = 2$ or $\Delta M = 3$ transition with $\nu_i \approx 3\nu_j$ would then permit generation and/or detection and amplification at millimeter wavelengths on a pulsed basis with a rather simple arrangement. For instance, 10^{19} spins radiating at 300 kMc/sec

with a repetition rate of only 10 per second would yield an average power of 20 milliwatts—a power somewhat above that presently available (considerably less than 1 μw). If multiple pumping could be employed, pulsed fields of the order of a kilo-oersted would be sufficient.

We are indebted to B. Feldman and J. J. Kelley for valuable assistance, and to Dr. R. H. Kingston, Dr. H. J. Zeiger, and Dr. S. H. Autler for informative discussions.

---

*The work reported in this paper was performed at Lincoln Laboratory, a center for research operated by Massachusetts Institute of Technology with the joint support of the U. S. Army, Navy, and Air Force.

†Present address: Convair, San Diego, California.

[1]S. Foner, Colloque International de Magnétisme de Grenoble, July 2-6, 1958, Contribution No. 32 [J. phys. radium 20, 336 (1959)], and Lincoln Laboratory Quarterly Progress Reports, February 1, 1958 et seq. (unpublished).

[2]An alternate proposal has recently been made by R. H. Hoskins, J. Appl. Phys. 30, 797 (1959).

[3]The energy level diagram is shown for $D<0$ as indicated by recent measurements of Geusic, Peter, and Schulz-du Bois, Bell System Tech. J. 38, 291 (1959).

[4]In principle $\Delta M=3$ pumping may be feasible, and/or spin inversion by a 180 degree pulse or adiabatic fast passage may be employed for higher efficiency.

[5]Bloembergen, Shapiro, Pershan, and Artman, Phys. Rev. 113, 445 (1959).

[6]N. Bloembergen, Phys. Rev. 104, 324 (1956).

[7]Pink ruby (nominally 0.1% Cr^{3+}) supplied by Linde Air Products Company.

[8]S. Foner and H. H. Kolm, Rev. Sci. Instr. 28, 799 (1957).

[9]Makhov, Kikuchi, Lambe, and Terhune, Phys. Rev. 109, 1399 (1958).

[10]A. H. Cooke, Reports on Progress in Physics (The Physical Society, London, 1950), Vol. 13, p. 276.

[11]Kikuchi, Lambe, Makhov, and Terhune, Project Michigan Report No. 2144-377-T, March, 1959 (unpublished).

[12]A similar proposal has recently been made by A. E. Siegman and R. J. Morris, Phys. Rev. Letters 2, 302 (1959).

SMEKAL-RAMAN TYPE MODIFIED X-RAY SCATTERING

K. Das Gupta*
Department of Physics and Astronomy, Ohio State University, Columbus, Ohio
(Received June 4, 1959)

The spectroscopic analysis of x-ray beams, scattered from some low atomic number elements, viz., carbon, beryllium, and aluminium, made with the help of the two-crystal spectrometer, multicrystal spectrograph, and focusing spectrograph by DuMond,[1] Bearden,[2] Gingrich,[3] Ehrenberg,[4] and a few others, verified the existence of Rayleigh (unchanged frequency) and Compton scattering but could not detect the existence of the phenomenon of the partial absorption of photons of Smekal-Raman type.

With scatterer carbon and a monochromatic incident x-ray beam of energy $h\nu$, the frequency ν' of the modified line of Smekal-Raman type can be calculated from the equation $h\nu'=h\nu-\delta E$, where δE in a typical process will correspond to the energy difference between the initial ($1s^2 2s^2 2p^2$) and the final ($1s^1 2s^2 2p^3$) state of the carbon atom. The value of δE for the element carbon as obtained from the x-ray K-absorption data is 282.2 ev and the wavelengths of the Smekal-Raman type modified lines due to incident copper and molybdenum radiations, viz. (1) Cu $K\alpha_1=1537.4$, (2) Cu $K\alpha_2=1541.2$, (3) Cu $K\beta_1=1389.4$, (4) Mo $K\alpha_1=707.8$, (5) Mo $K\alpha_2=712.1$, and (6) Mo $K\beta_1=630.98$ xu (Siegbahn x units), will be (1) 1593.3, (2) 1597.4, (3) 1434.9, (4) 719.5, (5) 723.9, and (6) 640.2 xu, respectively.

With the help of a bent mica ($d=2.554$ A) Cauchois spectrograph (diameter of the focal circle = 9 inches) and also a bent quartz ($d=1.178$ A) spectrograph (diameter of the focal circle = 5.5 inches) and using $K\alpha$ and $K\beta$ radiations of copper and molybdenum from the sealed-off x-ray tubes, with graphite (reactor quality), polystyrene (for carbon), and beryllium as scattering specimens, the modified lines of Smekal-Raman type have been observed in calculated positions using both the spectrographs for each of the scattering specimens. Figures 1 and 2 are the tracings of the original microphotometer records, clearly showing (1) Rayleigh lines, (2) Compton bands, and (3) Smekal-Raman type of modified lines in x-ray scattering.

The sealed-off x-ray tubes (Matchlett) were run at 12 to 15 ma at 40 kv and the period of exposure

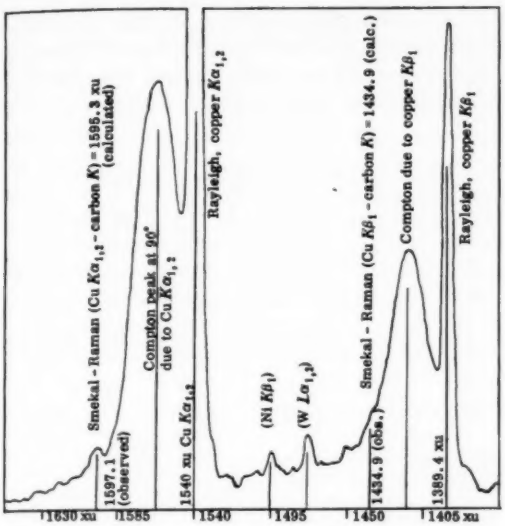

FIG. 1. Spectroscopic analysis of Cu target radiation scattered at ~90° by polystyrene with the help of the bent mica Cauchois spectrograph. The photometer record clearly shows (1) Rayleigh lines, viz., Cu $K\alpha_{1,2}$ and $K\beta_1$; (2) Compton bands due to $K\alpha_{1,2}$ and $K\beta_1$; (3) modified Smekal-Raman lines due to Cu $K\alpha_{1,2}$ and $K\beta_1$. Dispersion on the film = 21.6 xu/mm. The $K\alpha_{1,2}$ lines are not resolved.

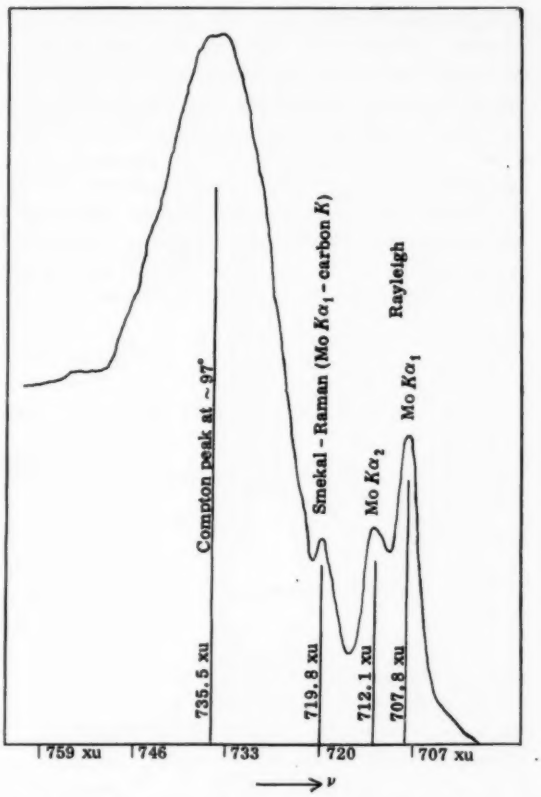

FIG. 2. Spectroscopic analysis of Mo target radiation scattered at ~97° by graphite, with the bent quartz Cauchois spectrograph. The photometer record shows clearly (1) Rayleigh lines, viz., Mo $K\alpha_1$ and $K\alpha_2$, (2) strong Compton band, and (3) the modified Smekal-Raman line due to Mo $K\alpha_1$; that due to $K\alpha_2$ overlaps with the short-wavelength end of the Compton band and is just visible in the original negative. The dispersion as measured in the original negative = 16.1 xu/mm.

varied between 100 and 150 hours. The target radiations from both copper and molybdenum were spectroscopically analyzed by giving prolonged exposures, and, only in the case of the copper target tube, $K\alpha$ lines of nickel and $L\alpha$ of tungsten appeared in the spectrum. The molybdenum target was, however, free from any such surface contamination of nickel and tungsten. The scattered radiation from graphite and polystyrene has been studied at scattering angles of approximately 90° (Fig. 1) and 97° (Fig. 2). The effective width of the bent crystal was about 6 mm and the slit in between the scatterer and the bent crystal is made of pure copper which allowed a beam of 6 mm×4 mm. The approximate distance between the scatterer and the focal spot of the target is about 1.5 inches. The effective irradiated area of the piece of graphite of 5 mm thickness is 1 cm×6 mm. The piece of graphite was kept at 45° to the direction of the incident beam. The scattering experiments with carbon and with beryllium have been done by keeping the spectrograph setting exactly the same, only the piece of graphite is replaced by a similar piece of beryllium. The observed modified lines due to carbon appeared at 282-ev gap and that due to beryllium at 116-ev gap on the low-energy side of the primary $K\alpha$ of copper or of molybdenum. The preliminary experiments made with the samples of extra pure magnesium and aluminium as scatterers, at different setting angles of the spectrograph, confirmed beyond doubt that the modified lines due to graphite, polystyrene, and beryllium appearing at the calculated positions cannot be due to any impurities either in the target or in the sample.

Although modified lines have been obtained with

different scatterers, viz., Be, C (graphite, polystyrene, apiezon oil), Mg, Al, Cu, and Fe at calculated positions, most of them are, however, extremely weak in intensity and it has not been possible to take their microphotometer records. It is hoped that by using the high light gathering power spectrograph, high contrast films, strong x-ray sources, and selecting suitable angles of scattering so as to have the minimum background due to the tail of the Compton band or the higher order Bragg reflections due to the white part of the target radiation, it will be possible to study, from this newly observed modified scattering, the term values of the elements and also the energy levels of the solid state.

---

* Permanent address: Department of Physics, University of Calcutta, Calcutta, India.

[1] J. W. M. DuMond, Phys. Rev. 37, 136 (1931).
[2] J. A. Bearden, Phys. Rev. 36, 791 (1930).
[3] N. S. Gingrich, Phys. Rev. 36, 1050 (1930).
[4] W. Ehrenberg, Z. Physik 53, 234 (1929).

GROUND STATE Λ-DOUBLING TRANSITIONS OF OH RADICAL*

G. Ehrenstein and C. H. Townes
Department of Physics, Columbia University, New York, New York

and

M. J. Stevenson
Research Laboratory, International Business Machines Corporation, Poughkeepsie, New York

(Received June 4, 1959)

One of the molecules whose presence in interstellar space may be detectable by means of its radio-frequency spectrum is the OH radical.[1] Attempts at observing it with radio telescopes have been unsuccessful thus far.[2] To make future searches more fruitful, frequencies of the appropriate absorption lines were measured in the laboratory with a Zeeman-modulated spectrometer.

For OH, at temperatures prevailing in interstellar space, only the lowest rotational state ($J=\frac{3}{2}$) of the $^2\Pi_{3/2}$ electronic state will be appreciably populated. This lowest energy level is split by Λ doubling into two levels 1666.4 Mc/sec apart. Each of the two Λ-doublet levels is split further by hyperfine interactions with the hydrogen nucleus, so that the spectrum consists of four absorption lines. The two stronger transitions, having no change in the total angular momentum $F(\Delta F=0)$, were measured and their frequencies are given in Table I together with frequencies calculated from expressions given by Dousmanis, Sanders, and Townes.[3] According to theory, the intensity ratio between the $F=2\leftarrow F=2$ and $F=1\leftarrow F=1$ transitions should be 9:5, and this was verified experimentally. Substantially the same ratio should prevail in interstellar space. The transitions with $\Delta F=\pm 1$ are expected to be about ten times weaker and have not been observed as yet.

Table I. Observed and calculated frequencies for Λ-doubling transitions in $J=\frac{3}{2}$ rotational state of $^2\Pi_{3/2}$ electronic state of OH radical.

Hyperfine transition	Experimental frequency (Mc/sec)	Calculated frequency (Mc/sec)
$F=2\leftarrow F=2$	1667.34 ± 0.03	1666.5
$F=1\leftarrow F=1$	1665.46 ± 0.10	1664.6

OH radicals were produced outside the absorption cell by an electrodeless radio-frequency discharge.[3] The microwave spectrometer was conventional in design except for the Zeeman-modulation technique. The absorption cell was a glass-lined, coaxial waveguide about $2\frac{1}{2}$ feet long and $1\frac{1}{4}$ inches in diameter. This coaxial cell was used both to propagate low-frequency microwave power and to provide Zeeman modulation. The modulating magnetic field was obtained by passing a large current through the center rod and back along the outer conductor. This produces a magnetic field between the two conductors which ideally does not extend outside the waveguide. The very small leakage fields which were obtained produced only very low pickup in the detecting circuits, whereas the pickup was quite troublesome when a conventional solenoid was wound around the

waveguide and used for Zeeman modulation. The modulating current consists of a 100-kc/sec sine wave current superimposed on a direct current, in such ratio that the minimum of the sin wave corresponds to zero current. With a modulator whose maximum output was 25 peak-to-peak amperes, adequate modulation fields were obtained for both $^2\Pi_{1/2}$ and $^2\Pi_{3/2}$ states of OH. This technique for Zeeman modulation can also be applied to a standard Stark cell with the Stark septum acting as the center conductor.

The authors wish to thank the Sperry Gyroscope Company and Professor Yardley Beers for lending us klystron tubes used in these measurements.

*This work is supported jointly by the U. S. Army Signal Corps, the Office of Naval Research, and the Air Force Office of Scientific Research.

[1]C. H. Townes, International Astronomical Union Symposium (Cambridge University Press, Cambridge, 1957), No. 4, p. 92; A. H. Barrett, Proc. Inst. Radio Engrs. 46, 250 (1958).

[2]A. H. Barrett and A. E. Lilley, Astron. J. 62, 5 (1957).

[3]Dousmanis, Sanders, and Townes, Phys. Rev. 100, 1735 (1955).

EVIDENCE FOR SHELL-MODEL STATES IN Sc^{41}†

C. M. Class, R. H. Davis,* and J. H. Johnson
The Rice Institute, Houston, Texas
(Received April 6, 1959)

The excited states of the mirror nuclei Ca^{41} and Sc^{41} are of considerable interest because of the possibilities they present for testing the predictions of the shell model under quite favorable circumstances. According to this model, the ground states of these nuclei are described by single particles in the $f_{7/2}$ shell outside a Ca^{40} core described by closed $(1s)^4(1p)^{12}(1d, 2s)^{24}$ shells. Single-particle excited states are predicted approximately in the order $p_{3/2}$, $p_{1/2}$, $f_{5/2}$, $g_{9/2}$, $d_{3/2}$, and $g_{7/2}$. In addition, states of more complex character are expected due to the excitation of nucleons from the Ca^{40} core.[1] These states should be bound in the case of Ca^{41} for which the separation energy of a neutron is 8.37 Mev, while for Sc^{41} they are expected to be unbound since the separation energy for a proton is only 1.63 Mev.[2] Whether or not the difference in the binding of the states has an important effect on their ordering is unclear.

The experimental evidence supporting the existence of the single-particle states is rather scant and comes for the most part from the $Ca^{40}(d, p)Ca^{41}$ reaction.[3] By application of stripping theory to the angular distributions of the resolved proton groups, it is possible to assign the orbital angular momenta of the captured neutrons and by a comparison of the relative cross sections at the maxima of the angular distributions, a distinction can be made between states of mainly single-particle character and those of more complex character. On this basis, the $p_{3/2}$ and $p_{1/2}$ levels have been tentatively assigned at energies of 1.947 and 3.950 Mev, respectively.[4] Seven other levels between 2 and 4 Mev have been assigned l values ($l \leq 2$), but none of these are formed with sufficient intensity to suggest possible single-particle character. In addition, thirteen states in this interval have been located which show no stripping maxima. The data available on the states of Sc^{41} are less complete. States formed by $l=1$ protons in the $Ca^{40}(d, n)Sc^{41}$ reaction have been reported at excitation energies of 1.86 and 2.07 Mev,[5] one of which by analogy with Ca^{41} is probably the $p_{3/2}$ single-particle state. Levels at 2.25 and 3.44 Mev are known from (p, γ) measurements,[6] and at energies above 6 Mev a number of states have been located by the study of the $Ca^{40}(p, p'e^{\pm})Ca^{40}$ reaction.[7]

In the work reported here, additions to the body of information available on Sc^{41} have been made by studying the elastic scattering of protons from Ca^{40}.[8] As is well known, when elastic scattering measurements are made with good resolution, one is able not only to locate excited states of the compound system but also to make spin and parity assignments for the states by an analysis of the resonance shapes. This analysis is much simplified when, as in the case at hand, the target nucleus has zero spin.[9] Another feature of interest in this case results from the low excitation energy with which Sc^{41} can be formed, which enables one to examine much of the energy interval relevant to shell-model considerations.

The details of the experimental method and the complete analysis of the results will be published elsewhere.[10] To summarize briefly the essential points here, the measurements were carried out at bombarding energies between 1.2 and 5.5 Mev, corresponding to excitation energies in Sc^{41} between 2.8 and 7 Mev. The region below an excitation energy of about 2.8 Mev was inaccessible because of the weak penetration of the Coulomb barrier by low-energy protons. The protons, scattered from thin (~2 kev) Ca targets evaporated onto 100-$\mu g/cm^2$ thick carbon foils, were detected at 90, 125, and 150 degrees with respect to the beam direction by a CsI crystal spectrometer which satisfactorily resolved the elastic groups from calcium and carbon. The shapes of the resonances were analyzed by application of dispersion theory, aided by the use of an electronic computer.[11] Essentially unambiguous assignments of the l values of the protons forming forty-two states were made as a result of this analysis, and it was possible to make j-value assignments to about twenty states with considerable certainty. In addition to $l(j)$ and π, the widths of the levels were also obtained from the analysis after suitable corrections were made for the effects of finite target thickness and energy spread of the beam. The Γ's so obtained needed no correction for effects of competing reactions in this case since the (p, p) process is the only particle reaction which occurs until a bombarding energy of about 5 Mev is reached, when the (p, p') reaction develops. The (p, γ) partial width is assumed negligible. From knowledge of the Γ and the l value of a state, the reduced width γ^2, given by $\gamma^2 = \Gamma/2kRP_l$, is readily obtained, where P_l is the penetrability of a proton having angular momentum l, k is its wave number, and R is the nuclear radius which in this case was taken to be 5.13 fermis. The magnitude of this quantity relative to the Wigner limit for this quantity gives a measure of the single-particle character of the state involved. In Fig. 1 the values of $\gamma^2/\gamma_w{}^2$ for states of given l (or j) are plotted as a function of the excitation energy.

The results shown in Fig. 1 display several noteworthy features:

(1) The marked peaking of $\gamma^2/\gamma_w{}^2$ for different $l(j)$ values suggests the influence at these energies of the single-particle states expected from the shell model although these states appear in a somewhat different order than predicted.[1] The discrepancy of order is not surprising and calls for the choice of a more suitable potential for determining the positions of these states. It might also be remarked that s states, for which the efficiency of detection is greatest due to the favorable penetrability factors, are relatively few and that their reduced widths are significantly smaller than for those states expected from the shell model. This would seem to imply that the s states in this region of excitation involve a complex mode of excitation of the Ca^{40} core.

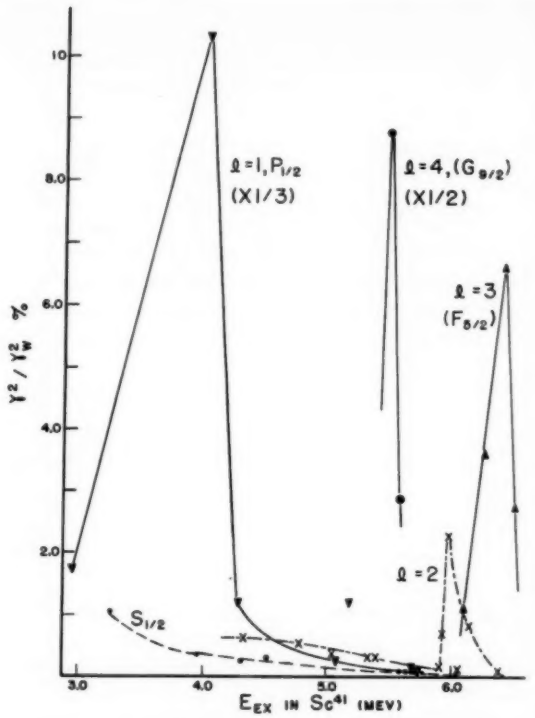

FIG. 1. The reduced widths of the states observed in elastic scattering of protons, expressed as a fraction of the Wigner single-particle limit, are shown as a function of the excitation energy in Sc^{41}. The lines connect the data points for states formed by protons of a fixed l value.

(2) While there are too few states contributing to make a strong argument, it appears that the envelope of the reduced widths of states formed by protons of a given $l(j)$ value shows a character which is illustrative at relatively low energies of excitation of the giant resonances discussed in the complex potential model[12] and in a more detailed fashion in the intermediate-coupling model of Lane, Thomas, and Wigner.[13] The occurrence of these maxima may also be viewed as supporting the interpretation of the strong maxima found in

Table I. Experimental single-particle level spacings.

Levels	ΔE (Mev) (present work)	ΔE (Mev) (reference 3)
$1f_{5/2}-1f_{7/2}$	6.4	≥ 4
$2p_{1/2}-2p_{3/2}$	2.2	~ 1.8
$2p_{3/2}-1f_{5/2}$	4.5	≥ 1
$1g_{9/2}-2p_{1/2}$	1.5	...
$2d_{5/2}-2p_{1/2}$	1.9	...

the spectra of protons from (d,p) reactions for this region of nuclei as due to the influence of single-particle states on the level structure.[14]

(3) If one assumes that the groups of states according to $l(j)$ value are in fact identifiable with the appropriate single-particle states, then the mean energy spacings of these states are of interest in connection with theories of the origin and magnitude of the spin-orbit force. The spacings observed in our measurements are summarized in Table I, and for comparison previous estimates of these spacings are included when available.

†Supported in part by the U. S. Atomic Energy Commission.

*Now at Florida State University, Tallahassee, Florida.

[1]C. A. Levinson and K. W. Ford, Phys. Rev. 100, 13 (1955).

[2]Nuclear Level Schemes, $A=40-A=92$, compiled by Way, King, McGinnis, and van Lieshout, Atomic Energy Commission Report TID-5300 (U. S. Government Printing Office, Washington, D. C., 1955).

[3]C. K. Bockelman and W. W. Buechner, Phys. Rev. 107, 1366 (1957); J. R. Holt and T. N. Marsham, Proc. Phys. Soc. (London) A66, 565 (1953).

[4]R. H. Nussbaum, Revs. Modern Phys. 28, 423 (1956).

[5]H. S. Plendl and F. E. Steigert, Bull. Am. Phys. Soc. 4, 18 (1959); (private communication).

[6]J. W. Butler (private communication).

[7]R. D. Bent and T. H. Kruse, Phys. Rev. 109, 1240 (1958).

[8]See also Davis, Prosser, Spencer, Young, and Johnson, Bull. Am. Phys. Soc. 2, 304 (1957).

[9]J. M. Blatt and L. C. Biedenharn, Revs. Modern Phys. 24, 258 (1952).

[10]Johnson, Kashy, Perry, and Class, Phys. Rev. (to be published).

[11]We should like to acknowledge the important contribution of E. Kashy and R. Perry who programmed the phase shift analysis for application to this problem. We are also indebted to the Shell Development Company, Houston, Texas for generously making their computing facility available to us.

[12]Feshbach, Porter, and Weisskopf, Phys. Rev. 96, 448 (1954).

[13]Lane, Thomas, and Wigner, Phys. Rev. 98, 693 (1955).

[14]Schiffer, Lee, Yntema, and Zeidman, Phys. Rev. 110, 1216 (1958); Schiffer, Lee, and Zeidman, Phys. Rev. (to be published).

ENERGY SPECTRUM OF PHOTONEUTRONS FROM OXYGEN

Carmelo Milone

Istituto di Fisica dell' Università, Centro Siciliano di Fisica Nucleare, Catania, Italia

(Received March 30, 1959; revised manuscript received June 2, 1959)

The energy spectrum of the photoneutrons from oxygen has been studied by irradiation of a water target with a 31-Mev collimated bremsstrahlung beam from the Brown Boveri betatron of Torino University.

Photoneutrons emitted at about 90° with the γ-ray beam have been recorded by means of the proton recoil tracks in Ilford L_4 plates 400 μ thick. A water wall 60 cm thick screened the plates against the spurious neutrons coming directly from the betatron, as in a previous work.[1]

Plates were scanned and proton recoil tracks were selected following the method used previously.[1]

The neutron spectrum is deduced from the proton recoil spectrum taking into account the cross section for (n,p) collisions in the hydrogen of the emulsion. The relation $E_n=E_p/\cos^2\theta$ was introduced only for $\theta>10°$. Small corrections are due to the probability of escape of the tracks from the emulsion[2] and to the absorption and scattering of neutrons in the target. The experimental energy spectrum is given in Fig. 1(a).

Under the restrictive assumption that only the direct $O(\gamma,n)$ process is effective and that the residual O^{15} nucleus is left in the ground state, the expected neutron spectrum may easily be inferred from the $O(\gamma,n)$ cross section,[3] taking

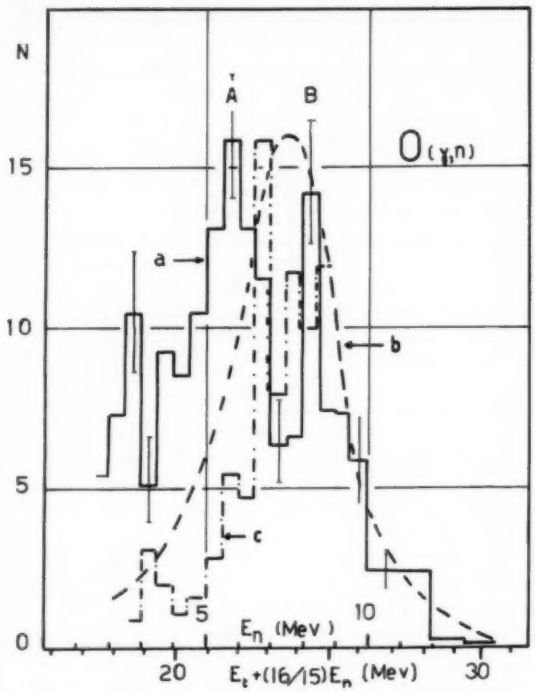

FIG. 1. (a) Experimental photoneutron spectrum. N = neutrons per $\Delta E_n = 0.5$ Mev (arbitrary units). (b) and (c) Spectra calculated from the $O(\gamma, n)$ cross sections.

account of the bremsstrahlung spectrum. The behavior of the neutron spectrum thus inferred is given in Fig. 1(b).

Although the above assumption is very restrictive and the $O(\gamma, n)$ cross section[3] is available only in large energy steps, a rough agreement may be observed in the high-energy region between the experimental and calculated spectra. This gives evidence of a large contribution of direct process in the $O(\gamma, n)$ reaction. On the other hand, for all elements previously investigated,[4] evaporation accounts for the greater part of the emitted neutrons. A more detailed comparison between the experimental and the calculated spectra in the high-energy region may be made up to $E_\gamma = 25.1$ Mev taking into account Spicer's cross section[5] calculated in 0.5-Mev steps. The spectrum (c) in Fig. 1 inferred from Spicer's cross section in the giant resonance region shows a fine structure as the experimental spectrum.

In the low-energy region a contribution of the evaporative process may account for the difference between the experimental and calculated spectra.

The neutron peak around 2.5-3 Mev may be due to neutrons leaving O^{15} in excited states. The two neutrons peaks A and B are to be attributed to photons of energy E_γ around 22 and 24 Mev, respectively. Indeed, taking into account (*i*) the $O^{16}(\gamma, n)$ threshold energy ($E_t = 15.6$ Mev), (*ii*) the energy of the first excited level in O^{15} ($E_1 = 5.3$ Mev), and (*iii*) the behavior of the $O(\gamma, n)$ cross section beyond 27 Mev,[3] it appears that after the emission of the neutron groups A and B the O^{15} must be left in its ground state. In this particular case $E_\gamma = 15.6 + (16/15)E_n$.

It gives this writer great pleasure to express his thanks to Professor R. Ricamo and Professor G. Wataghin for their generous help and to Professor G. Cortini for valuable discussion of the program of the research. Grateful thanks are due to the Catania and Torino laboratory colleagues for their friendly collaboration.

[1]Cortini, Milone, Rubbino, and Ferrero, Nuovo cimento 9, 85 (1958).

[2]L. Rosen, Nucleonics 11, No. 7, 32 (1953); 11, No. 8, 38 (1953).

[3]J. H. Carver and K. H. Lokan, Australian J. Phys. 10, 312 (1957).

[4]Cortini, Milone, Papa, and Rinzivillo, Nuovo cimento (to be published).

[5]B. M. Spicer, Australian J. Phys. 10, 326 (1957).

SHELL EFFECTS AT HIGH EXCITATION ENERGIES*

H. W. Newson and M. M. Duncan
Duke University, Durham, North Carolina
(Received May 25, 1959)

It has been known for some time that a plot of the level spacings of rather highly excited compound nuclei (as measured by s-wave neutron resonances) fluctuates rapidly as a function of mass number.[1,2] The fluctuations are evidently connected in some manner with the shell structure of nuclei since prominent maxima of the level spacings appear at neutron numbers of 50, 82, and 126. Rosenzweig[3] has calculated relative shell-model level densities. We are presenting similar calculations based on an even simpler model.

We shall attempt to account for level spacings of even-A compound nuclei by considering the most significant mode of excitation of compound nuclei to be excitations of 0^+ pairs of like nucleons among the levels of a spherical shell-model scheme. For our calculations we assume that there are a minimum number of unpaired particles (i.e., two in odd-odd or even-even compound nuclei with nonzero angular momentum). One can make a simple count of the number of possible different ways of arranging the two unpaired nucleons in a shell scheme and still obtain a J^π consistent with the spin and parity of the target nucleus and an incident s-wave neutron. This count, which has been carried out only for odd-odd compound nuclei between $N=50$ and 82, is roughly proportional to $2J+1$ (as long as J is not too large), in qualitative agreement with the predictions of a simple Fermi gas model.[4] We therefore define a level spacing $D_0=2(2I+1)D_{\text{obs}}\equiv 1/\rho_0$ which should be approximately independent of all but pair excitations of nucleons; I is the spin of the target nucleus and D_{obs} is the observed spacing including all s-wave channels.

If one assumes, for the moment, that a major shell (only partially filled) is isolated, it is easy to calculate the number of possible ways of arranging indistinguishable pairs in the shell as a function of an excitation energy which is measured in units of S, an average spacing for pairs between subshells of a major shell. These simple pair excitations alone are not enough to account for the observed level densities. However, there are two (complex pair) modes of excitation available: Because of the large separation energy (about 2 Mev per nucleon[5]) between major shells, one and only one pair can be excited into a higher major shell. As an alternative, one or possibly more pairs may be brought up from the filled subshells below the unfilled major shell, as will be discussed later. These complex pair excitations can occur in a number of different ways (index i) which leaves an energy $E'-E_i$ for the simple pair excitations. It is clearly possible to calculate the number of possible configurations at a given nuclear excitation energy, E' above the lowest energy state with J^π, by sharing the available energy in all possible ways between simple and complex pair excitations. If the distribution of the number of simple pair excitations, $r(E'-E_i)$, is calculated from a shell model, and r is assumed independent of i, then the total configuration density at E' is the sum over all possible values of E_i. If, for simplicity, one assumes $E_i=nS'$, where $n=0, 1, \ldots$, then

$$1/D_0=\rho_0(E')=\sum_{n=0}^{E'/S'} r(E'-nS')=\int_0^{E'} r(E'-E)\,dE/S'. \tag{1}$$

The maximum energy, M, which can be absorbed by simple pair excitation in the partially filled shells, is roughly equal to or less than the excitation energy, B, of the compound nuclei when $35<N<90$ and between 120 and 130 if the pair spacing, S', is about 0.5 Mev. For these cases Eq. (1) becomes

$$\rho_0(B\gtrsim M)=1/D_0=n_Z n_N/S'. \tag{2}$$

n_Z and n_N are the number of arrangements of the indistinguishable proton pairs and neutron pairs, respectively, within their major unfilled shells.

The results of these calculations based on Eq. (2) are shown in Fig. 1(a) for odd-odd compound nuclei. The predicted spacings near the rare earths are much too low (dashed curve) due to the fact that $M\gg B$ for these compound nuclei so that Eq. (2) breaks down very badly. The higher calculated points in this region are based on an approximate correction which assumes a triangular distribution for r, and that $B=6$ Mev, $S'=50$ kev, and $S=500$ kev. In Fig. 1(b) the predic-

tions of Eq. (2) are compared to some of the even-even compound nuclei. It is seen that the general trend of the experimental results and in some cases their detailed behavior are correctly predicted.

Sample counts have shown that the general trend of the predicted spacings is unaffected by assuming four rather than two unpaired nucleons. In any case, this number must be small since the pairing energies[8] [about $23(2j+1)A^{-1}$ Mev] limit it. The effect of this restriction on the number of possible configurations is now being investigated in detail by Rosenzweig.[7] However, sample calculations (based on the simplest cases) indicate that a count of all the energetically possible "broken pair" configurations predicts too low a spacing and, hence, we must assume that the stability of most of these configurations does not permit them to be observed as sharp resonances. Consequently, we are unable (in general) to estimate the value of S' from the shell model, since some of the observed resonances may be due to an unknown fraction of the broken pair configurations. In addition, we may also observe configurations arising from the excitation of pairs out of the filled subshells below the shell of interest. Since the conventional shell-model diagram is only a semiempirical summary of information about excitations above the Fermi level, we cannot predict the energetics of this last mode of excitation. It is rather surprising that a single value of S' (50 kev) yields as good agreement between calculated and measured values as that in Fig. 1.

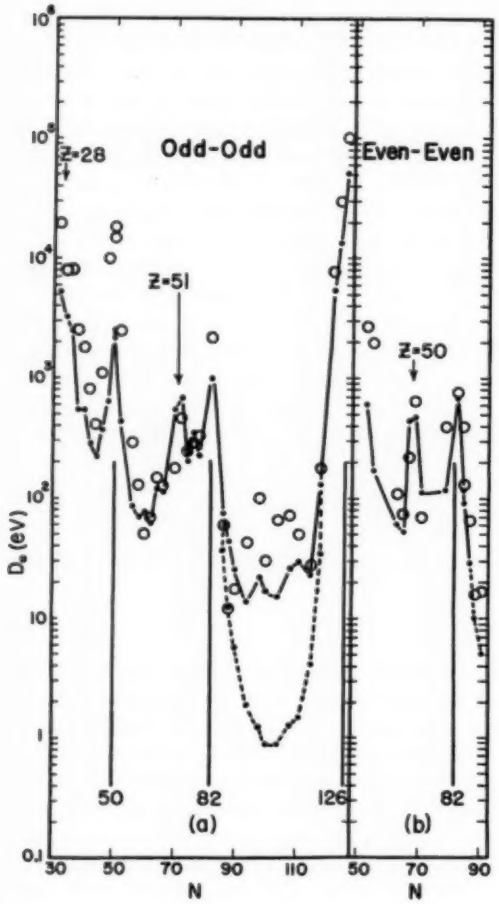

FIG. 1. Calculated and measured values of D_0 are plotted against the number of neutrons N in the target nucleus for even-even and odd-odd compound nuclei. Experimental points are shown as circles. Calculated points are shown as small solid dots connected by straight solid lines except that the predictions of Eq. (2), where it is invalid, are connected by dashed lines. Experimental errors are not indicated. The best known spacings (in general the smallest) are uncertain by ± 20% or more; the most uncertain points are those near $N=50$ where the errors are of the order of a factor of two or more in either direction. The same value of S' (50 kev) has been used in all calculations.

We have profited greatly from discussion with Dr. M. F. L. Pryce and Dr. E. Merzbacher. We are also indebted to Dr. J. A. Harvey for his valuable estimates of spacings from the experimental data[8] and to Miss E. Winton for help with the calculations.

*Work supported in part by the U. S. Atomic Energy Commission.

[1] H. W. Newson and R. H. Rohrer, Phys. Rev. 94, 654 (1954).

[2] Hughes, Garth, and Levin, Phys. Rev. 91, 6 (1953).

[3] N. Rosenzweig, Phys. Rev. 108, 817 (1957).

[4] J. M. B. Lang and K. J. Le Couteur, Proc. Phys. Soc. (London) A67, 586 (1954).

[5] J. A. Harvey, Phys. Rev. 81, 353 (1951).

[6] M. Nomoto, Progr. Theoret. Phys. (Kyoto) 18, 483 (1957).

[7] N. Rosenzweig, Bull. Am. Phys. Soc. 4, 272 (1959).

[8] The necessary data or references thereto may be found in Neutron Cross Sections, compiled by D. J. Hughes and R. B. Schwartz, Brookhaven National Laboratory Report BNL-325 (Superintendent of Documents, U. S. Government Printing Office, Washington, D. C., 1958), second edition.

TRIPLE ISOMERISM IN Ir^{192}†

Gertrude Scharff-Goldhaber and Michael McKeown
Brookhaven National Laboratory, Upton, New York
(Received June 12, 1959)

About eight years ago we started a systematic program to search for long-lived isomers produced by pile neutron irradiation. Samples of most elements, weighing ~50 mg, were placed for one month inside the Brookhaven reactor and were then allowed to "cool." An analysis of the radiations from these samples carried out two years after the irradiation gave evidence only of well-known activities. A renewed study undertaken in the beginning of this year revealed a new activity induced in the Ir sample: Although the well-known 74.37-day ground-state activity[1] Ir^{192g} should have decayed to ~1 disintegration per sec, according to our computation, we observed a gamma spectrum, identical with that of Ir^{192g} (see Fig. 1), but corresponding to a source strength of 2820 ± 140 disintegrations per sec. As Ir^{192g} is known to have a 1.45-min isomer,[1] decaying mainly by a 58-kev isomeric ($E3$) transition to the 74-day ground state, we are forced to conclude that the activity observed stems from a third, longer lived isomer of Ir^{192}. This then constitutes a case of a nuclear isomeric triplet. Only one other case of triple isomerism is known, again in an odd-odd nucleus: Sb^{124}.[2] No definite spin assignments were possible so far for the metastable states in Sb^{124} because of the very low energies of the isomeric transitions. Hence, it seemed of particular interest to study the mode of decay of the new long-lived isomer of Ir^{192}.

We shall distinguish the two metastable states of Ir^{192} by naming the 1.45-min isomer Ir^{192m_1} and the new long-lived isomer Ir^{192m_2}. Measurements of the source intensity of Ir^{192m_2} through several weeks showed no decay within the statistical limits of error, allowing us to state a lower limit $T_{1/2} > 5$ yr.

The identity of the gamma-ray spectrum accompanying the decay of Ir^{192m_2} with that of Ir^{192g} indicates that Ir^{192m_2} decays by an isomeric transition. In order to determine the multipole order of this transition, we first studied the L x-rays emitted from a thin source of Ir^{192m_2}, using a 3-mm-thick NaI(Tl) crystal as detector. We found that the ratio I_L x-rays:I_{316} kev from this sample was ~16 times larger than that from an equally thin Ir^{192g} source, studied in the same geometry. There was no measurable difference, however, between the I_K x-rays:I_{316} kev ratios of the two sources. This implies that the isomeric transition is mainly converted in the L shell and is therefore a high electric multipole. Next we examined the conversion electrons from this transition by using a thin Ir^{192m_2} source placed on a 1-cm-thick anthracene scintillator, covered with a 0.2-mg/cm² Al foil. We found unresolved L and M conversion electron lines from a 161 ± 5 kev transition. (See Fig. 2, curve A.) The electron spectrum was compared with that of Ir^{192g} (see Fig. 2, curve B), which was quite flat in the same energy region. The energy calibration was carried out by means of the conversion lines of the isomeric transitions in Te^{125m} (See Fig. 2, curve C.)

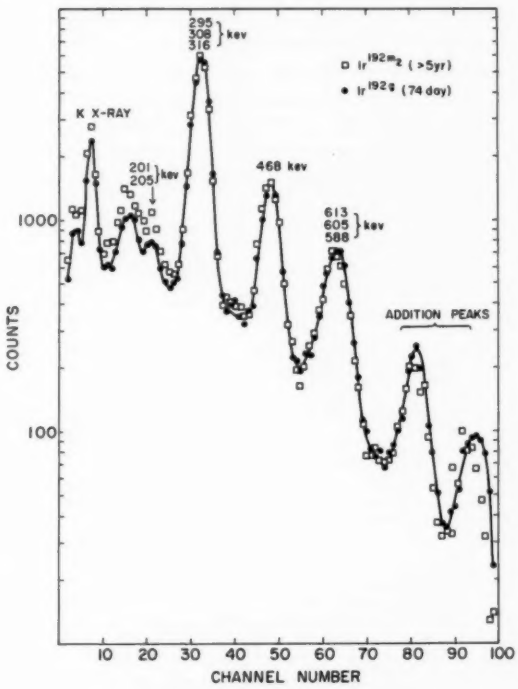

FIG. 1. Comparison of the scintillation spectra of the gamma rays from Ir^{192g} (•) and Ir^{192m_2} (>5 yr) (□). The slightly higher gamma-ray intensity in the low-energy region is due to increased backscattering in the thicker Ir^{192m_2} source. The peak between the K x-ray peak and the 201-205 kev photopeak is due to backscattering in the lead shield.

No unconverted 161-kev gamma rays were found. However, because of the weak Ir^{192m_2} activity at our disposal we can only say that $I_{161\ kev}:I_{316\ kev} < 0.1$. From the energy, the low K/L ratio, and the lower limit for the half-life of the isomeric transition, the most probable multipole assignment is $E5$, as follows from the values for the computed half-lives and activation cross sections given in Table I. For an $E5$ transition of 161 kev for $Z = 77$, $\alpha_K = 6.3$, $\alpha_L = 568$ (Sliv),[3] $\alpha_M = 238$ (Rose).[4] The theoretical half-life for a single proton $E5$ transition of this energy is 19.6 yr. Assuming that this is the actual half-life, we compute from the observed source strength an activation cross section $\sigma = 5.2 \times 10^{-27}$ cm^2 for pile neutrons. Since natural Ir was used as the target, we estimate that a fraction of this cross section, $\leq 3 \times 10^{-27}$ cm^2, is due to an $(n, 2n)$ process in Ir^{193}.

As Fig. 2, curve A, shows, no conversion electrons from a 58-kev transition were observed in the electron spectrum of Ir^{192m_2}. Therefore, the $E5$ transition does not end in the 1.45-min state Ir^{192m_1}. Unless it is followed by a low-energy (< 30 kev) transition, which would have

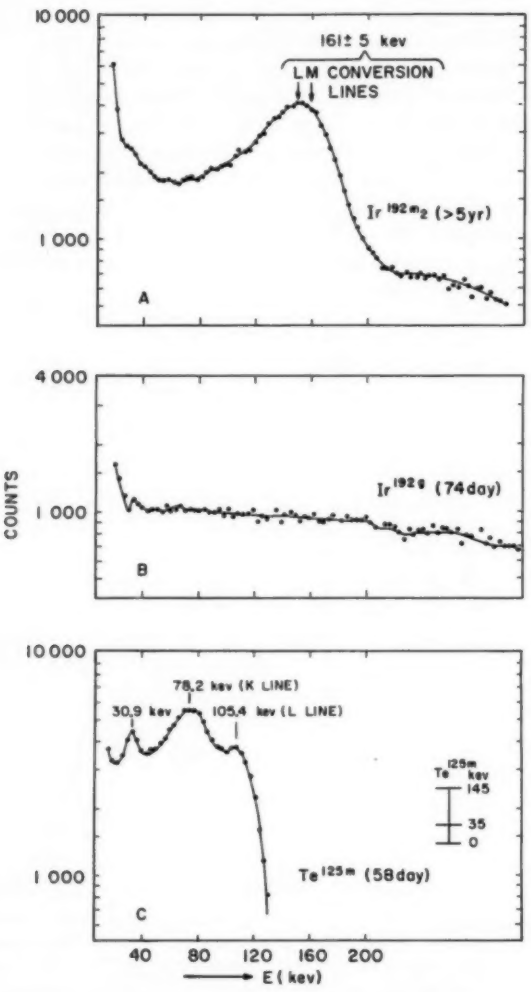

FIG. 2. Conversion electron spectra of Ir^{192m_2} (> 5 yr) (curve A) and Ir^{192g} (74 day) (curve B). The energy calibration was carried out by means of the K and L conversion electron lines of the 110-kev transition and of the L conversion electron line of the 35-kev transition in Te^{125m} (curve C). The positions of the L and M conversion lines of the isomeric transition in Ir^{192m_2} were determined by taking the theoretical conversion coefficients (see Table I) into account.

Table I. Relation between electric multipole order, half-life, and activation cross section computed for a 161-kev transition.

	$E4$	$E5$	$E6$ [a]
α_K	1.5	6.3	11.6
α_L [b]	122.2	568	5730
α_M [c,d]	21.4	238	3760
α_{tot}	145.1	912.3	9501.6
T_γ (sec) [e]	1.55×10^5	5.65×10^4	8.82×10^{19}
T (yr)	3.38×10^{-5}	19.6	2.79×10^8
σ_{act} (cm^2) [f]	...	5.2×10^{-27}	5.7×10^{20}

[a] The values for the $E6$ conversion coefficients were obtained by extrapolating logα versus electric multipole order.

[b] See reference 3.

[c] See reference 4.

[d] In order to take screening effects roughly into account, the M-shell conversion coefficients for $Z_{eff} = 70$ were used.

[e] The gamma half-lives were computed using the formulas given by S. A. Moszkowski, in Beta- and Gamma-Ray Spectroscopy, edited by K. Siegbahn (Interscience Publishers, Inc., New York, 1955), p. 391.

[f] The activation cross sections σ_{act} were computed using the observed number of disintegrations/sec, the total neutron flux, and the computed half-life given in the line above. The following relation between half-life T (in years) and activation cross section (in cm^2) holds:

$$\sigma_{act}(Ir^{192m_2}) = 2.04 \times 10^{-28} Te^{5.06/T}$$

escaped detection, it may be assumed to go directly to the 74-day ground state which is known to have a character 4± or 5-.[1] From this it follows that if $I_{Ir^{192}g} = 4\pm$, then $I_{Ir^{192}m_2} = 9\mp$ and $I_{Ir^{192}m_1} = 1\mp$. On the other hand, if $I_{Ir^{192}g} = 5-$, then $I_{Ir^{192}m_2} = 10+$ or $0+$, and $I_{Ir^{192}m_1} = 2+$ or $8+$, respectively. Since a weak beta continuum had been reported for Ir^{192m_1},[1] of unknown end-point energy, we decided to study which states in Pt^{192} are populated by beta decay of this isomer. Thus we hoped to be able to make a spin assignment for Ir^{192m_1}, from which the spins of the other two isomers would follow. The Ir^{192m_1} sources consisted of enriched Ir^{191} (85.9%), irradiated for 10 sec by neutrons from our reactor. We measured the beta-spectrum of the 1.45-min activity and the beta-gamma coincidences, as well as the gamma spectrum and the gamma-gamma coincidences. From our results it follows that the Pt^{192} ground state (0+) and also the two lowest excited states at 316 kev (2+) and 611 kev (2+) are populated in the beta decay of Ir^{192m_1}. The branching ratios found were 7×10^{-5}, 8×10^{-5}, and 2.5×10^{-5} per disintegration, respectively.[5] Figure 3 shows the proposed disintegration scheme of the isomeric triplet. It contains the unique spin assignments for the three isomeric states derived from this work. (The assignment 2- for Ir^{192m_1}, although compatible with the beta branching, is excluded, because Ir^{192g} would then be 5+.) Also, the previously established[1] spin assignments of the levels of Pt^{192}, which are fed in the beta decay of Ir^{192m_1} and Ir^{192g}, are given. From these it follows that either all three beta branches of Ir^{192m_1} are allowed and the three high-energy beta branches from Ir^{192g} (representing ~99% of all beta decays) first forbidden, or vice versa, depending on which parities (upper or lower) are chosen. The log*ft* values derived from our studies of the beta decay of Ir^{192m_1} are almost the same as those for the beta branches of Ir^{192g} reported previously. It is therefore not possible to make definite parity assignments for the three isomeric states.

By studying the 1.45-min growth of the intensity of the 468-kev gamma ray from the 4+ state of Pt^{192} which is not populated in the decay of Ir^{192m_1}, we obtained the ratio for the initial activation cross sections $\sigma_i(Ir^{192m_1})$: $\sigma_i(Ir^{192g}) = 0.84$. Taking the total activation cross section from the literature,[6] $\sigma_t(Ir^{192g}) = (7.0\pm2.0)\times10^{-22}$ cm², we obtain $\sigma_i(Ir^{192g}) = (3.8\pm1.1)\times10^{-22}$ cm² and $\sigma_i(Ir^{192m_1}) = (3.2\pm0.9)\times10^{-22}$ cm². The latter value is to be compared with the value of $(2.6\pm1.0)\times10^{-22}$ given in the literature.[6]

The small cross section found for formation of Ir^{192m_2} is in agreement with expectations from the rule[7] that σ_{act} decreases with increasing $|I - I_C|$, where I_C denotes the spin of the compound state. For $Ir^{191} + n$, $I_C = \frac{3}{2} \pm \frac{1}{2}$.

We wish to thank E. der Mateosian and G. Harbottle for their kind collaboration in various phases of this work.

†Work performed under the auspices of the U. S. Atomic Energy Commission.

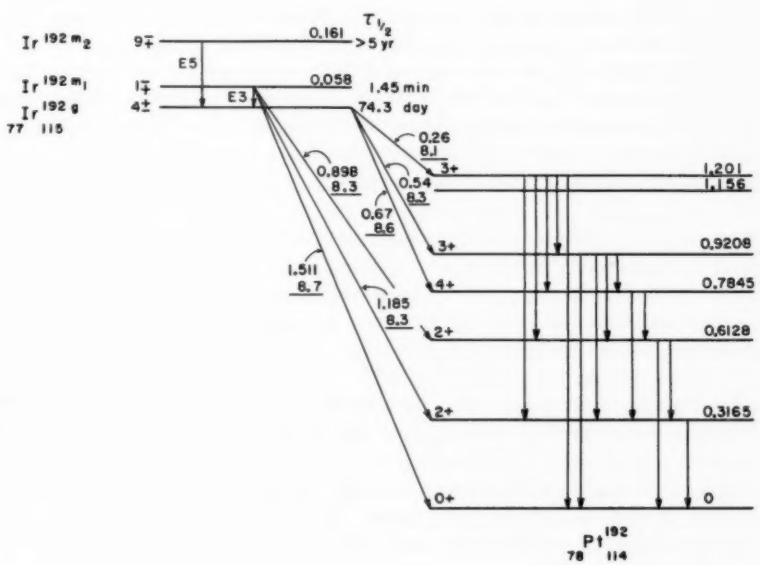

FIG. 3. Disintegration scheme of the triple isomers of Ir^{192}. The decay of Ir^{192m_2} and the analysis of the beta decay of Ir^{192m_1}, as well as the spin assignments for the three isomers, result from the present work. Because the log*ft* values for the beta transitions from Ir^{192g} and from Ir^{192m_1} are comparable, it is not possible to decide which set of the beta transitions is allowed and which is first forbidden. Hence the ambiguity in the parities (upper or lower set) still persists. Only that part of the decay scheme of Ir^{192g} which is relevant for the discussion is shown.

[1]Strominger, Hollander, and Seaborg, Revs. Modern Phys. 30, 585 (1958); B. S. Dzelepow and L. K. Peker, Decay Schemes of Radioactive Nuclei [Academy of Sciences of the U.S.S.R. Press, Moscow, 1958)].

[2]der Mateosian, Goldhaber, Muehlhause, and McKeown, Phys. Rev. 72, 1271 (1947).

[3]L. A. Sliv and I. M. Band, Tables of Internal Conversion Coefficients (Academy of Sciences of the U.S.S.R. Press, Moscow, 1958), Part II.

[4]M. E. Rose, Internal Conversion Coefficients (North Holland Publishing Company, Amsterdam, 1958).

[5]A weak β-branch (~8.5%) of 2.6-Mev end-point energy, decaying with an effective half-life of approximately 1.5 min, seems to be due to an impurity (Rh^{104} and $Rh^{104???}$?).

[6]Neutron Cross Sections, compiled by D. J. Hughes and R. B. Schwartz, Brookhaven National Laboratory Report BNL-325 (Superintendent of Documents, U. S. Government Printing Office, Washington, D. C., 1958), second edition.

[7]E. der Mateosian and M. Goldhaber, Phys. Rev. 108, 766 (1957).

OXYGEN-20*

Nelson Jarmie and Myron G. Silbert
Los Alamos Scientific Laboratory, University of California,
Los Alamos, New Mexico
(Received June 10, 1959)

This is a preliminary report of the observation of the nuclide O^{20}, heretofore unknown. This isotope of oxygen is of interest because it is new, because it is a member of the group of nuclides with a closed shell of eight protons, and particularly because it is the lightest nucleus known with isotopic spin $T=2$.

We observed O^{20} by detecting the protons from the $O^{18}(t,p)O^{20}$ reaction. The experimental arrangement and equipment have been described in detail previously.[1] Briefly, 2.6-Mev tritons from an electrostatic accelerator bombard a gas target enriched in O^{18}. Reaction fragments are analyzed in a double-focussing magnetic spectrometer and are detected in a CsI crystal scintillation spectrometer. The varying sensitivity of the CsI to different particles and the momentum analysis of the fragments determine the mass and energy of these fragments. As an additional check that the fragments in the O^{20} reaction were protons, their behavior was observed when a thin aluminum foil was placed over the CsI crystal. Protons from targets of normal oxygen, 25% O^{18},[2] and 96% O^{18} were observed. Background runs were also taken with nitrogen and methane in the target to check on possible contaminant reactions. All target gases were analyzed with a mass spectrometer. To eliminate the possibility that the proton groups could have come from (He^3,p) reactions caused by the He^{3+} component of the beam, runs were taken using a HT^+ beam. It was shown that the results below were definitely from the $O^{18}(t,p)O^{20}$ reaction.

Two proton groups associated with O^{20} were observed. These are assumed to be due to the ground state and first excited state of O^{20}. The Q for the reaction $O^{18}(t,p)O^{20}$ is 3.12 ± 0.04 Mev. This then gives a preliminary value for the mass of O^{20} of 20.01036 ± 0.00004 amu or a mass excess of 9.65 ± 0.04 Mev. The beta disintegration energy[3] for the O^{20}-F^{20} decay is calculated to be 3.75 Mev. The first excited state of O^{20} is found to be at an energy of 1.70 ± 0.05 Mev above the ground state. No other energy level was seen up to about 4.05 Mev. The errors stated are standard deviations.

This mass for O^{20} indicates a more stable nucleus than has been expected. For instance, Talmi and Thieberger[4] with a shell-model calculation predicted a mass excess of 11.4 Mev. The measured mass of O^{20} corresponds to a 6.5-Mev excited level in F^{20} and to a 16.7-Mev level in Ne^{20}. These levels should be the positions of the first $T=2$ state in these nuclei.

More precise values on O^{20}, as well as information on the energy levels of O^{18}, N^{16}, and N^{17}, will be reported in a complete paper.

Our thanks go to Eugene Haddad for some helpful advice on this experiment.

*Work performed under the auspices of the U. S. Atomic Energy Commission.

[1]Nelson Jarmie and Robert C. Allen, Phys. Rev. 111, 1121 (1958).

[2]The 25% O^{18} was kindly furnished by A. O. Nier, University of Minnesota.

[3]See S. Katcoff and J. Hudis, J. Inorg. Nuclear Chem. 3, 253 (1956), for an attempt to measure the O^{20} half-life.

[4]I. Talmi and R. Thieberger, Phys. Rev. 103, 718 (1956).

DIRECT PROOF OF θ_1^0 NEUTRAL DECAY*

J. L. Brown, H. C. Bryant, R. A. Burnstein, R. W. Hartung, D. A. Glaser, J. A. Kadyk, D. Sinclair, G. H. Trilling, J. C. Vander Velde, and J. D. van Putten
Harrison M. Randall Laboratory of Physics, University of Michigan, Ann Arbor, Michigan
(Received June 9, 1959)

Although the neutral decay mode $\theta_1^0 \rightarrow \pi^0 + \pi^0$ is expected to occur in addition to the well-known charged mode $\theta_1^0 \rightarrow \pi^- + \pi^+$, there has been no complete experimental proof of its existence because of the difficulty of detecting the neutral decay products with high efficiency. Ridgway, Berley, and Collins[1] and Osher, Moyer, and Parker[2] have reported counter experiments in which they observed gamma rays of roughly the correct energy originating several centimeters downstream of internal targets in the Cosmotron and Bevatron. The latter authors also report that the decrease in the numbers of such gamma rays with distance downstream from the target is consistent with the assumption that the gamma rays originate from Σ^+, θ^0, and Λ^0 decays whose lifetime is roughly that measured for the ordinary charged decays of these particles. Eisler et al.[3] have reported some gamma rays associated with strange particle production in a propane bubble chamber; Crawford et al.[4] have reported similar results from a hydrogen bubble chamber; and Boldt et al.[5] have observed showers occurring in conjunction with charged Λ^0 and θ^0 decays in a multiplate cloud chamber. In none of these experiments has it been possible to observe individual events in which all four gamma rays arising from the neutral θ^0 events were detected.

In order to study this process in detail, as well as others involving gamma rays, we have constructed a liquid xenon bubble chamber 30 cm in diameter and 25 cm in depth. The chamber operates at -21°C at a vapor pressure of 370 psi. The liquid xenon has a density of 2.18 g/cm^3 and a radiation length of 3.9 cm. We have taken about 160 000 photographs of this chamber exposed to a 1.0-Bev π^- beam at the Berkeley Bevatron.

Figure 1 shows the production of a Λ^0 followed by the decay $\Lambda^0 \rightarrow p + \pi^-$. Also visible in the picture are four electron pairs whose parent gamma rays appear to have originated at a common point about 1.2 cm from the origin of the Λ^0. If the measured directions of the pairs are used to extend the lines of flight of the gammas back toward their origin, it is found that these lines all pass through a cube less than 5 mm on a side. The volume of this cube is fully accounted for by

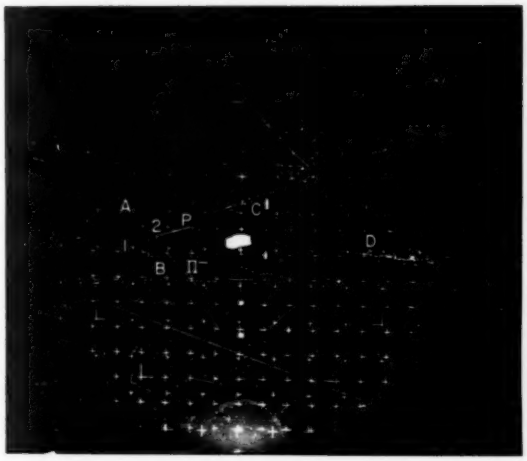

FIG. 1. Example of the decay $\theta_1^0 \rightarrow 2\pi^0 \rightarrow 4\gamma$. The θ^0 is produced at point 1 in association with a Λ^0 which decays into a proton and π^- (as indicated) both of which stop in the chamber. The lines of flight of the four gamma rays, given by the measured direction of the electron pairs A, B, C, and D, intersect near 2 where the θ_1^0 decay took place.

measurement errors, and therefore it can be concluded that within these errors the four gammas do originate at a common point. These four gamma rays are interpreted most naturally as arising from the decays $\theta_1^0 \rightarrow \pi^0 + \pi^0$, $\pi^0 \rightarrow 2\gamma$; the θ^0 having been produced in association with the Λ^0. We have found nine other four-gamma events of this same type in analyzing about one-half of the pictures.

In support of the interpretation of these events as neutral decay modes of θ_1^0 particles the following points should be noted: (1) The background of such four-electron-pair events arising either from prongless neutron stars in which two π^0 are created, or from the chance association of unrelated gamma rays is completely negligible. (2) Although the photographs were scanned for all charged V^0 decays, with or without associated gamma rays, every charged V^0 decay associated with four electron pairs was a $\Lambda^0 \rightarrow p + \pi^-$, unaccompanied by any other visible strange-particle

decay. This fact strongly indicates that the four gamma rays are indeed to be attributed to a particle of strangeness +1. (3) On the basis of the known θ_2^0 lifetime,[6] less than one of our ten events can be attributed to a neutral decay mode of the θ_2^0. Although these considerations leave little doubt as to the fact that the four-gamma events do arise from neutral θ_1^0 decay modes, some question may remain as to whether these decay modes are indeed of the type $\theta_1^0 \rightarrow \pi^0 + \pi^0$ followed by $\pi^0 \rightarrow 2\gamma$ or whether perhaps some of the gammas are produced directly in the decays. If one knows how to pair the gammas belonging to the same π^0, it is possible to compute the θ^0 mass from the observed directions of the θ^0 and the four gammas, thus making a direct check that the decay scheme $\theta_1^0 \rightarrow \pi^0 + \pi^0$ has really been observed. Unfortunately the results of this calculation are quite sensitive even to small measurement errors. Making use of the lower limit for the energy of each gamma ray imposed by the visible ionization loss of its associated electron shower, however, we were able to pick assignments of gamma rays which made the kinematics for the decays consistent with the mode $\theta_1^0 \rightarrow \pi^0 + \pi^0$ followed by $\pi^0 \rightarrow 2\gamma$ for both π^0's. We therefore believe that the decay scheme $\theta_1^0 \rightarrow 2\pi^0$ is the most likely interpretation of the events, although on the basis of our data such schemes as $\theta_1^0 \rightarrow \pi^0 + 2\gamma$ or $\theta_1^0 \rightarrow 4\gamma$ cannot be ruled out.

Work is in progress on other aspects of the experiment, including branching ratios for neutral decay of Λ^0 and θ^0.

We wish to express our gratitude to the staff of the Lawrence Radiation Laboratory for making this work possible, and especially to our many friends at the Bevatron who helped us very much during this experiment.

---

*Supported in part by the U. S. Atomic Energy Commission.

[1]Ridgway, Berley, and Collins, Phys. Rev. 104, 513 (1956).

[2]Osher, Moyer, and Parker, Bull. Am. Phys. Soc. 1, 185 (1956).

[3]Eisler, Plano, Samios, Schwartz, and Steinberger, Nuovo cimento 5, 1700 (1957).

[4]Crawford, Cresti, Douglass, Good, Kalbfleisch, Stevenson, and Ticho, Phys. Rev. Letters 2, 266 (1959).

[5]Boldt, Bridge, Caldwell, and Pal, Phys. Rev. 112, 1746 (1956).

[6]Crawford, Cresti, Douglass, Good, Kalbfleisch, and Stevenson, Phys. Rev. Letters 2, 361 (1959).

EXPERIMENT ON CHARGE INDEPENDENCE IN PION INTERACTIONS

D. Harting, J. C. Kluyver, A. Kusumegi, R. Rigopoulos, A. M. Sachs,* G. Tibell, G. Vanderhaeghe, and G. Weber
CERN, Geneva, Switzerland
(Received May 28, 1959)

Although the existing experimental results in pion physics are consistent with the assumption of charge independence of pion-nucleon forces, the statistical accuracy of the data leads to an uncertainty of ±15% in quantitative tests of the concept.[1] Direct experimental tests[2] offer the possibility of substantially reducing this uncertainty before being limited by the accuracy of theoretical calculations of the Coulomb and mass difference effects in the specific reactions studied.

The present paper describes an experiment at 600-Mev proton energy on the reactions

$$p + d \rightarrow H^3 + \pi^+,$$

$$p + d \rightarrow He^3 + \pi^0,$$

for which (apart from Coulomb and mass corrections) the charge independence hypothesis predicts the ratio of the differential cross sections to be 2 at any c.m. angle. The c.m. energy of the emerging pions is 220 Mev, well above the $(\frac{3}{2},\frac{3}{2})$ resonance. The cross sections are compared by detecting only the recoiling nuclei, which are identified by momentum and time-of-flight selection, with pulse-height analysis as an additional check.

A sketch of the experimental arrangement is given in Fig. 1. The 600-Mev proton beam traverses a 2-cm thick liquid deuterium target with 0.1-mm thick Mylar windows and then a secondary emission chamber monitor. The solid angle for the scattering is defined by a 2×3 cm^2 tungsten collimator, 4 cm thick, which is placed 500 cm from the target at an angle of 11.3° to the incident proton beam. Of the H^3 and He^3 nuclei transmitted, the higher energy group, corresponding to 52° in

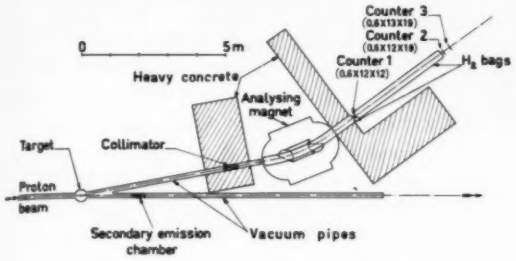

FIG. 1. Experimental arrangement. The counter dimensions are given in cm.

the c.m. system, was measured. A few properties of these particles are given in Table I. The particles passed by the collimator are analyzed by a magnet, the current in which is adjusted to bend the beam of either the H^3 or the He^3 nuclei over 26° into a telescope of three scintillation counters. The separation between counter 1, just after the magnet, and the pair of counters 2 and 3 is 400 cm. The signal from counter 1 is delayed by a cable of a length corresponding to the time of flight of the H^3 and He^3 nuclei over this 400-cm path and triple coincidences are recorded simultaneously with two coincidence circuits, one with 5.5 mμsec and the other with 4.0 mμsec resolution. The selectivity of this momentum–time-of-flight system ensures that no particles with a mass number different from three can be counted if they come directly from the target, i.e., are not scattered in or after the collimator. The identity of the counted particles is confirmed by recording, from one of the counters, the amplitude of the pulses that give rise to triple coincidences. These pulses are split and fed through two fast gates in parallel, each triggered by a different coincidence circuit. The output of each gate is recorded on a separate multichannel pulse-height analyzer. By taking the data from the well-defined H^3 and He^3 peaks of the pulse-height spectra (shown for He^3 in Fig. 2), particles of the wrong charge and accidentals producing small pulse heights are eliminated.

Measurements on H^3 are alternated with He^3 runs. The thickness of counter 1 is reduced from 6 to 1.5 mm for the He^3 measurements to equalize the multiple scattering for both kinds of particles. Other effects of the larger multiple scattering of He^3 are negligibly small, as the trajectory of the heavy particles goes through vacuum from the target to the analyzing magnet and from there on through hydrogen.

The main difficulty of the experiment is the very small cross section of the reactions which, at the angle considered, is 14 μb/sterad for H^3. Three H^3 particles are counted for every 10^{11} protons in our geometry, whereas the number of protons and deuterons scattered into the same solid angle is a factor of 10^4 higher. Most of these particles are removed by the analyzing magnet, but Fig. 3, which gives the relative number of triple coincidences as a function of the delay in counter 1, shows that the time-of-

Table I. Properties of the H^3 and He^3 nuclei counted in the present experiment. The range and energy loss are for plastic scintillator, the time of flight for 400-cm pathlength.

	T (Mev)	pc/Z (Mev)	Time of flight (mμsec)	Range (g cm^{-2})	Energy loss (Mev cm^2 g^{-1})
H^3	300	1332	31.1	23.2	7.2
He^3	300	666	31.1	5.8	28.9

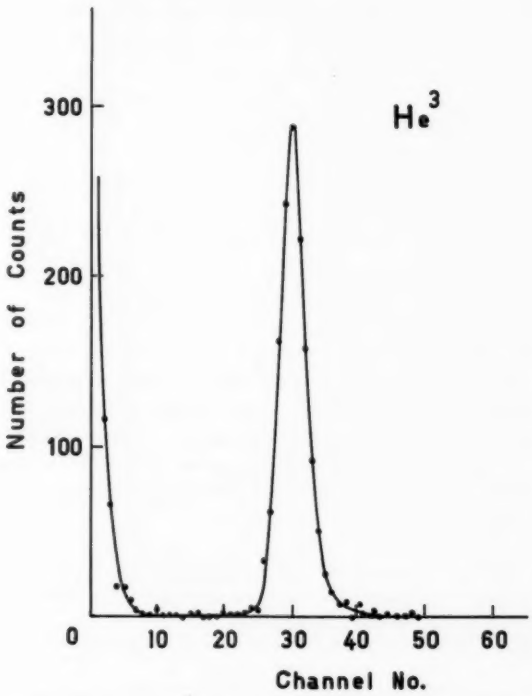

FIG. 2. Pulse-height spectrum in counter 2, gated by triple coincidences, for He^3 settings. The number of counts is given per channel for 8×10^{13} incident protons.

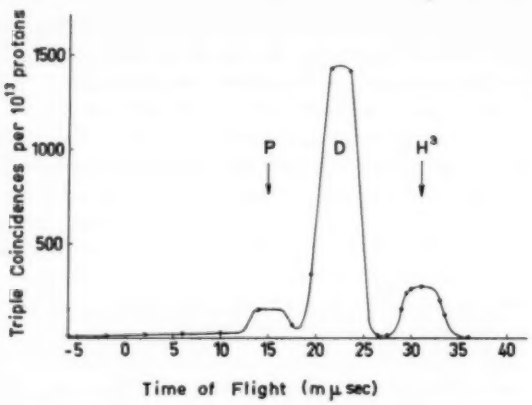

FIG. 3. Time-of-flight curve for H^3 settings.

flight selection still has to discriminate against rather a large number of deuterons.

The direct proton beam crosses the experimental room in a vacuum pipe but nevertheless contributes most to the background in the counters, approximately one thousand singles for each heavy particle recorded, notwithstanding the heavy shielding. To avoid corrections for accidental coincidences, the measurements have been made with a proton beam of 2×10^{10} protons per second, one-fifth of the maximum intensity.

The results of the counting, with their statistical errors, are listed in Table II. The value for the ratio of the measured cross sections following from these numbers is 2.29 ± 0.05.

In addition to the statistical uncertainty, possible sources of systematic errors must be considered. The reliability of the result depends mainly on two assumptions: first, that all the H^3 and He^3 nuclei, passing through the collimator, are counted and secondly, that all the recorded counts with the correct pulse height originate in H^3 and He^3 nuclei going through the three counters. To test the validity of these assumptions all measurements were repeated under marginal conditions. When the delay in counter 1 was set off from its correct value by an amount equal to the resolving time of the coincidence circuits, less than 1% of the counting rate was left. In the ratio this effect can be neglected. When the counters 2 and 3 were shifted together by their own width in the horizontal direction, the counting rate dropped to less than 1% of the central position value. The corresponding figure after vertical movement was at most 2% for both H^3 and He^3. Depending on their origin these marginal counts would have to be added to or subtracted from the measured numbers, leading to a negative or positive correction of $(2\pm2.8)\%$ in the ratio. As this origin is unknown (the counts might be due to multiply scattered H^3 and He^3 nuclei or to other scattered particles with the correct time of flight) no corrections were applied, but the uncertainty was expressed in an additional error to the ratio of 4%. Other sources of uncertainty are the drift in the monitor and possible deviations from 100% efficiency of the counting system, each contributing a 1% error.

Table II. Results of the experiment. The number of counts is given for 10^{13} incident protons. The errors include only counting statistics.

	H^3	He^3
Full target	279.8 ± 2.6	136.2 ± 1.6
Empty target	16.1 ± 1.1	21.2 ± 1.2
Full - empty	263.7 ± 2.8	115.0 ± 2.0

After transformation to the c.m. system and combining the errors in quadrature, the final result for the ratio of the cross sections at a c.m. angle of 52° is

$$R=2.26\pm0.11.$$

The difference between this result and the value 2 predicted by isotopic spin considerations alone is somewhat larger than the 4% which, according to a preliminary calculation by Köhler,[3] should be added for Coulomb and mass corrections. Measurement of the ratio at a different angle is now planned.

The authors wish to thank Professor G. Bernardini for helpful discussions, Dr. G. Fidecaro who kindly lent us the target, and Dr. B. Hedin for his work on the extraction of the proton beam. We are indebted to Mr. V. Beck and Mr. P. Actis for technical assistance and to the cyclotron staff for their co-operation.

*National Science Foundation Senior Postdoctoral Fellow on leave from Columbia University.

[1]A. Stanghellini, Nuovo cimento 10, 398 (1958).

[2]A. M. L. Messiah, Phys. Rev. 86, 430 (1952); Fliagin, Dzhelepov, Kiseler, and Oganesian, J. Exptl. Theoret. Phys. U.S.S.R. 35, 854 (1958)[translation: Soviet Phys. JETP 35, 592 (1959)]; Bandtel, Frank, and Moyer, Phys. Rev. 106, 802 (1957); Crewe, Garwin, Ledley, Lillethun, March, and Marcowitz, Phys. Rev. Letters 2, 269 (1959).

[3]S. Köhler (private communication).

SEARCH FOR RARE DECAY MODES OF THE μ^+ MESON*

Juliet Lee and N. P. Samios
Columbia University, New York, New York
(Received June 4, 1959)

With the use of a hydrogen bubble chamber we have endeavored to detect the following two decay modes of the μ^+ meson:

$$\mu^+ \to e^+ + e^- + e^+,$$

$$\mu^+ \to e^+ + \nu + \bar{\nu} + e^+ + e^-.$$

The decay $\mu^+ \to e^+ + e^- + e^+$ has not been observed although there are no known selection rules which would forbid it. Its nonexistence, however, has been well enough accepted to be incorporated into theoretical proposals such as the universal V-A theory[1,2] which excludes neutral currents. Recently Kinoshita and Sirlin[3] and also Eckstein and Pratt[4] have calculated the photon energy spectrum and decay rate for the process $\mu^+ \to e^+ + \nu + \bar{\nu} + \gamma$. As a result, the decay mode $\mu^+ \to e^+ + \nu + \bar{\nu} + e^+ + e^-$, where the photon is internally converted, should occur a small fraction of the time. This last process would appear similar to the direct decay of the $\mu^+ \to e^+ + e^- + e^+$ in that three prongs would emerge from the end of a μ^+ stopping.[5] A separation between these two processes is possible since the energy of the three electrons for the non-neutrino decay would be equal to the μ mass (i.e., 106 Mev) and their vector momentum would be zero. On the other hand, in the neutrino decay the energy of the secondaries would be less than 106 Mev and momentum would not balance. It is of interest to investigate both of these reactions in order to determine the validity of the above assumptions and calculations.

Slow π^+ mesons were stopped in a liquid hydrogen bubble chamber 12 in. in diameter, 6 in. in depth, placed in a magnetic field of 8800 gauss. On the average, 10 π^+'s stopped per picture, decaying into $e^+ + \nu + \bar{\nu}$. The π^+ meson served to identify the μ^+ meson and 2.2×10^5 such μ^+'s were observed. The experiment consisted in examining the μ^+ endings for those events which had 3 prongs and then measuring the vector momenta of these secondaries.

The possible sources of background were the following:

(1) $\mu^+ \to e^+ + \nu + \bar{\nu} + \gamma$, where the ray was externally converted within 2 mm of the vertex. The probability for this process can be calculated using the γ-ray energy distribution given by Kinoshita and Sirlin[3] and the known conversion probability in liquid hydrogen. Using a length of 2 mm, the number of these events expected is 0.03.

(2) A γ ray produced by an interaction in the walls accidentally materializing on a μ^+ ending. In all the pictures, 170 such random pairs were observed. A μ^+ ending can be located to within a cube whose side is 2 mm. Therefore, the probability that one of the 170 pairs could have occurred at the end of one of the μ^+ endings is $=170 \times 10 \times (0.2)^3/10^4 = 1.4 \times 10^{-4}$.

Both of these effects are negligible. The scanning efficiency was determined by looking for events in which the positron from a μ^+ decay made a visible knock-on electron within 2 mm of the vertex. The comparison of two independent scannings of the film gave 90% efficiency for finding these two-prong events. The detection of the three-prong events should be much easier, corresponding to an efficiency of the order of 95%.

From a total sample of 2.2×10^5 μ^+'s, three events were found where three charged prongs (2 positrons and 1 electron) emerged from the μ^+ ending. The total energy of the three secondaries was in each case 51 ± 3.5 Mev, 55 ± 1.5 Mev, and 33 ± 2 Mev and their resultant momenta 47 ± 3.5 Mev/c, 54 ± 1.5 Mev/c, 29 ± 2 Mev/c, respectively. Figure 1 is a picture of one of the above events.

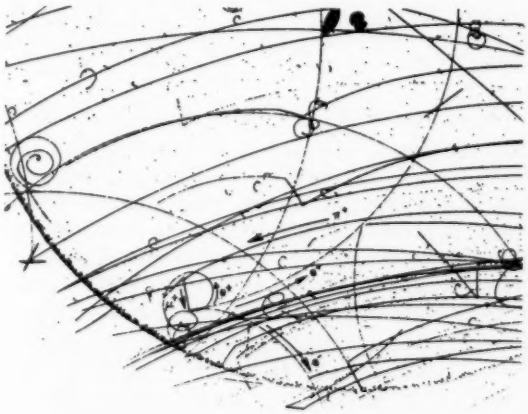

FIG. 1. Example of an event where 3 secondary prongs emerge from the μ-meson ending. It is identified as

$$\pi^+ \to \mu^+ + \bar{\nu}$$
$$\quad \searrow e^+ + e^+ + e^- + \nu + \bar{\nu}.$$

Of the three, none can be attributed to the direct decay $\mu^+ \to e^+ + e^- + e^+$ since the total energy of the secondaries was less than 106 Mev and there was a net momentum unbalance. If the events from this decay mode were distributed according to a Poisson distribution, this would correspond to a branching ratio

$$R = (\mu^+ \to e^+ + e^- + e^+)/(\mu^+ \to e^+ + \nu + \bar{\nu}) = 1 \times 10^{-5}$$

for 90% confidence.

According to the previous criteria, the three-prong events are all examples of the decay $\mu^+ \to e^+ + \nu + \bar{\nu} + e^+ + e^-$. This gives a ratio

$$R' = (\mu^+ \to e^+ + \nu + \bar{\nu} + e^+ + e^-)/(\mu^+ \to e^+ + \nu + \bar{\nu})$$
$$= (1.5 \pm 1.0) \times 10^{-8}.$$

This ratio R' can be estimated using the internal conversion probability, ρ_T, as given by Kroll and Wada,[6]

$$\rho_T = \frac{2\alpha}{3\pi}\left[\ln\left(\frac{2E_\gamma}{m}\right) - \frac{11}{6} - \frac{5}{24}\left(\frac{E_\gamma}{m_\mu - E_\gamma}\right)^2\right],$$

where E_γ = photon energy, m = electron mass, m_μ = meson mass [terms of order $(E_\gamma/m_\mu)^2$ have been neglected], and using also the transition probability for the radiative decay as given by references 3 and 4. Using a lower energy cut-off of 5 Mev for the γ ray, this gives for R' a value of approximately 5×10^{-5} which is essentially in agreement with the experimental result.

An accurate determination of the branching ratio is not feasible by means of a bubble-chamber experiment of this type, the purpose of the present endeavor being to show the existence of the decay mode and an order of magnitude of the decay rate.

We wish to thank our scanners, Mrs. Dina Goursky, Mr. John Impeduglia, Miss Mary Johnson, and Mr. Alex Rytow for their painstaking work and the Columbia Bubble Chamber Group for taking the pictures.

---

*This work is supported in part by the U. S. Atomic Energy Commission and the Office of Naval Research.

[1]R. P. Feynman and M. Gell-Mann, Phys. Rev. 109, 193 (1958).

[2]E. C. G. Sudarshan and R. E. Marshak, Phys. Rev. 109, 1860 (1958).

[3]T. Kinoshita and A. Sirlin, Phys. Rev. Letters 2, 177 (1959).

[4]S. G. Eckstein and R. H. Pratt (private communication).

[5]The decay mode $\mu^+ \to e^+ + \gamma$ with the γ ray internally converting would have a branching ratio $= 1/10^6 \times 160 \approx 10^{-8}$ which is undetectable with the present experiment.

[6]N. Kroll and W. W. Wada, Phys. Rev. 98, 1355 (1955).

PION PRODUCTION BY PIONS*

Walton A. Perkins, John C. Caris, Robert W. Kenney, Edward A. Knapp, and Victor Perez-Mendez

Lawrence Radiation Laboratory, University of California, Berkeley, California

(Received June 4, 1959)

The existence of a pion-pion interaction has been postulated to explain the nucleon structure[1] and the peak[2-4] in the π^--proton total cross section near 1 Bev. The direct interaction of the incident pion and a virtual pion in the meson cloud surrounding the nucleon could contribute significantly to the production of an extra pion in pion-nucleon collisions. In order to study this interaction, we have investigated the reaction $\pi^- + p \to \pi^+ + \pi^- + n$ in the energy region from 260 to 430 Mev. The π^+ meson in the final state provides a unique signature for this reaction, since the highest energies are just barely above the threshold for the production of two secondary pions.

The experimental arrangement is shown in Fig. 1. Negative pion beams produced by the 730-Mev proton beam of the Berkeley synchrocyclotron striking an internal target were magnetically selected and collimated as shown in the figure. The resulting pion beams, with kinetic energies of 260, 317, 371, and 427 Mev and energy spread of ±2.5%, impinged on a 4-inch-thick liquid hydrogen target.

The positive pion was unambiguously identified by its characteristic μ decay, by use of the electronic gating equipment described elsewhere.[5] In this experiment the coincidence $12345\bar{6}$ triggered the delayed gate which made a coincidence with the μ pulse; the energy band of the detected pions was determined by the thickness of the copper absorber placed between counters No. 3 and No. 4. The detection efficiency of the counter tele-

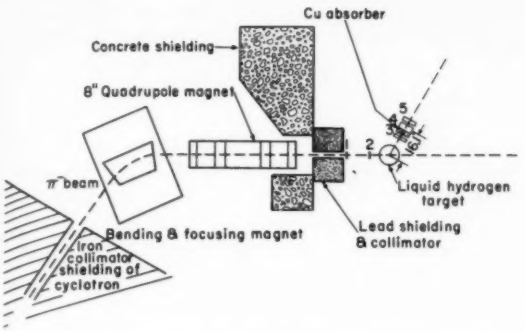

FIG. 1. Experimental arrangement (not to scale).

scope was previously determined by using a magnetically analyzed beam of positive pions.

Measurements were taken for π^+ mesons emitted at 60°, 90°, 125°, and 160° in the barycentric system for incident π^- kinetic energies of 317, 371, and 427 Mev; for π^- kinetic energy of 260 Mev only a single measurement was made at 90° (lab). To obtain the angular differential cross section an integration was performed over the energy of the π^+ meson at each angle. The angular differential cross sections are nearly isotropic at 317 and 371 but are peaked forward at 427 Mev. The differential cross sections were integrated over the angle of the π^+ meson to give the total cross sections shown in Fig. 2. The errors shown are the combined errors of counting statistics and of integration over energy and angle.

Recent measurements have been made by Zinov and Korenchenko[6] at incident energies of 307, 333, and 370 Mev for the combined reactions $\pi^-+p\rightarrow\pi^++\pi^-+n$ and $\pi^-+p\rightarrow\pi^-+\pi^0+p$. These measurements, taken for charged pions emitted at 106° (c.m.), are in reasonable agreement with the results presented here.

The dashed line in Fig. 2 represents the theoretical prediction according to Rodberg[7] and Kazes[8] based on the static model which assumes only a direct pion-nucleon interaction. We interpret the large systematic discrepancy between this theory and experiment as evidence for a pion-pion interaction (i.e., here the π^- interacts directly with the π^+ in the meson cloud surrounding the nucleon).

The following Letter[9] discusses the effect of a pion-pion interaction on the total cross section for this reaction. The solid line in Fig. 2 shows the result of including this interaction in the

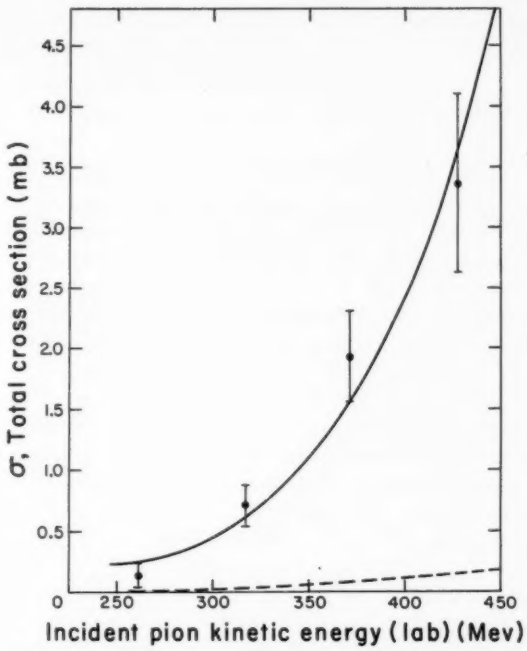

FIG. 2. Total cross section for $\pi^-+p\rightarrow\pi^++\pi^-+n$ as a function of the incident π^- kinetic energy. The dashed curve represents the static-model prediction by Rodberg[7] and Kazes[8]; the solid curve is the pion-pion interaction result by Rodberg.[9]

theoretical prediction.

We should like to acknowledge the continued interest and support of Professor A. C. Helmholz. We also wish to thank Mr. James Vale and the cyclotron crew for their assistance and cooperation during the course of the experiment.

---

*Work done under the auspices of the U. S. Atomic Energy Commission.

[1]W. R. Frazer and J. R. Fulco, Phys. Rev. Letters 2, 365 (1959).

[2]F. J. Dyson, Phys. Rev. 99, 1037 (1955).

[3]G. Takeda, Phys. Rev. 100, 440 (1955).

[4]Cool, Piccioni, and Clark, Phys. Rev. 103, 1082 (1956).

[5]Imhof, Kalibjian, and Perez-Mendez, Rev. Sci. Instr. 29, 476 (1958).

[6]V. G. Zinov and S. M. Korenchenko, Zhur. Eksptl. i Teoret. Fiz. 34, 301 (1958) [translation: Soviet Phys. JETP 34(7), 210 (1958)].

[7]L. S. Rodberg, Phys. Rev. 106, 1090 (1957).

[8]E. Kazes, Phys. Rev. 107, 1131 (1957).

[9]L. S. Rodberg, following Letter [Phys. Rev. Letters 3, 58 (1959)].

PION PRODUCTION AND THE PION-PION INTERACTION*

Leonard S. Rodberg
Department of Physics, University of California, Berkeley, California
(Received June 4, 1959)

In the preceding Letter[1] the cross sections for $\pi^- + p \to \pi^- + \pi^+ + n$ at incident energies between 260 and 430 Mev were presented. In this note we wish to discuss the theoretical interpretation of these results.

One may first attempt to understand this process using the well-known pion-nucleon interaction. This has been done previously[2] within the framework of the static model, which should remain applicable for the low energies involved here. In this model the incident pion interacts directly with the nucleon, and the nucleon "shakes off" the final pions. This approach yields a cross section for $\pi^- + p \to \pi^- + \pi^+ + n$ which is less than 0.1 mb for $E_{\text{inc}} \lesssim 400$ Mev. This small cross section results from (a) the relatively small, nonresonant, cross section for scattering of the initial and final pions on the nucleon (the incident energy is more than 100 Mev above the position of the 3-3 resonance, and the mean kinetic energy of the final-state pions is more than 50 Mev below the resonance energy); (b) the weak pseudovector coupling ($f^2 \approx 0.08$) which produces the extra meson; and (c) the small amount of phase space available to the outgoing P-wave pions. Thus the direct pion-nucleon interaction makes a negligible contribution to pion production in the 250-450 Mev region.

We have therefore attempted to fit the results of the preceding Letter using a direct pion-pion interaction. The contribution from the interaction of the incident pion with a pion in the nucleon cloud has been computed using the impulse approximation. The sizable cross section at low energies suggests an S-wave π-π interaction, and the rapid rise of the cross section with energy requires a P-wave interaction (all angular momenta are in the π-π center-of-mass system). The S-wave interaction has been described by phase shifts satisfying $[\nu/(\nu+1)]^{1/2} \times \cot \delta_0^I = 1/a_I$ with the isotopic spin $I=0$ and 2, ν the square of the π-π c.m. momentum, and $a_0 = 5\lambda$, $a_2 = 2\lambda$.[3] The P-wave cross section has been computed from the low-energy form $[\nu^3/(\nu+1)]^{1/2} \cot \delta_1^2 = 1/a_1$. A fit to the observed total cross section was obtained with $|\lambda| \approx 1/10$ and $|a_1| \approx 1/5$ (units $\mu_\pi = 1$); the result is shown in Fig. 2 of the preceding Letter. The P-wave phase shift obtained here is consistent with that found by Frazer and Fulco[4] in their investigation of nucleon structure.

The calculation was performed assuming that only the one-meson exchange term contributes. The meson-nucleon rescattering corrections can be computed by incorporating a π-π interaction into the formalism of reference 2. In the one-meson approximation which was used in reference 2, this adds an additional inhomogeneous term to the integral equations obtained there. These new equations can be solved using the same methods as in the earlier work. If the production amplitude is represented by D_0, the correction due to the rescattering of meson k is $\sim [ie^{i\delta_{33}(k)} \sin\delta_{33}(k)] D_0$, assuming that only pion-nucleon scattering in the $T = J = \frac{3}{2}$ - state is important. There should then not be large corrections in the present energy region. As in the case of photomeson production,[5] this is because the pion production takes place far from the nucleon. At higher energies, since the momentum transfer is of the order of the incident c.m. momentum, the mean radius of interaction becomes smaller and the rescattering corrections become correspondingly larger.

Over the energy range considered here the ratio of S-wave to P-wave contributions varies from 15 to 1/3; they become equal at $E_{\text{inc}} \approx 400$ Mev. The present experiment does indicate a sharp break within this region. For a given partial wave in the π-π system, the present model predicts a pion angular distribution in the overall center-of-mass system favoring forward angles, and a pion energy distribution tending slightly toward higher energies than predicted by phase space. Both the angular distribution and the energy spectrum[6] of the π^+ are consistent with this at 317 and 427 Mev, but differ markedly at 371 Mev. This abrupt change can be interpreted as a manifestation of the rapid change in the S/P ratio and the resulting the S-P interference. It does not seem possible to make quantitative estimates of these effects since the intermediate pion is far off the mass shell. Its "mass" varies with the angle and energy of the emitted pions, and the dependence of the cross section on this mass is difficult to estimate. The "free"

π-π scattering cross section can be determined only by the extrapolation procedures recently suggested by Goebel and Chew and Low.[7]

The angular- and energy-correlations in the π-π c.m. system should also be sensitive to the S/P ratio: a fore-aft asymmetry should appear within this energy range, and higher c.m. energies should be favored as the P-wave interaction becomes dominant. An observation of both final pions is required to determine the relevant angle and energy. As discussed in the previous paragraph, it is difficult to make a reliable estimate of these effects using the present phenomenological approach.

According to the model proposed here, the P-wave, $T=1$, π-π interaction should dominate for $E_{\text{inc}} > 400$ Mev. It follows that the charged-to-neutral production ratio $(\pi^- + p \to \pi^- + \pi^+ + n)/(\pi^- + p \to \pi^- + \pi^0 + p)$ is predicted to be 2, the square of the ratio of the pion-nucleon coupling constants for charged and neutral meson emission. This interaction also yields no production of $2\pi^0$. For $\pi^+ + p$, only the reaction $\pi^+ + p \to \pi^+ + \pi^0 + p$ is permitted by the $T=1$ interaction. As a result, the inelastic cross section for $\pi^+ + p$ should be 1/3 that for $\pi^- + p$; experimentally,[8,9] for $E_{\text{inc}} \approx 500$ Mev, this ratio is about 1/4. Since the probability of finding two pions in the nucleon cloud is small, this model also predicts that double-pion production should be unlikely compared to single-pion production.

*This work was supported in part by a grant from the National Science Foundation.

[1]W. A. Perkins et al., preceding Letter [Phys. Rev. Letters 3, 56 (1959)].

[2]L. S. Rodberg, Phys. Rev. 106, 1090 (1957); E. Kazes, Phys. Rev. 107, 1131 (1957).

[3]This relation is suggested by the dispersion-theoretic approach of G. F. Chew and S. Mandelstam, University of California Radiation Laboratory Report UCRL-8728 (unpublished).

[4]W. R. Frazer and J. R. Fulco, Phys. Rev. Letters 2, 365 (1959). The π-π energies involved in our problem are too small to obtain any indication of the resonance which they require. At higher energies there is some indication of a peak in the inelastic cross section at the expected energy (reference 8). See also G. Takeda, Phys. Rev. 100, 440 (1955).

[5]G. F. Chew and R. E. Low, Phys. Rev. 101, 1579 (1956).

[6]V. Perez-Mendez (private communication).

[7]C. Goebel, Phys. Rev. Letters 1, 337 (1958); G. F. Chew and F. E. Low, Phys. Rev. 113, 1640 (1959). As these authors point out, the sharp diffraction peak observed in elastic pion-nucleon scattering provides another indication of a strong π-π interaction.

[8]Blevins, Block, and Leitner, Phys. Rev. 112, 1287 (1958).

[9]R. R. Crittenden et al., Phys. Rev. Letters 2, 121 (1959).

CONSEQUENCES OF ATOMIC CONVERSION FOR THE INTERPRETATION OF EXPERIMENTS ON THE SPIN-DEPENDENCE OF MUON ABSORPTION*

V. L. Telegdi
The Enrico Fermi Institute for Nuclear Studies, The University of Chicago, Chicago, Illinois
(Received June 1, 1959)

The ground state of a μ-mesonic atom of nonzero nuclear spin I is split by the hyperfine interaction into two states, of total angular momenta $F = I \pm \frac{1}{2}$. It was pointed out by Bernstein, Lee, Yang, and Primakoff[1] (hereinafter referred to as BLYP) that (a) the lifetimes of the members of this doublet may, as a consequence of the incoherence of the two states, be distinct, and that (b) these lifetimes will actually differ if the muon absorption rate depends on F, i.e., if the relevant weak interaction is at least partly spin-dependent. The total muon disappearance rate is the sum of the absorption and the decay rates, and the latter is indeed to an excellent approximation independent of F. BLYP estimated the fractional difference δ between the two lifetimes on the basis of a simple nuclear model,[2] and suggested an experimental test for the spin-dependence of muon absorption: Demonstrate that the rate of appearance of decay electrons (originating from μ^- bound in a monoisotopic target with $I \neq 0$) does not, as a function of time, follow a simple exponential. The logarithm of the decay curve should indeed exhibit (in the sense defined below) a positive curvature proportional to δ^2. This quadratic dependence would of course prevent one, as BLYP emphasized, from establishing which member of the doublet absorbs faster, i.e., from settling a question of particular theoretical significance.

In the discussion of BLYP it was assumed implicitly that atomic processes do not contribute to the lifetime of either state, and in particular that the energetically higher member of the doublet cannot be converted into the lower one at an appreciable rate. Such a conversion could take place in principle by the ejection of Auger electrons and, to a lesser extent, by $M1$ radiation. It is the purpose of this note to explore the experimental consequences of such atomic conversion processes which, in our opinion, may not be negligible in situations of actual physical interest.

We refer to the higher state of the doublet by 1, to the lower one by 2, and indicate the muon disappearance rates by λ_1 and λ_2, respectively; let R stand for the conversion rate from 1 to 2. The populations n_1 and n_2 of 1 and 2 are governed by

$$dn_1/dt = -(\lambda_1 + R)n_1,$$
$$dn_2/dt = -\lambda_2 n_2 + Rn_1, \qquad (1)$$

as a function of time, t. The rate of appearance of decay electrons is for all t proportional to $\lambda_0(n_1+n_2)$, indicating with λ_0 the muon decay rate (by hypothesis the same for 1 and 2). In the experiment proposed by BLYP, one measures the curvature K of $f(t) = \log(n_1+n_2)$. We adopt the standard definition

$$K = f''(1+f'^2)^{-3/2}, \qquad (2)$$

where the primes indicate differentiation with respect to t. The sign of K is determined by the sign of f''. From (1) one has directly

$$f'' = [(\lambda_1-\lambda_2)^2 n_1 n_2 + (\lambda_1-\lambda_2)Rn_1(n_1+n_2)]/(n_1+n_2)^3, \qquad (3)$$

which shows that $K \geq 0$ when $R = 0$, i.e., in the case considered by BLYP. The curvature will, however, necessarily be negative ($K < 0$) when the inequalities

$$\lambda_1 - \lambda_2 < 0, \qquad (4a)$$
$$R > |\lambda_1 - \lambda_2|/(1 + n_1/n_2), \qquad (4b)$$

obtain under the conditions of the experiment. (4b) is of course a function of time; as K goes monotonically to zero with increasing t,

$$R > |\lambda_1 - \lambda_2|/[1 + n_1(0)/n_2(0)], \qquad (4b')$$

is sufficient to ensure, with (4a), $K < 0$ for all t.

Odd Z - odd A nuclei, the most suitable targets for the BLYP experiment, have in general magnetic moments μ_N in agreement with the picture of an $I_{L\pm\frac{1}{2}}$ unpaired proton. The sign of μ_N determines which of the states $F = I \pm \frac{1}{2}$ lies lowest, so that (4a) can be written as

$$\lambda_- > \lambda_+ \quad \text{when} \quad \mu_N > 0, \quad (I = L + \tfrac{1}{2}) \qquad (5a)$$
$$\lambda_+ > \lambda_- \quad \text{when} \quad \mu_N < 0, \quad (I = L - \tfrac{1}{2}) \qquad (5b)$$

indicating with $\lambda_{+(-)}$ the disappearance rate in the $F = I + (-)\frac{1}{2}$ state. [Note that N^{15} is the sole relevant nuclide for which (5b) applies.] The extreme case of a nucleus with $\mu_N > 0$ is the proton; condition (5a) requires hence that muon absorption proceed faster from the singlet than from the triplet state in the basic absorption act. This will be the case when the ratio of the Gamow-Teller and of the Fermi coupling constants is negative,[3] e.g., for the V-A interaction now well established in many weak reactions. Condition (5b) may also be fulfilled by the <u>same</u> type of coupling, because here the muon and the proton are in a relative singlet state when $F = I + \frac{1}{2}$.

Assuming that the members of the doublet are statistically populated at $t = 0$, condition (4b′) becomes

$$R/|\lambda_+ - \lambda_-| > I/(2I+1) \quad \text{when} \quad \mu_N > 0, \qquad (6a)$$
$$R/|\lambda_+ - \lambda_-| > (I+1)/(2I+1) \quad \text{when} \quad \mu_N < 0. \qquad (6b)$$

For Al ($Z = 13$, $I = \frac{5}{2}$) a detailed calculation,[2] based on a $V - xA$ type interaction and the measured[4] muon absorption rate, gives $\lambda_- - \lambda_+ = 1.2\times10^5$ sec^{-1}. According to a recent estimate,[5] the conversion by Auger effect on the conduction electrons in metallic Al should occur at a rate $R \approx I(2I+1)^{-1}\times 1.5\times10^6$ sec^{-1}. Thus, even if this estimate were too high by a factor two, (6a) should be amply fulfilled for Al. As $|\lambda_+ - \lambda_-| \sim 1/Z$, while $R \sim Z^a$ (with $a > 1$), elements with $Z > 13$ should <u>a fortiori</u> yield $K < 0$.

We conclude that in the BLYP experiment

(a) a negative <u>curvature</u> can arise only if the basic muon absorption process is faster for antiparallel muon and proton spins, e.g. for a V-A type interaction;

(b) a zero curvature does not necessarily imply the absence of spin dependence;

(c) the conversion rates from the higher to the lower member of the μ-mesonic hyperfine doublet are for $Z \geq 13$ sufficiently large to lead to a negative curvature once the condition (a) holds.

These conclusions, in particular (c), have an obvious bearing on the neutron asymmetry ef-

fects in μ-capture recently discussed by Überall.[6]

The author was prompted to the considerations presented here some time ago by preliminary experimental results[7] which suggest that $K<0$ for Al; he is grateful to R. Winston for assistance with the analytic formulation of the curvature problem. He takes pleasure in thanking H. Primakoff and J. Bernstein, who had independently drawn similar conclusions, for much friendly advice.

---

* Research supported by a joint program of the Office of Naval Research and the U. S. Atomic Energy Commission.

[1]Bernstein, Lee, Yang, and Primakoff, Phys. Rev. 111, 313 (1958).

[2]For more detailed and model-independent calculations, see H. Primakoff, Revs. Modern Phys. (to be published).

[3]T. D. Lee gave a particularly simple argument for this at the 1958 Midwest Theoretical Physics Conference at St. Louis (p. 189 of the mimeographed proceedings).

[4]J. C. Sens, Phys. Rev. 113, 679 (1959).

[5]This estimate was made by H. Primakoff and the author, and supersedes the one in footnote 16a of reference 2. R depends primarily on the probabilities for finding the $3s$ conduction electrons and the Auger emitted electrons near $r=0$. In this estimate $|\psi_{3S}(0)|^2 = y/\pi a_0^3$, and $|\psi_v(0)|^2 = 2\pi Z^*\alpha c/v$ were assumed, and $y=2.2$ was inferred from Knight shift and optical hfs data. One finds, for an $F=I+\frac{1}{2}\rightarrow F=I-\frac{1}{2}$ transition,

$$R = I(2I+1)^{-1}(64\pi/9)Z^*\alpha^5 y(m_e/m_\mu)^3 m_\mu c^2/\hbar,$$

and $10 \leq Z^* < 12$ for Al.

[6]H. Überall (to be published).

[7]Lathrop, Lundy, Swanson, Telegdi, Yovanovitch, and Winston (unpublished).

SUPPRESSION OF P-STATE CAPTURE IN (K^-, p) ATOMS*

T. B. Day, G. A. Snow, and J. Sucher
Department of Physics, University of Maryland, College Park, Maryland
(Received June 3, 1959)

It is of obvious importance, in studying the reactions of K^- mesons at rest in liquid hydrogen or deuterium, to have some idea of the atomic orbit from which the K mesons are captured. Since the low-energy scattering data[1] seem to indicate a large S-wave interaction, it is simplest to ignore P-wave contributions and assume that the reactions take place from the $1S$ orbit. (In the case of deuterium, even the neglect of P-wave interactions does not prevent an appreciable capture from the $2P$ orbit.[2])

However, this neglect, in the case of hydrogen, of the $2P$ orbit contributions has been very hard to justify. Since transition rates due to K^--p interactions are so very much greater than those of radiative transitions, even a very small P-wave interaction can compete favorably with the radiative $2P\rightarrow 1S$ transition rate, as long as the $2P$ state is occupied at all. Moreover, it is usually argued that the cascading mesons will predominantly pass through the $2P$ state (except for loss due to the direct capture from higher nS orbits) since the nature of the selection rules for dipole radiation favors populating the circular orbits.

We would like to point out in this note that successive Stark effect collisions of a highly excited (K^-, p) atom with nearby protons in the liquid hydrogen will drastically reduce the probability that the K^- meson ever reaches the $2P$ orbit.

Consider the following picture. The (K^-, p) atom is moving with some velocity $v(\sim 10^5$ cm/sec from considerations of thermal motion, recoil from previous radiative transitions, and possible pickup of the K^- in flight) through the liquid hydrogen. The average radius of a unit sphere (hereinafter called a unit cell) in liquid hydrogen (density 0.07 g/cc)[3] is ~1.8 A. Hence, on the average about one in ten traversals of a unit cell will result in the mesonic atom's passing within a distance of one electron Bohr radius from a proton, and thus being subjected to the intense electric field of the proton.[4] To estimate the transition rates due to this Stark effect, let us compute it in the $n=6$ level, between the $6P$ and $6S$ states.

A measure of this rate is given by

$$\gamma_S(6P\rightarrow 6S) = |\langle 6S|\vec{E}\cdot\vec{r}|6P\rangle| \simeq E_{\mathrm{Av}}(a_0)\langle 6S|r\cos\theta|6P\rangle, \quad (1)$$

where $E_{\mathrm{Av}}(a_0)$ is some average electric field due to the proton at one Bohr radius, and $r\cos\theta$ refers to the K^- meson's coordinate. One ob-

tains[5]

$$\langle 6S|r\cos\theta|6P\rangle = 30.8\, a_{K^-}, \tag{2}$$

where a_{K^-} is the K-meson Bohr radius, and

$$E_{\mathrm{Av}}(a_0) \sim e^2/a_0^2. \tag{3}$$

Then, we find

$$\gamma_S(6P\text{–}6S) \simeq 2.0\times10^{15}\ \mathrm{sec}^{-1}. \tag{4}$$

This is comparable to the direct capture transition rate from the $6S$ level,[6] given by

$$\gamma_c(nS) = (4.7\times10^{17})/n^3\ \mathrm{sec}^{-1}, \tag{5}$$

$$\gamma_c(6S) = 2.2\times10^{15}\ \mathrm{sec}^{-1}. \tag{6}$$

The radiative $6P$–$1S$ transition rate (obtained from Table XV of reference 5 upon multiplication by the K^--p reduced mass $= 648m_e$) is

$$\gamma_R = 1.26\times10^{10}\ \mathrm{sec}^{-1}. \tag{7}$$

Stark transition rates for other possible $(n, l \rightarrow n, l\text{-}1)$ transitions will be comparable in magnitude to that of Eq. (4), and decrease as n decreases, so that at $n=2$,

$$\gamma_S(2P\text{–}2S) \simeq 0.2\times10^{15}\ \mathrm{sec}^{-1}. \tag{8}$$

Note that γ_S is much larger than the reciprocal of the transit time ($\sim10^{13}\ \mathrm{sec}^{-1}$), which, in turn, is much larger than γ_R. Hence, during the time that a highly excited mesonic atom is within a Bohr radius of a hydrogen atom,[7] radiative transitions can be ignored, while many Stark transitions can take place, so that some steady-state distribution is approached. Ignoring, for the moment, the capture from the nS state, we approximate the equilibrium distribution due to the Stark transitions with a simple $(2l+1)$ distribution.[8] Now, when the capture from the nS state is included, the nP (and, of course, the nS) states are immediately depopulated.[9] Hence, we expect that in each close collision, an appreciable fraction of the K^- mesons in the n level are lost due to capture from the nS state.

We are now in a position to make a quantitative estimate of the total effect. Since the Bethe and Salpeter tables only go up to $n=6$, we use that level as an example of a starting level and proceed as follows. Take 3600 K mesons distributed in the $6S$ to $6H$ level with a $(2l+1)$ weighting at time equal to zero. Let the mesonic atoms move and decay via radiative transitions for the time necessary to cross 10 unit cells.[10] After that time consider the atoms as passing within a Bohr radius of a neighboring proton. This has the effect, as noted above, of completely depopulating the $6P$ level and reshuffling the remaining particles into a $(2l+1)$ distribution again. Then start again with the new $(2l+1)$ distribution on another 10-cell journey, etc.

A lower limit for the total loss in the first 10-cell journey is[11] 300 particles from $6P$ plus 16.9 from $6D$, $6F$, $6G$, and $6H$ combined. When the 3600 K^- mesons are gone, the loss due to $6P$–$6S$ $\rightarrow$capture will be $(3/3.169)\times3600$ $(=3408)$. The remaining K^- mesons are lost by direct radiative transitions and are distributed as in Table I. Thus, Table I shows that only ~45 K^- mesons of the original 3600 get to the $2P$ level by direct $6D$–$2P$ radiative transitions. On following the cascading mesons through the lower levels, which are also subject to the Stark effect, one finds that the population of the $2P$ level is raised to ~52 out of the original 3600.

So $\lesssim1.4\%$ of the K^- mesons starting in the $n=6$ level distributed according to a $(2l+1)$ distribution reach the $2P$ level. Furthermore, similar considerations apply at even higher n levels. To estimate the percentage of those starting in a higher level which reach the $2P$ level, we use the fact obtained from the $n=6$ level calculation, that most of the particles reaching $2P$ came via direct $6D$–$2P$ radiative transitions. This percentage was directly proportional to the radiative transition rate for $6D$–$2P$. For a given initial l, the radiative transition rate goes as n^{-3} (see reference 4).

For example, at $n=15$, the S-state nuclear capture rate is still much faster than all radiative rates and the inverse of the transit time. Hence, our conditions are still fulfilled, and

Table I. Distribution by radiation from $n=6$ levels, starting with 3600 particles distributed in the $6S$ to $6H$ states with a $(2l+1)$ weighting. (All levels shown are taken as stable for purposes of the diagram.)

5P/3.71	5D/8.9	5F/17.5	5G/31
4P/7.98	4D/16.0	4F/21.5	
3P/17.36	3D/26.1		
2P/44.59			

now, of those mesons which start in an $n=15$ level, the percentage that reaches the $2P$ state becomes ~0.1%. Thus, our calculations indicate that of the K^- mesons captured by protons in liquid hydrogen in highly excited states, $\lesssim 1\%$ will ever reach the $2P$ level.[12]

The above result implies that when a K^- meson comes to rest in liquid hydrogen, the nuclear capture reaction essentially always occurs with the relative orbital angular momentum of the (K^-,p) system equal to zero. This has many important consequences:

1. The isotropic angular distributions of the decays of Σ^+, Σ^-, and Λ^0 hyperons[13] produced from (K^-,p) captures at rest shows, according to the arguments of Treiman,[14] that the spins of these three hyperons are each equal to one-half.

2. The relation between the data for (K^-,p) reactions in flight and those for (K^-,p) captures at rest, assumed by many authors,[15] is now justified. In addition, the $(\Lambda^0,2\pi)$ production data from (K^-,p) atoms can be used to determine the parity of the K^- meson relative to the (Λ^0,p) system.[16]

3. The predictions of Amati and Vitale[17] concerning the branching ratios from (K^-,p) capture reactions at rest, based on the assumption of global symmetry, may now more significantly be compared with existing data. Subject to the reservations pointed out by Dalitz,[18] the data violate the predicted inequality.

4. It is expected that the Stark effect transitions will also dominate in the capture at rest of $\bar{p}$, Σ^-, and Ξ^- hyperons in hydrogen, so that it is justified to assume that the capture reactions take place from S states.

5. Similar considerations are expected to hold for captures at rest of K^-, Σ^-, and Ξ^- particles in deuterium.

The results of this calculation indicate that essentially no mesonic x-rays should be produced when a K^- meson comes to rest in liquid hydrogen. This result can be checked experimentally with a search for such x-rays.

We are indebted to Professor L. Madansky for suggesting the possible importance of the Stark effect in (K^-,p) mesonic atoms, and to Dr. R. G. Glasser for directing our attention to the higher n levels.

*This research was supported in part by the U. S. Air Force through the Air Force Office of Scientific Research of the Air Research and Development Command and in part by the U. S. Atomic Energy Commission.

[1] Norden, Rosenfeld, Solmitz, Tripp, and Watson, Bull. Am. Phys. Soc. 4, 24 (1959); A. H. Rosenfeld, Bull. Am. Phys. Soc. 3, 363 (1958); M. F. Kaplon, 1958 Annual International Conference on High-Energy Physics at CERN, edited by B. Ferretti (CERN, Geneva, 1958), p. 171. R. S. White (private communication); R. D. Hill (private communication).

[2] T. B. Day and G. A. Snow, Phys. Rev. Letters 2, 59 (1959).

[3] For experiments in a hydrogen bubble chamber, a density of 0.059 g/cc should be used. This has the effect of increasing the population of the $2P$ state slightly over the estimates given in this paper.

[4] We assume that the electron shields the proton's field completely beyond one Bohr radius, and that there is no shielding within a Bohr radius.

[5] H. A. Bethe and E. E. Salpeter, Quantum Mechanics of One- and Two-Electron Atoms (Springer-Verlag, Berlin, 1957), p. 253.

[6] G. Frye, Phys. Rev. 113, 688 (1959).

[7] For distances of approach to the proton, R, smaller than a_0, $\gamma_S(R)=\gamma_S(a_0)(a_0/R)^2$.

[8] We have looked at the simple problem of three degenerate levels coupled by Stark transitions (radiative and capture transitions are ignored) and find that in the Stark reshuffling very good mixing is achieved.

[9] If we consider only the nP and nS levels as being coupled by Stark transitions, but include the capture from the nS state, the population of the nP level decays exponentially with a decay constant Γ given by

$$\Gamma \sim \tfrac{1}{2}\gamma_c(nS), \quad 4\gamma_S \gtrsim \gamma_c, \tag{a}$$

$$\Gamma \sim \tfrac{1}{4}\gamma_c(nS)\,|\,4\gamma_S/\gamma_c|^2, \quad 4\gamma_S \ll \gamma_c\,. \tag{b}$$

For $n \gtrsim 4$, Γ is much larger than the reciprocal of the transit time. However, for $n=2$, $\Gamma \sim 2\times10^{12}$ sec^{-1} compared with $\gamma_R(2P\to1S)=4\times10^{11}$ sec^{-1}. Thus, in integrating over the path of the (K^-,p) system in a $2P$ state, the Stark effect is rather small, especially when the $2S$ level shift due to nuclear capture is included [not done in Eq. (b) above].

[10] This average time for crossing one unit sphere is $\frac{3}{4}(2R_0/v)$ where R_0 is the radius of the unit sphere ~1.8 A, and v is the velocity. The same factor $\frac{3}{4}$ applies in crossing, on the average, a sphere of radius equal to one Bohr radius.

[11] This estimate of the loss underestimates the true effect since successive repopulation and depletion of the nP level many times within one collision is ignored.

[12] Clearly the results depend on the exact value chosen for the velocity. The loss due to radiation, and hence the percentage reaching the $2P$ state, is inversely proportional to this velocity. However, the velocity would have to be changed by a large factor to change the absolute percentages appreciably.

[13] L. Alvarez et al., Nuovo cimento 5, 1026 (1957).

[14] S. B. Treiman, Phys. Rev. 101, 1216 (1956).

[15] R. H. Dalitz and S. F. Tuan, Ann. Phys. (to be

published); Jackson, Ravenhall, and Wyld, Nuovo cimento 9, 834 (1958).

[16] L. B. Okun' and I. Ia. Pomeranchuk, J. Expti. Theoret. Phys. (U.S.S.R.) 34, 997 (1958) [translation: Soviet Phys. JETP 34, 688 (1958)].

[17] D. Amati and B. Vitale, Nuovo cimento 9, 895 (1958).

[18] R. H. Dalitz, 1958 Annual International Conference on High-Energy Physics at CERN, edited by B. Ferretti (CERN, Geneva, 1958), p. 197.

S-MATRIX POLES IN THE DETERMINATION OF PARITIES*

G. Feldman and T. Fulton
John Hopkins University, Baltimore, Maryland
(Received May 18, 1959)

Recently it has been conjectured[1] that there exist dispersion relations in momentum transfer variables. A number of authors[2,3] have suggested using an approximation to these relations in order to determine such physical quantities as parities, coupling constants, etc. This approximation consists of extracting the contribution of certain single-particle intermediate states ("the pole terms") to S-matrix elements, and analyzing the experimental data on the assumption that these contributions predominate. In this note we wish to point out some potential difficulties inherent in such an analysis.

One of the processes which has been examined in reference 2 is the production of Λ's in π-proton collisions, that is

$$\pi^- + p \rightarrow \Lambda + K^0. \qquad (1)$$

If we assume that the Mandelstam conjecture[1] is justified, there is a term in the matrix element of process (1) from the K-meson intermediate state illustrated in Fig. 1(a). This term will contribute provided the vertex parts

$$\langle K^0 | j_{\pi^+} | K^+ \rangle, \quad \langle \Lambda | j_{K^+} | p \rangle \qquad (2)$$

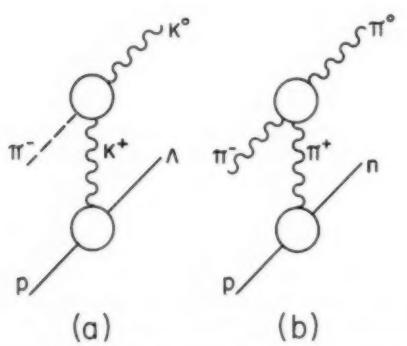

FIG. 1. Possible pole contributions for the processes $\pi^- + p \rightarrow \Lambda + K^0$ and $\pi^- + p \rightarrow n + \pi^0$.

do not vanish. In this case the matrix element will have a pole in $\cos\theta$ (θ being the angle between the incoming π meson and outgoing K in the center-of-mass system) at a point α_0. This point is in the nonphysical region, but can be near $\cos\theta = 1$. There are, of course, contributions to the matrix element arising from other intermediate states, for example the ones in which there is both a K and a π meson. These terms lead to a branch point in $\cos\theta$ at the point α_1. Specifically, for a π-meson lab energy of 1.9 Bev, $\alpha_0 = 1.24$ and $\alpha_1 = 1.40$.

If one plots $F(\cos\theta)$ using the experimental data, where

$$F(\cos\theta) = (\alpha_0 - \cos\theta)^2 d\sigma/d\Omega, \qquad (3)$$

it is claimed that one can obtain direct evidence for or against the presence of the pole term. The single experiment, namely the angular distribution for process (1) at a fixed energy, could be used to prove that the vertex parts (2) do not vanish. Hence it would follow that the relative K^+-K^0 parity is odd.

We wish to examine reactions analogous to process (1). Our aim is to show that use of the type of analysis discussed above may lead to ambiguous, and possibly incorrect, conclusions. Accordingly, we shall first consider the experimental angular distribution[4] for the process

$$\pi^- + p \rightarrow \pi^0 + n \qquad (4)$$

at a fixed π-meson kinetic energy of 220 Mev in the laboratory system. In strict analogy to the method outlined for process (1), we consider whether the experimental information sheds any light on the existence of the π^+-meson intermediate state illustrated in Fig. 1(b). The matrix element $M(\cos\theta)$ (θ is the center-of-mass scattering angle) for process (4) is, apart from kinema-

tic factors, of the form

$$M(\cos\theta) \sim \frac{f g \bar{u}_p \Gamma u_n}{(c_0 - \cos\theta)} + T(\cos\theta), \qquad (5)$$

where

$$f = \langle \pi^+ | j(0)_{\pi^0} | \pi^+ \rangle, \qquad (6)$$

$$g \bar{u}_p \Gamma u_n = \langle p | j(0)_{\pi^-} | n \rangle, \qquad (7)$$

and $\Gamma = 1\,(\gamma_5)$ depending on whether the π^+ has even (odd) parity relative to the p-n system. The constant c_0 is given by

$$c_0 = 1 + \tfrac{1}{2}\mu^2/k^2, \qquad (8)$$

where k is the π-meson momentum in the center-of-mass system. The next singularity, a branch point arising from intermediate states of two π mesons, occurs at c_1, where

$$c_1 = 1 + 2\mu^2/k^2. \qquad (9)$$

At 220-Mev lab energy,

$$c_0 = 1.16 \quad \text{and} \quad c_1 = 1.64. \qquad (10)$$

We define

$$G(\cos\theta) = (c_0 - \cos\theta)^2 d\sigma/d\Omega. \qquad (11)$$

$G(\cos\theta)$ is a function regular at $\cos\theta = c_0$. Since the nearest singularity is at $\cos\theta = c_1$, one may expand G about c_0 in a power series whose radius of convergence is $c_1 - c_0$. Chew[3] suggests the use of experimental data within this circle of convergence in extrapolation to the pole.[5] If we further assume that the pole is dominant in this region, we obtain the result

$$G(\cos\theta) = (c_0 - \cos\theta)^2 \sum_{\text{spins}} |M(\cos\theta)|^2$$

$$\sim f^2 g^2 (1 - \cos\theta), \qquad (12)$$

where we have taken $\Gamma = \gamma_5$. (The result using $\Gamma = 1$ is markedly different.)

In Fig. 2 we plot the experimental points for $G(\cos\theta)$ in the region $1 \geq \cos\theta \geq 0$. We observe that these points can be fitted to a straight line passing through $\cos\theta = 1$, i.e., the distribution (12). One might consider this as evidence for the presence of the π^+-meson intermediate state. This implies that the vertex part (6) is nonzero and forces the untenable conclusion that the π^0 meson is a scalar (or that parity is not conserved in strong interactions). Also plotted in Fig. 2 is the result obtained using the best fit for the experimental $d\sigma/d\Omega$ as determined in reference 4.

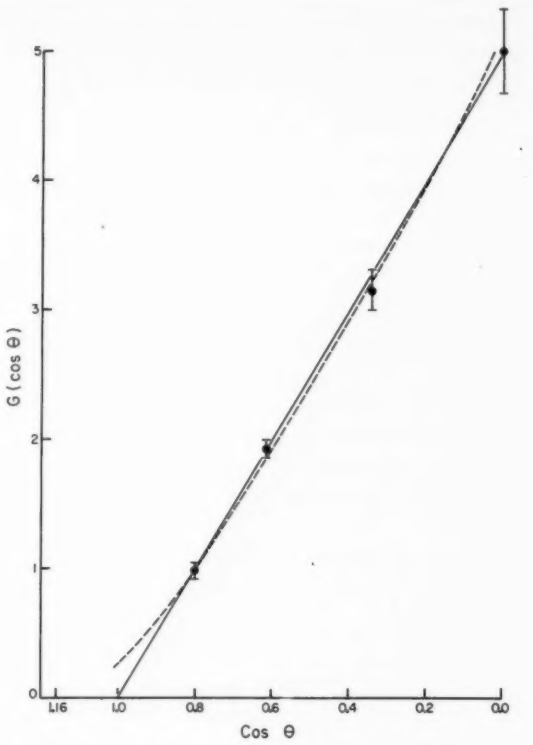

FIG. 2. Plot of $G(\cos\theta) = (c_0 - \cos\theta)^2 d\sigma/d\Omega$ ($c_0 = 1.16$) for π^--p charge-exchange scattering at 220 Mev. The experimental data are from reference 4. The straight line is obtained on the assumption that the pole term is dominant. The dashed curve is based on the best fit to $d\sigma/d\Omega$ given in reference 4. Errors in this curve are not shown.

If we apply the Chew criterion[3] to this case, we would be restricted to using experimental data in the region $1 \geq \cos\theta \geq 0.68$. The best fit to the experimental data extrapolated to this region no longer lies on the straight line through $\cos\theta = 1$. However, one need not have assumed that only the pole contributes. To prove that the pole term is not present, it is necessary to show unambiguously that $G(\cos\theta)$ has a second order zero at $\cos\theta = c_0$.

One can carry out a similar procedure for the reaction

$$\pi^- + p \to \pi^- + p, \qquad (13)$$

at 220 Mev. Again, in the absence of other information, we can ask whether the experimental angular distribution indicates the existence of the π^0 intermediate state. The analysis proceeds

as before. Once more, one cannot rule out the presence of this pole. Its existence would imply, in this case, that parity is not conserved in strong interactions.

The illustrations we have employed indicate that attempts to establish the presence or absence of certain vertex parts (and thus determine parities) by the above means are, at best, questionable. Of course, to make our point we have been selective in the choice of experiments. Nevertheless, this is in keeping with the spirit of the pole approximation as presently advocated.

The conjecture that poles in $\cos\theta$ appear in the S matrix is no doubt reasonable. However, an analysis of experiments which assumes that the poles predominate may require accurate measurements sufficiently close to the pole, yet far from other singularities. What is meant by "accurate," "sufficiently close," and "far" is somewhat nebulous. In fact, in the above illustrations [and in process (1)], in order to establish the presence or absence of a pole, it is necessary to distinguish between a possible zero near $\cos\theta = 1$ and a double zero at $\cos\theta = c_0$ (or α_0). At higher energies the poles approach the physical region, that is the points $\cos\theta = \pm 1$. Analysis of experiments at these higher energies probably would not eliminate the ambiguities, since the other singularities also approach these limit points.

---

*Supported in part by the National Science Foundation and the Office of Scientific Research.

[1]S. Mandelstam, Phys. Rev. 112, 1344 (1958).

[2]J. G. Taylor, Nuclear Phys. 9, 357 (1959); J. G. Taylor (to be published).

[3]G. F. Chew, Phys. Rev. 112, 1380 (1958); G. F. Chew and F. E. Low, University of California Radiation Laboratory Report UCRL-8427 (unpublished); Taylor, Moravcsik, and Uretsky, Phys. Rev. 107, 563 (1957); M. Moravcsik, Phys. Rev. Letters 2, 352 (1959); S. Barshay and S. Glashow, Phys. Rev. Letters 2, 371 (1959).

[4]Ashkin, Glaser, Feiner, and Stern, Phys. Rev. 105, 724 (1959).

[5]The corresponding circle of convergence for process (1) lies entirely outside of the physical region. Nevertheless, Taylor[2] has suggested using data in the region $1 \geq \cos\theta \geq 0$.

ERRATA

INTEGRATION OF SECONDARY CONSTRAINTS IN QUANTIZED GENERAL RELATIVITY. P. W. Higgs [Phys. Rev. Letters 1, 373 (1958)].

In this Letter[1] it was stated that three of the secondary constraints[2] in the quantized theory of gravitation are equivalent to the statement that the wave functional $\Psi\{g_{rs}(x)\}$ is invariant under general transformations of the three coordinates x. From this the conclusion was drawn that Ψ must depend only on the three eigenvalues of the Ricci tensor $R_{rs}(x)$. (As before, Latin indices run from 1 to 3; Greek indices from 0 to 3.) It appears on more careful examination of the transformation properties of Ψ that the former statement is not quite correct, so the conclusion is erroneous. The purpose of the present note is to clarify the invariance properties of Ψ and to present the correct solution of the secondary constraints

$$\mathcal{H}_u \Psi = 0, \tag{1}$$

where

$$\mathcal{H}_u = g_{rs,u}\pi^{rs} - 2(g_{ru}\pi^{rs})_{,s} \quad \text{with} \quad \pi^{rs} = -i\delta/\delta g_{rs}$$

Let us consider just the localized transformations of the three spatial coordinates, $x'^r = x^r + a^r(x)$, where the infinitesimal functions $a^r(x)$ vanish at infinity. Then

$$\delta g_{rs}(x) = -(a^u g_{rs,u} + a^u{}_{,r} g_{us} + a^u{}_{,s} g_{ru}),$$

and so, the primary constraints having been

satisfied already,

$$\delta\Psi = \int d^3x\, \delta g_{rs}(x)\delta\Psi/\delta g_{rs}(x)$$

$$= -i\int d^3x\, a^u(x)\mathcal{H}_u(x)\Psi - 2i\int dS_r\, a^u(x) g_{us}\pi^{rs}\Psi.$$

The first term vanishes if the constraint (1) is satisfied; the second is an integral over the surface at infinity which vanishes only if $a^u(x)$ is localized. We therefore have to construct functionals $\Psi\{g_{rs}(x)\}$ which are invariant only under localized transformations.

The problem is solved by transforming g_{rs} into a form which satisfies certain transversality conditions:

$$g_{rs}(x) = y^a{}_{,r}\, y^b{}_{,s}\, g^T{}_{ab}(y).$$

If $y^a(x)$ are three independent functions such that the differences $y^a - x^a$ are localized and $g^T{}_{ab}$ satisfies suitable conditions, then we know that Ψ is independent of y^a. By suitable conditions we mean that $g^T{}_{ab}$ has only three independent components and the functions y^a are uniquely determined by $g_{rs}(x)$ together with these conditions. It turns out that the well-known harmonic coordinate conditions fulfill these criteria.

It is convenient to introduce the contravariant densities h^{rs}, related to g_{rs} by $h^{rs}g_{st} = (-g)^{1/2}\delta^r{}_t$. Then we define the "transverse gravitational potentials"

$$h^{Tab}(y) = (\det y^c{}_{,t})^{-1} y^a{}_{,r}\, y^b{}_{,s}\, h^{rs}(x), \qquad (2)$$

where $y^a(x)$ is the regular solution of the generalized Laplace equation

$$(h^{rs}y_{,r})_{,s} = 0 \qquad (3)$$

which satisfies the asymptotic condition (localization)

$$\lim_{|x|\to\infty}(y^a - x^a) = 0 .$$

The functions y^a and consequently also the transverse potentials are uniquely determined by $g_{rs}(x)$. The constraints (1) now tell us that $\Psi = \Psi\{h^{Tab}(y)\}$. The transversality condition, which follows from (2) and (3), is

$$h^{Tab}{}_{,b} = 0, \qquad (4)$$

so there are only three independent transverse components. They may be exhibited explicitly by performing a Fourier transformation and resolving the transform of h^{Tab} parallel and perpendicular to the wave vector k_a: we define

$$\gamma^{ij}(k) = \int d^3y \exp(-ik\cdot y) e^i{}_a e^j{}_b [h^{Tab}(y) + \delta^{ab}], \qquad (5)$$

where $e^i{}_a(k)$ is an orthonormal triad of vectors (the scalar product here is Euclidean) such that $k_a = |k| e^3{}_a$. Then, by (4) and (5), the only non-vanishing components of γ^{ij} are γ^{11}, γ^{22}, $\gamma^{12} = \gamma^{21}$. [In addition, the reality condition $\gamma^{ij}(-k) = \gamma^{*ij}(k)$ is to be imposed.] Finally, the wave functional may be written as $\Psi\{\gamma^{ij}(k)\}$.

The transverse potentials which have been defined here reduce in the linearized theory to those which were obtained by Arnowitt and Deser,[3] except that their γ^{ij} was traceless on account of the eighth constraint. It remains to be seen whether Dirac's $\mathcal{H}_L$ condition implies a similar restriction in the full theory.

[1]Equation (11) of this paper should read

$$[\mathcal{H}_u(x), \mathcal{H}_L(y)] = i\mathcal{H}_L(x)\partial/\partial x^u \delta^{(3)}(x-y).$$

[2]P. A. M. Dirac, Proc. Roy. Soc. (London) A246, 333 (1958).

[3]R. Arnowitt and S. Deser, Phys. Rev. 113, 745 (1959).

EFFECT OF NUCLEAR ELECTRIC DIPOLE MOMENTS ON NUCLEAR SPIN RELAXATION IN GASES. P. A. Franken and H. S. Boyne [Phys. Rev. Letters 2, 422 (1959)].

In this Letter it was estimated that careful measurements of nuclear spin relaxation times in noble gases such as He^3 and Xe^{129} could reveal the existence of nuclear electric dipole moments as small as 10^{-3} or 10^{-4} nuclear magneton. (One nuclear magneton $= eh/2Mc = e \times 10^{-14}$ cm.) Indeed, we interpreted the already available measurements on these gases to indicate upper limits of order 10^{-1} to 10^{-2} nuclear magneton.

Professor E. M. Purcell has brought to our attention that we have made a serious error in

our implicit assumption that the velocity changes due to collisions in the gas are uncorrelated. Whereas an atom does experience a random walk in its displacements it is not true that the changes in velocity due to collisions are random. For example, if an atom is moving in the x direction it is more than 50% probable that the next collision will decrease the x component of velocity. Were this not true the atoms in the gas would rapidly depart from the Maxwell-Boltzmann velocity distribution.

Since we implicitly assumed that the changes of velocity are uncorrelated, it becomes apparent that our calculation must be modified. Purcell has found, and we entirely agree, that our calculation is valid only when $\omega\tau_c \geq 1$, where ω is the Larmor frequency of the nuclear magnetic moment in the applied magnetic field and τ_c is the mean time between collisions.

In the event that $\omega\tau_c < 1$, Purcell finds, and we entirely agree, that the relaxation time we computed [Eq. (2) of the Letter] must be multiplied by the approximate factor $[1/\omega\tau_c]^2$.[1] Therefore the estimated maximum electric dipole moment must be multiplied by the approximate factor $[1/\omega\tau_c]$, which is of order 10^3 for the experiments discussed in the Letter.

It seems entirely possible that experiments could be done with He and Xe under conditions where $\omega\tau_c \cong 1$, in which case the formulas of the Letter are applicable. For magnetic fields of ~20 000 gauss and room temperature we estimate that gas pressures of ~1/20 atmosphere would be satisfactory. We see no objection to compressing or even liquifying the gases for short periods of time in order to perform the necessary spin polarization measurements. We estimate that upper limits of $\sim 10^{-2}$ nuclear magneton could still be established, but the experiments are difficult. Such upper limits would still be an improvement over what can be obtained by previously discussed methods.[2]

We wish to express our gratitude to Professor Purcell for bringing this correction to our attention, and for several valuable discussions.

---

[1]Professor Purcell has performed an exact calculation of this factor which will be submitted to the Physical Review.

[2]E. M. Purcell and N. F. Ramsey, Phys. Rev. 78, 807 (1950).

ABSTRACTS

In this section are printed the abstracts of Articles that have been forwarded to The American Institute of Physics for publication in THE PHYSICAL REVIEW. In quoting information obtained from this section before the appearance of the corresponding Article, reference should be made to "Physical Review (to be published)" rather than to this Journal.

SINGLE-PARTICLE ENERGIES IN THE MANY-FERMION SYSTEM. David J. Thouless, Lawrence Radiation Laboratory, University of California, Berkeley, California (Received January 19, 1959).

We have examined the ground state of the many-fermion system, using perturbation theory, with particular attention to Brueckner's method. A study of the single-particle propagators in the ground state of the system sheds some light on the relation between the single-particle energies used, for example, in the optical model of nuclear reactions, and Brueckner's self-consistent energies. This leads naturally to the use of a renormalization factor to allow for propagation off the energy shell. It is possible to formulate the perturbation theory entirely in terms of graphs with no fermion self-energy parts, and this method is used to examine the approximations used for this problem, and to relate more closely the calculations of the ground-state energy and of other properties of the ground state.

LOW-TEMPERATURE TRANSPORT PROPERTIES OF COPPER AND ITS DILUTE ALLOYS: PURE COPPER, ANNEALED AND COLD-DRAWN. Robert L. Powell, Hans M. Roder, and William J. Hall, Cryogenic Engineering Laboratory, National Bureau of Standards, Boulder, Colorado (Received January 22, 1959).

Experimental results between 4° and 300°K are given for (1) the thermal conductivity, electrical resistivity, and thermoelectric force and power of two high-purity coppers, one annealed and one cold-drawn 26%; and (2) the electrical resistivity of a series of seven samples of high-purity copper cold-drawn between 0% and 20% elongation. The total electronic thermal resistivities each consist of three terms: the intrinsic resistivity, W_i; the imperfection resistivity, W_0; and a deviation term, W_{i_0}, indicating the departure from strict additivity of W_i and W_0. The intrinsic thermal resistivity and intrinsic electrical resistivity vary as $T^{2.8}$ and $T^{4.5}$, respectively, contrary to the predictions of the usual transport theory using Bloch approximations and assumptions. The resistivity of pure copper is 1.545 μohm cm at 0°C. The increase in imperfection electrical resistivity is approximately linear with increase in cold-drawn elongation. However, the added resistivity is not independent of temperature (Matthiessen's rule), but is about twice as great at the ice point as it is at 4°K. The change in thermoelectric power with drawing is positive at the lower temperature, but negative above 38°K. The Lorenz number does not approach the Sommerfeld value at the lowest temperatures, but flattens out to a value considerably smaller. A qualitative discussion for each of the various effects is given.

RECOVERY OF ELECTRON-IRRADIATED COPPER. I. CLOSE PAIR RECOVERY. J. W. Corbett, R. B. Smith,* and R. M. Walker, General Electric Research Laboratory, Schenectady, New York (Received January 28, 1959).

Stage I recovery (14-65°K) of electron-irradiated, high-purity copper is shown to be composed of at least five substages: I_A, 14-24°K; I_B, 24-28.5°K; I_C, 28.5-33°K; I_D, 33-48°K, and I_E, 48-65°K. I_A, I_B, and I_C recovery are discussed in further detail. (Discussion of I_D and I_E recovery is deferred to the following paper.) I_B and I_C are shown to have the characteristics of close pair recovery. It is inferred that I_A also has these characteristics. The values of the activation energy for recovery are $E_A = 0.05 \pm 0.01$ ev, $E_B = 0.085 \pm 0.01$ ev, and $E_C = 0.095 \pm 0.01$ ev. An attempt to relate the observed close pair spectrum to specific interstitial-vacancy configurations is described.

*Now at Hanford Laboratory Operations, Hanford Atomic Products Operations, Richland, Washington.

RECOVERY OF ELECTRON-IRRADIATED COPPER. II. INTERSTITIAL MIGRATION. J. W. Corbett, R. B. Smith,* and R. M. Walker, General Electric Research Laboratory, Schenectady, New York (Received January 28, 1959).

Several experiments are presented dealing with substages I_D and I_E of stage I (10°K - 80°K) recovery in electron-irradiated pure copper. It

is concluded that both I_D and I_E represent the recovery due to the free diffusion of a defect, presumably an interstitial atom, with an activation energy for motion $E_m = 0.12 \pm 0.005$ ev. I_D is the result of correlated recovery (the interstitial returns to the vacancy from which it came) while I_E is the result of uncorrelated recovery (the interstitial travels to a distant sink). The migrating interstitial is shown to interact with vacancies, traps, and other interstitials leading, respectively, to annihilation, trapping, and cluster formation. The interaction between two interstitials leading to cluster formation is found to be comparable with the annihilation interaction between an interstitial and a vacancy. Clusters containing more than two interstitials are also formed. Previous work in copper is discussed, and it is concluded that this previous work is consistent with the above description of stage I recovery. The relationship of the present work to the general problem of assigning defect processes to the higher temperature recovery states in copper is also discussed.

*Now at Hanford Laboratory Operations, Hanford Atomic Products Operations, Richland, Washington.

SPIN-WAVE SPECTRA FOR CANTED ANTIFERROMAGNETS AND FERROMAGNETS. R. Orbach, Department of Physics, University of California, Berkeley, California (Received January 16, 1959).

The magnetic resonance conditions and the spin-wave spectra are found for canted antiferromagnetic and ferromagnetic lattices, where the cant is produced by magnetocrystalline anisotropy fields which are noncollinear. The sublattices are thereby caused to cant towards each other in antiferromagnets and away from each other in ferromagnets. The cant of the antiferromagnetic sublattices may produce a net moment (weak ferromagnetism) but does not alter appreciably the usual antiferromagnetic spin-wave spectrum in the presence of anisotropy. The static susceptibility parallel ($\chi_\parallel$) and at right angles ($\chi_\perp$) to the vector difference of the anisotropy fields is calculated, and is shown to be altered from the noncanted result. It is shown that in antiferromagnets with no apparent weak ferromagnetism, canted sublattices may still be present, and can be detected by a nonzero ratio of $\chi_\parallel$ to $\chi_\perp$ at 0°K. The ferromagnetic spin-wave spectrum shows a sudden change from the normal spectrum as soon as one introduces the noncollinear anisotropy fields. An optical branch is formed and a high-frequency $\vec{k}=0$ magnetic resonance is expected. This resonance is a consequence of the two-sublattice character of the canted ferromagnet and may be termed an exchange resonance.

PRESSURE EFFECTS IN LUMINESCENCE. II. ISOBARIC EXPERIMENTS ON NaI(Tl). L. Reiffel, Physics Research Division, Armour Research Foundation, Chicago, Illinois (Received January 5, 1959).

The effect of steady-state hydrostatic pressure on the properties of luminescent systems, with particular reference to the phosphorescence of NaI(Tl), is examined. It is shown that readily observable changes in decay mean life may be produced by very modest pressures. An interpretation of these effects is developed from a configurational coordinate model and also from thermodynamic considerations. Experimental results are in good agreement with these theoretical expectations. For a 0.66-ev trap in NaI(Tl), the change in center volume at the point of transition from metastable to emitting state is found to be $+17.5\times10^{-24}$ cm^3. Assuming a specific model for the center allows computation of the sign and magnitude of the critical displacement of ions required for trap collapse—in this case +0.19 A. The force constant for the metastable state is computed to be 5.8×10^5 dynes/cm; and the vibrational frequency, assuming an effective mass equal to six I^- ions, is 3.4×10^{12} sec^{-1} corresponding to a zero-point energy for this trap of 0.007 ev and crossover at a vibrational quantum number of about 47. The transmission coefficient for crossover to the emitting state appears to be of the order of 0.03%. Other possible experiments involving steady-state or transient pressure effects are outlined.

TEMPERATURE DEPENDENCE OF THE WORK FUNCTION OF SILVER, SODIUM, AND POTASSIUM. C. R. Crowell and R. A. Armstrong,* Department of Physics, McGill University, Montreal, Quebec, Canada (Received October 31, 1958).

Measurements have been made of the temperature dependence of the work functions of freshly evaporated films of silver, sodium, and potassium deposited at pressures of the order of 10^{-9}

mm of mercury. The results for silver (-13.4×10^{-5} volt/°K) were obtained by a capacitive contact potential method, those for sodium and potassium (-51×10^{-5} and -26×10^{-5} volt/°K, respectively) by the diode retarding-field method.

The theoretical outline by Herring and Nichols has been extended to produce quantitative predictions in fair agreement with the experimental results. Quantum defect calculations of the internal energy have been used to determine the effect of thermal expansion. Some allowance for anisotropy and dispersion has been included in the calculations of the electrostatic effect of thermal vibrations at constant volume. This effect is the largest contribution to the temperature dependence of the work functions of monovalent metals. The calculations point out the importance of the predominantly transverse modes of vibration. The effect of thermal vibration at constant volume on the chemical potential has also been calculated allowing for anisotropy and dispersion, and is shown to be small ($\sim -2 \times 10^{-5}$ volt/°K for monovalent metals). The theoretical predictions (representing the assumed model within an estimated 25%) are -12×10^{-5}, -45×10^{-5}, and -28×10^{-5} volt/°K for silver, sodium, and potassium, respectively.

*Now at Radio and E. E. Division, National Research Council, Ottawa, Canada.

NEW APPROACH TO THE THEORY OF SUPEREXCHANGE INTERACTIONS. P. W. Anderson, Bell Telephone Laboratories, Murray Hill, New Jersey (Received February 4, 1959).

The theory of indirect exchange in poor conductors is examined from a new viewpoint in which the d (or f) shell electrons are placed in wave functions assumed to be exact solutions of the problem of a single d electron in the presence of the full diamagnetic lattice. Inclusion of d-electron interactions leads to three spin-dependent effects which, in the usual order of their sizes, we call: superexchange per se, which is always antiferromagnetic; direct exchange, always ferromagnetic; and an indirect polarization effect analogous to nuclear indirect exchange. Superexchange itself is shown to be closely related to the poor conductivity, in agreement with experiment. By means of crystal field theory the parameters determining superexchange can be estimated, and in favorable cases (NiO, $LaFeO_3$) the exchange integrals can be evaluated with an accuracy of several tens of percent. Qualitative understanding of the whole picture of exchange in iron group oxides and fluorides follows from these ideas.

VIBRATION FREQUENCY SPECTRA OF DISORDERED LATTICES. I. MOMENTS OF THE SPECTRA FOR DISORDERED LINEAR CHAINS. C. Domb* and A. A. Maradudin, Physics Department, University of Maryland, College Park, Maryland, and E. W. Montroll and G. H. Weiss, Institute for Fluid Dynamics and Applied Mathematics, University of Maryland, College Park, Maryland (Received January 19, 1959).

Using the theory of random walks on lattices, a combinatorial expression has been obtained for the even moments of the vibrational frequency spectrum of a randomly disordered, two-component, isotopic linear chain as functions of the concentrations of the two kinds of particles and of their mass ratio. Expressions for the even moments up to μ_{20} are presented.

*On leave from Physics Department, King's College, University of London, London, England.

VIBRATION FREQUENCY SPECTRA OF DISORDERED LATTICES. II. SPECTRA OF DISORDERED ONE-DIMENSIONAL LATTICES. C. Domb* and A. A. Maradudin, Physics Department, University of Maryland, College Park, Maryland, and E. W. Montroll and G. H. Weiss, Institute for Fluid Dynamics and Applied Mathematics, University of Maryland, College Park, Maryland (Received January 19, 1959).

Using a combination of the moment-trace method and a new method, the "delta-function" method, the vibrational frequency spectrum of a randomly disordered, two-component, isotopic linear chain has been computed for a wide range of the concentrations of the two kinds of particles and of their mass ratios. In addition the particular case of a chain in which the mass of one of the isotopic constituents becomes infinite can be treated exactly, and the results of this analysis shed light on the form of the spectra for lattices with large but finite mass ratios for the two constituents. The spectra are characterized by the disappearance of the square-root singularity at

the maximum frequency which is found in ordered one-dimensional lattices, and by the appearance of impurity bands, the nature of which is discussed. Finally, the zero-point energy of a randomly disordered lattice is calculated and compared with the zero-point energy of an ordered lattice and of the separated phases.

*On leave from Physics Department, King's College, University of London, London, England.

ELECTROLUMINESCENCE OF AlN. G. A. Wolff, I. Adams, and J. W. Mellichamp, United States Army Signal Research and Development Laboratory, Fort Monmouth, New Jersey (Received January 12, 1959).

Electroluminescence in the visible region is observed when AlN is excited by either ac or dc. The emitted spectra consist of narrow bands in the 400-500 mμ region and broad continuous bands in the 500-700 mμ region. The broad bands vary according to the activator agents. With ac, the luminescence is in phase with the applied voltage. With dc, light is emitted in the vicinity of the cathode and decays with time. This decay can be explained by polarization. The presence of a barrier at the cathode is indicated. Impact excitation is proposed.

STUDIES OF THE SEMICONDUCTING PROPERTIES OF THE COMPOUND CsAu. W. E. Spicer, A. H. Sommer, and J. G. White, RCA Laboratories, Princeton, New Jersey (Received February 5, 1959).

Data are presented showing CsAu to be a semiconductor. The optical absorption curve is typical of a semiconductor with a threshold for direct optical excitation across the gap between 2.6 and 3.3 ev and exciton peaks at about 2.6, 3.0, and 3.3 ev. A relatively high optical absorption at smaller photon energies may indicate an indirect absorption process. Additional information has been obtained by measuring the spectral response curve of the photoemission from CsAu. The resistivity of the material is approximately 0.01 ohm-cm over the range from 410°K to 4.2°K, indicating either degeneracy or impurity banding. X-ray studies show that CsAu has a CsCl structure and a lattice constant of 4.263 ± 0.001 A. Finally, some preliminary results obtained with other alkali metal-gold compounds are described.

ELECTROMAGNETIC PROPERTIES OF SUPERCONDUCTORS. K. K. Gupta* and V. S. Mathur, Enrico Fermi Institute for Nuclear Studies and the Department of Physics, University of Chicago, Chicago, Illinois (Received January 2, 1959).

An integral relationship between the supercurrent and the vector potential of the electromagnetic field, similar to Pippard's phenomenological equation, is derived from the gauge-invariant theory of Wentzel. Expressions for coherence distance and penetration depth have been calculated.

*On leave of absence from the Tata Institute for Fundamental Research, Bombay, India.

D BANDS IN THE BODY-CENTERED CUBIC LATTICE. Joseph Callaway,* Department of Mathematics, Queen Mary College, University of London, London, England (Received February 2, 1959).

A model of a crystal, consisting of positive point charges neutralized by a uniform distribution of negative charge, is employed to study the form of the d-bands in a body-centered cubic lattice as a function of the lattice spacing. The wave functions are expressed as linear combinations of plane waves and the potential treated as a perturbation. It is shown that the perturbation series for the energy is a power series in Za, where Z is the atomic number and a is the lattice parameter. The leading term in the series is of the order $(1/a)^2$, and the coefficients of successive terms in the series decrease rapidly. The first three terms are evaluated for the states of predominantly d symmetry at the center of the Brillouin zone, and the corner H.

*Permanent address: Department of Physics, University of Miami, Coral Gables, Florida.

FREQUENCY SHIFTS IN HYPERFINE SPLITTING OF ALKALIS CAUSED BY FOREIGN GASES. H. Margenau, P. Fontana, and L. Klein, Yale University, New Haven, Connecticut (Received February 2, 1959).

The difference in the dispersion force between an alkali atom in a particular hyperfine level belonging to the ground state and a perturbing molecule is computed. These asymptotic forces, if

active alone, generally produce red shifts and suffice to account for the results obtained for the heavier buffer gases. Experimental data exhibit blue shifts for the lighter gases and therefore indicate that the net frequency shifts are the result of exchange as well as dispersion forces. The former cannot be determined theoretically. Therefore, a simple model is devised in which the difference in the forces is given a positive trend at distances of separation smaller than d, while beyond d it is given the calculated form. The experimental data for all alkali-rare gas interactions can then be fitted by values of d which, for the different foreign gases, are of order of their gas-kinetic diameters.

ABSORPTION OF GASEOUS HELIUM IN THE EXTREME ULTRAVIOLET. Norman N. Axelrod and M. Parker Givens, Institute of Optics, University of Rochester, Rochester, New York (Received February 2, 1959).

The absorption of gaseous helium at room temperature has been studied in the spectral region 550 A to 150 A. The measurements of Lee and Weissler have been confirmed and extended. The data are in substantial agreement with the theoretical predictions of Huang.

NEUTRON ELASTIC AND NONELASTIC CROSS SECTIONS FOR BERYLLIUM. J. B. Marion, Los Alamos Scientific Laboratory, Los Alamos, New Mexico, and University of Maryland, College Park, Maryland, and J. S. Levin and L. Cranberg, Los Alamos Scientific Laboratory, Los Alamos, New Mexico (Received January 29, 1959).

A time of-flight technique has been used to measure angular distributions for the elastic scattering of neutrons from beryllium in the energy range from 2.6 to 6.0 Mev. Neutron total cross sections were also measured and the following nonelastic (total minus elastic) cross sections obtained: 2.60 Mev, 0.27 ± 0.13 barn; 3.50 Mev, 0.43 ± 0.10 b; 4.10 Mev, 0.51 ± 0.08 b; 5.00 Mev, 0.60 ± 0.08 b; and 6.00 Mev, 0.73 ± 0.07 b. Differential cross sections were also obtained for the inelastically scattered neutrons leaving Be^9 in the 2.43-Mev excited state. Integration of these angular distributions yielded the following inelastic scattering cross sections: 3.50 Mev, 0.23 ± 0.04 barn; 4.10 Mev, 0.25 ± 0.04 b; and 5.00 Mev, 0.34 ± 0.05 b. A continuous spectrum of neutrons was observed which corresponds to the direct $(n, 2n)$ reaction and/or the excitation of the Be^9 "level" at 1.7 Mev. This continuum was found to have an angular distribution roughly symmetric about 90°. The 2.43-Mev state of Be^9 was found to decay by neutron emission to the ground state of Be^8 with a branching ratio of 12 ± 5 %.

ELASTIC SCATTERING OF 3.7-Mev NEUTRONS FROM S, Fe, Co, Ni, Cu, AND Zn. M. K. Machwe,* D. W. Kent, Jr., and S. C. Snowdon, Bartol Research Foundation of the Franklin Institute, Swarthmore, Pennsylvania (Received December 15, 1958).

The differential cross section for the elastic scattering of 3.7-Mev neutrons from sulfur, iron, cobalt, nickel, copper, and zinc has been measured in a ring geometry using a modified Bonner-type scintillation detector. The measurements were taken over an angular range between 10° and 160°. Angular resolution effects have been removed by a suitable iterative procedure. Multiple-scattering effects have been removed by an approximate analytical treatment.

* Now at Université de Montreal, Montreal, Canada.

POLARIZATION OF 6- AND 7-Mev PROTONS ELASTICALLY SCATTERED BY NUCLEI. Robert E. Warner and W. Parker Alford, Department of Physics and Astronomy, University of Rochester, Rochester, New York (Received December 31, 1958).

Polarization measurements have been made by first scattering from the target of interest and second scattering in a carbon polarimeter for which the mean second scattering angle is 48° and for which the mean value of the polarization is greater than +70 % for 5 Mev $\leq E_2 \leq$ 6 Mev. The polarization as a function of angle at 15° intervals from 45° to 135° is reported near 6 Mev for Al, Ti, V, Cr, Fe, Co, Ni, Cu, and Zn, and near 7 Mev for Al, Fe, Ni, and Cu. $P(\theta)$ usually shows an oscillatory behavior, with the magnitude of the maxima and minima never greater than about 40 %. The polarization as a function of energy is reported for C at 45° from 5.7 to 6.8 Mev, and for Fe and Cu at 60° and 120°

from 5.8 to 6.4 Mev. For C, $P(45°)$ decreases from +92% at 5.7 Mev to +36% at 6.8 Mev. For Cu, $P(60°)$ and $P(120°)$ vary slowly, if at all, with energy, but a rapid energy variation for Fe is observed, possibly due to resonance effects in compound elastic scattering.

CROSS SECTIONS FOR ELASTIC SCATTERING AND REACTIONS DUE TO PROTONS ON N^{15}. S. Bashkin, R. R. Carlson, and R. A. Douglas,* State University of Iowa, Iowa City, Iowa (Received January 28, 1959).

Absolute differential cross sections were measured for the reactions $N^{15}(p,p)N^{15}$, $N^{15}(p,\alpha_0)C^{12}$ (ground state), and $N^{15}(p,\alpha_1)C^{12*}$(first excited state). Thin gas targets, enriched up to 98% in N^{15}, and a 6-mil CsI(Tl) crystal detector were used. Numerous angles were studied for bombarding energies between 1 Mev and 3.6 Mev. Spins and parities are discussed where resonances suggest the existence of excited states in O^{16}. Results are as follows:

E_p (kev)	Resonant mode	Spin, parity
1028	$p\alpha_0\alpha_1\gamma$	1^-
1210	$p\alpha_0\alpha_1$	3^-
1640	$p \quad \alpha_1$	1^+
1890	α_0	
1985	α_1	2^-
3000	$p\alpha_0\alpha_1$	4^+
3300	$p \quad \alpha_1$	2^-
3350	α_0	2^+
3520	$p\alpha_0\alpha_1$	$1^-, 2^+, 3^-, 4^+$

At the 1210-kev resonance, the incident energy for which the α_0 yield is maximum depends on the angle of observation. This is probably the result of interference and has bearing on the spin and parity assignment of this level. The anomaly at 1890 kev cannot be positively identified as due to resonance.

*Now at Universidade de São Paulo, São Paulo, Brasil.

CROSS SECTION FOR ELASTIC SCATTERING OF PROTONS BY N^{14}. S. Bashkin, R. R. Carlson, and R. A. Douglas,* State University of Iowa, Iowa City, Iowa (Received January 28, 1959).

The elastic scattering cross section for protons on N^{14} was measured for bombarding energies from 900 kev to 4000 kev and for angles of 90°, 125.3°, 149.4°, and 160.9° in the center-of-mass system. A gas target chamber and a 6-mil thick CsI(Tl) crystal detector were used. The cross section was measured to an absolute accuracy of ±3.5%. An anomaly was observed at 3880±40 kev corresponding to a state in O^{15} at 11.00 Mev previously seen in the yield of inelastic gamma rays.

*Now at Universidade de São Paulo, São Paulo, Brasil.

TOTAL PHOTONUCLEAR ABSORPTION IN Al. M. V. Mihailović, G. Pregl, G. Kernel, and M. Kregar, J. Stefan Institute, Ljubljana, Yugoslavia (Received January 15, 1959).

A direct measurement of the total photonuclear absorption in Al was carried out with improved resolution using a Compton spectrometer for analysis of the bremsstrahlung and absorption spectrum. The maximum value for the cross section is found to be 100±10 mb; the integrated cross section is estimated to about 800 mb Mev.

SCATTERING OF 29.2-Mev He^3 NUCLEI BY DEUTERONS. J. S. C. McKee and D. R. Sweetman,* Department of Physics, University of Birmingham, Birmingham, England, P. V. March and W. T. Toner, Department of Natural Philosophy, University of Glasgow, Glasgow, Scotland, and W. M. Gibson, CERN, Geneva, Switzerland (Received February 3, 1959).

Differential cross sections for He^3 particles elastically scattered from deuterium are presented for angles from 10° to 40° (lab). Cross sections obtained previously for the same process are also shown, and there is good general agreement between the two sets of results.

*Now at Atomic Weapons Research Establishment, Aldermaston, Berks, England.

C^{14} - N^{14} MASS DIFFERENCE AND MASS EXCESSES OF SOME LIGHT NUCLIDES. L. Friedman, W. Henkes,* and D. Christman, Chemistry Department, Brookhaven National Laboratory, Upton, New York (Received February 5, 1959).

Mass excesses of the nuclides H^1, D^2, C^{12}, C^{14}, N^{14}, O^{18}, and A^{40} were determined by measurement of 18 parent molecule ion doublets with the

mass synchrometer. The $C^{14}-N^{14}$ difference, 156.44 ± 0.29 kev, was obtained from measurements on the doublets $[C^{14}O^{18}-O_2]$, $[N^{14}O^{18}-O_2]$, $[C^{14}H_4-H_2O]$, $[C^{14}CH_2-CO]$, and $[N_2H_4-O_2]$ and on other doublets which give some of those above. This is in excellent agreement with the value of 156 ± 1 kev obtained from determination of the C^{14} beta end point. The consistency of these data supports the 1-kev upper limit for the neutrino rest mass derived from the H^3-He^3 mass difference and the H^3 beta end point, and also supports the argument that mass synchrometer data are essentially free of systematic errors of the magnitude required to account for discrepancies between nuclear reaction and mass-spectrographic mass excesses of C^{12} and O^{16}. Mass excesses of the light nuclides determined were slightly higher than recently published mass synchrometer data, but agreement was generally within 1μMU.

*Present address: Robert Kochstrasse 8, Marburg/Lahn, Germany.

POSITIVE-PION PRODUCTION IN PROTON-PROTON COLLISIONS AT 450 Mev. Lee G. Pondrom,* Enrico Fermi Institute for Nuclear Studies, University of Chicago, Chicago, Illinois (Received January 28, 1959).

The external proton beam of the Chicago cyclotron has been used to study the reaction $p+p \rightarrow \pi^+ + n + p$ at 450 Mev. The reaction $p+p \rightarrow \pi^+ + d$ was also measured as a check on the equipment. A double-focusing wedge magnet was used to observe the momentum distribution of pions at angles of 14°, 20.5°, and 30° in the laboratory system. The over-all resolution of the magnet system varied from 1.5% to 2.2%. A least-squares fit of the $p+p \rightarrow \pi^+ + d$ data in the center-of-mass system gives $d\sigma/d\Omega \propto (0.38 \pm 0.20 + \cos^2\theta)$ with $\sigma = 1.47 \pm 0.12$ millibarns. The spectra for the unbound reaction were fitted to *Ss*, *Sp*, *Ps*, and *Pp* spectrum shapes predicted by the phenomenological theory of pion production. This fit gives $d\sigma/d\Omega \propto (0.40 \pm 0.08 + \cos^2\theta)$ with $\sigma = 1.80 \pm 0.7$ millibarns. The results of this fit have been compared with the cross section for neutral pion production at 450 Mev. This comparison was found satisfactory for the amounts of the *Ss*, *Sp*, and *Pp* spectrum shapes found in this experiment, but an excessively large amount of the *Ps* shape, 0.38 ± 0.10 millibarn, was required to fit the data. The results show that $\sigma_{10}(Pp)$ is much smaller than has been previously reported. An excitation function for the unbound cross section is predicted by this fit in terms of the phenomenological model, and is found to increase too rapidly at high bombarding energies.

*Now at the Aeronautical Research Laboratory, Wright-Patterson Air Force Base, Ohio.

PROTON COMPONENT OF THE PRIMARY COSMIC RADIATION. Frank B. McDonald, State University of Iowa, Iowa City, Iowa, and William R. Webber,* Imperial College, London, England (Received January 14, 1959).

The proton component has been extensively studied at high altitudes on a series of six Skyhook balloon flights at various latitudes using the Čerenkov-scintillation counter technique. The intensity of primary protons has been measured at 4°, 41°, 53°, and 55° geomagnetic latitude. The proton differential energy spectrum has been measured directly in the region 250-750 Mev. It is observed that primary alphas and protons have the same form of rigidity spectrum from 1 Bv to 17 Bv. A series of cutoff rigidities are measured in the vicinity of $\lambda = 53°$ and 55°. The intensity and composition of fast splash albedo is determined at $\lambda = 4°$, 53°, and 55°. Significant time variations are observed between the three high-latitude flights. Differences observed in the intensity and energy spectra of these three flights are discussed and strong restraints are placed on the possible modulating mechanism.

*Now at the Physics Department, University of Maryland, College Park, Maryland.

PRODUCTION OF Σ^+ HYPERONS BY 990-Mev POSITIVE PIONS IN LIQUID HYDROGEN. A. R. Erwin, Jr.,* and J. K. Kopp, Brookhaven National Laboratory, Upton, New York, and Harvard University, Cambridge, Massachusetts, and A. M. Shapiro, Brown University, Providence, Rhode Island, and Harvard University, Cambridge, Massachusetts (Received February 2, 1959).

The production and subsequent decay of six Σ^+ hyperons was observed in the central region of a hydrogen bubble chamber exposed to π^+ mesons

of kinetic energy 900 ± 30 Mev at the Cosmotron. The corresponding total production cross section, corrected for scanning inefficiencies, is $0.18^{+0.09}_{-0.07}$ mb. This value, combined with weighted averages of Σ^0 and Σ^- production cross sections in hydrogen obtained by Brookhaven, Columbia, and Berkeley groups, is used to compute the three triangular inequalities imposed by charge independence. The inequality $[\sigma(\Sigma^+)]^{1/2}+[\sigma(\Sigma^-)]^{1/2}-[2\sigma(\Sigma^0)]^{1/2}=0.14^{+0.12}_{-0.11}$ $(\text{mb})^{1/2}\geq 0$, is the only one that might not be satisfied. The near-zero value of the left-hand side indicates the difficulty to be encountered in demonstrating a failure of charge independence at this energy.

*Now at the Department of Physics, University of Wisconsin, Madison, Wisconsin.

MODEL OF A LINEAR HARMONIC OSCILLATOR IN THE GENERAL THEORY OF RELATIVITY. Henry Zatzkis, Mathematics Department, Newark College of Engineering, Newark, New Jersey (Received January 16, 1959).

A model of a linear harmonic oscillator in the general theory of relativity is examined. It is based on a classical model of a point mass vibrating harmonically about the center of an ideal liquid sphere. The motion is no longer harmonic. However, to a first approximation, it is still harmonic, but the period of vibration depends both on the amplitude and on the curvature of the space. Both quantities tend to slow down the motion. In the limiting case of flat space the classical frequency is again restored.

THREE-PION CONTRIBUTION TO THE ELECTROMAGNETIC STRUCTURE OF THE NUCLEON. B. Bosco and V. De Alfaro, Istituto di Fisica dell'Università, Torino, Italia, and Istituto Nazionale di Fisica Nucleare, Sezione di Torino, Italia (Received February 2, 1959).

In this paper the three-pion contribution to the scalar electromagnetic form factors of the nucleon is computed by using the fixed-source meson theory without rescattering corrections. The $(\gamma,3\pi)$ interaction is taken phenomenologically as a point interaction. It is shown that for those values of the $(\gamma,3\pi)$ coupling constant compatible with photoproduction experiments, the experimental charge distribution could be roughly fitted with a cutoff in the dispersion integrals of the order of 7 pion masses.

STRUCTURE THEOREM FOR THE PHOTON PROPAGATOR. Herbert M. Fried, Department of Physics, University of California, Los Angeles, California (Received February 3, 1959).

A simple theorem relating the structure of the bare and dressed photon commutators and propagators is derived, and its implication, with respect to the choice of photon gauge, is discussed.

$K_{\mu 2}$ DECAY AND LEPTONIC DECAY OF HYPERONS. B. Sakita, Department of Physics and Astronomy, University of Rochester, Rochester, New York (Received January 19, 1959).

The partial life time of $K\rightarrow\mu+\nu$ is calculated by dispersion techniques assuming that the K meson is pseudoscalar and that the relevant Fermi interactions are of the V-A type. The results are compared with experiments and it is concluded that the renormalized axial vector coupling which is responsible for the leptonic decay of hyperons is much smaller than the usual universal Fermi interaction.